

CARBON DIOXIDE SEQUESTRATION AND ENHANCED OIL RECOVERY  
CO-OPTIMIZATION

A THESIS SUBMITTED TO  
THE GRADUATE SCHOOL OF NATURAL AND APPLIED SCIENCES  
OF  
MIDDLE EAST TECHNICAL UNIVERSITY

BY

NURI AKHUNDOV

IN PARTIAL FULFILLMENT OF THE REQUIREMENTS  
FOR  
THE DEGREE OF MASTER OF SCIENCE  
IN  
PETROLEUM AND NATURAL GAS ENGINEERING

SEPTEMBER 2021



Approval of the thesis:

**CARBON DIOXIDE SEQUESTRATION AND ENHANCED OIL  
RECOVERY CO-OPTIMIZATION**

submitted by **NURI AKHUNDOV** in partial fulfillment of the requirements for the degree of **Master of Science in Petroleum and Natural Gas Engineering, Middle East Technical University** by,

Prof. Dr. Halil Kalıpçılar

Dean, Graduate School of **Natural and Applied Sciences**

---

Assoc. Prof. Dr. Çağlar Sınayuç

Head of the Department, **Petroleum and Natural Gas Engineering Dept., METU**

---

Assoc. Prof. Dr. Çağlar Sınayuç

Supervisor, **Petroleum and Natural Gas Engineering Dept., METU**

---

**Examining Committee Members:**

Assist. Prof. Dr. İsmail Durgut

Petroleum and Natural Gas Engineering Dept., METU

---

Assoc. Prof. Dr. Çağlar Sınayuç

Petroleum and Natural Gas Engineering Dept., METU

---

Assist. Prof. Dr. Doruk Alp

Petroleum and Natural Gas Engineering Dept., METU NCC

---

Date: 09.09.2021

**I hereby declare that all information in this document has been obtained and presented in accordance with academic rules and ethical conduct. I also declare that, as required by these rules and conduct, I have fully cited and referenced all material and results that are not original to this work.**

Name Last name : Nuri Akhundov

Signature:

## **ABSTRACT**

### **CARBON DIOXIDE SEQUESTRATION AND ENHANCED OIL RECOVERY CO-OPTIMIZATION**

Akhundov, Nuri  
Master of Science, Petroleum and Natural Gas Engineering  
Supervisor: Assoc. Prof. Dr. Çağlar Sinayuç

September 2021, 103 pages

The worldwide growth of industry leads to continuous rise of anthropogenic emission amount into the atmosphere, which causes greenhouse effect all over the world, that is heating up the atmosphere and changing the global climate. On the other hand, carbon dioxide injection into oil reservoirs for the purpose of enhancement of oil recovery (CO<sub>2</sub>-EOR) has been commercially used for nearly 50 years. The operations in petroleum sector are being carried out in a way to maximize the recovered oil while keeping the amount of CO<sub>2</sub> injected at its minimum due to the purchase cost of carbon dioxide. To overcome the economic restrictions for CO<sub>2</sub> sequestration during EOR, it is necessary to simultaneously maximize economic oil recovery and the volumes of CO<sub>2</sub> injected in oil reservoirs using an engineering approach. This process is named as co-optimization. For this purpose, several simulations for different scenarios are being carried out to find the maximum amount of CO<sub>2</sub> that can be stored, maximum amount of oil that can be produced, and an optimal point for simultaneous maximization of both numbers.

Results show, that using inverted 5 spot pattern and implementing water-alternating-gas (WAG) injection can significantly contribute to the co-optimization, while other

parameters, such as pattern area and injection rate need to be evaluated on case by case basis, considering economical factors as well.

Keywords: Climate Change, CO<sub>2</sub>, Storage, Sequestration, Enhanced Oil Recovery, Co-Optimization

## ÖZ

### **KARBON DİOKSİTİN DEPOLANMASI VE GELİŞMİŞ PETROL KURTARIMININ BİRLİKTE UYGULANMASI**

Akhundov, Nuri  
Yüksek Lisans, Petrol ve Doğal gaz Mühendisliği  
Tez Yöneticisi: Doç. Dr. Çağlar Sınayuç

Eylül 2021, 103 sayfa

Endüstrinin dünya çapında büyümesi, atmosfere yapılan insan kaynaklı emisyon miktarlarının sürekli artmasına neden olmakta, bu da tüm atmosferi ısıtan ve küresel iklimi değiştiren sera etkisini doğurmaktadır. Öte yandan, petrolün geri kazanımı amacıyla (CO<sub>2</sub>-EOR) petrol rezervuarlarına karbondioksit enjeksiyonu yaklaşık 50 yıldır ticari olarak kullanılmaktadır. Petrol sektöründeki çalışmalar, satın alma maliyetinin yüksek olması nedeniyle enjekte edilen CO<sub>2</sub> miktarını minimumda tutarken geri kazanılan petrolü maksimuma çıkaracak şekilde yürütülmektedir. EOR sırasında CO<sub>2</sub> sekestrasyonuna yönelik ekonomik kısıtlamaların üstesinden gelmek amacı ile, bir mühendislik yaklaşımı kullanarak ekonomik petrol geri kazanımını ve petrol rezervuarlarına enjekte edilen CO<sub>2</sub> hacimlerini eş zamanlı maksimize etmek gerekmektedir. Ortak optimizasyon adı verilen bu işlemin amacı, depolanabilecek maksimum CO<sub>2</sub> miktarını, üretilebilecek maksimum petrol miktarını ve her iki sayının eş zamanlı olarak maksimizasyonu için en uygun noktayı bulmak amacıyla farklı senaryolar için çeşitli simülasyonlar gerçekleştirilmektedir.

Sonuçlar, tersine çevrilmiş 5 nokta deseninin kullanılmasının ve su-alternatif gaz (WAG) enjeksiyonunun uygulanmasının, eş optimizasyona önemli ölçüde katkıda

bulunabileceğini gösterirken, desen alanı ve enjeksiyon hızı gibi diğer parametrelerin durum bazında ekonomik faktörleri de göz önünde bulundurarak değerlendirilmesi gerektiğini göstermektedir.

**Anahtar Kelimeler:** İklim Değişikliği, CO<sub>2</sub>, Depolanma, Ayrılma, Gelişmiş Petrol Kurtarımı, Ortak Optimizasyon

*To My Father*

## ACKNOWLEDGMENTS

I would like to express my sincere gratitude to my supervisor Assoc. Prof. Dr. Çağlar Sınayuç for his guidance, advice, support, encouragement, and patience throughout my graduate studies.

I want to thank TÜBİTAK and Assoc. Prof. Dr. Çağlar Sınayuç for awarding me a graduate research scholarship for a portion of my graduate studies.

I am very grateful to all my instructors at METU, especially in the Department of Petroleum & Natural Gas Engineering, who have played an important and irreplaceable role in my undergraduate and graduate education, and my career.

Note of appreciation to all the colleagues from METU, especially in the Department of Petroleum & Natural Gas Engineering, who supported me during both my undergraduate and graduate education.

Thanks to all the people, close to me, in Baku, Azerbaijan, who also supported and encouraged me, and provided feedback during the preparation of this thesis.

Finally, I want to thank my family, for their continuous support, patience, and encouragement during my studies. I am very grateful to my mother, Tarana Ahmadova, who focused on my education since my early childhood, and never compromised it no matter the circumstances. And I want to specially highlight my father, Nazim Akhundov, under whose guidance I was able to enroll METU with scholarship from bp, who supported, encouraged, and never stop believing in me during my education, whose priority was making sure that I graduate with MSc degree, and who unfortunately was not able to live long enough to see this happening.

## TABLE OF CONTENTS

ABSTRACT.....	v
ÖZ.....	vii
ACKNOWLEDGMENTS .....	x
TABLE OF CONTENTS.....	xi
LIST OF TABLES .....	xiv
LIST OF FIGURES .....	xv
LIST OF ABBREVIATIONS AND NOMENCLATURE .....	xx
CHAPTERS	
1 INTRODUCTION .....	1
2 LITERATURE REVIEW .....	5
2.1 Greenhouse gases and climate change.....	5
2.2 Carbon capture, utilization and storage (CCUS) .....	7
2.2.1 Carbon capture .....	8
2.2.1.1 Post-combustion capture (PCC) .....	9
2.2.1.2 Pre-combustion.....	11
2.2.1.3 Oxy-combustion .....	12
2.2.2 Carbon utilization.....	14
2.2.3 Carbon storage .....	15
2.2.3.1 Terrestrial sequestration.....	17
2.2.3.2 Ocean sequestration .....	18

2.2.3.3	Geosequestration .....	19
2.2.3.3.1	Coal seams .....	20
2.2.3.3.2	Deep saline aquifers .....	21
2.2.3.3.3	Oil and gas reservoirs .....	23
2.3	CO <sub>2</sub> -EOR .....	25
2.3.1	Miscible CO <sub>2</sub> -EOR .....	26
2.3.1.1	Minimum Miscible Pressure .....	28
2.3.2	Immiscible CO <sub>2</sub> -EOR .....	29
2.3.2.1	CO <sub>2</sub> solubility in oil .....	30
2.3.2.2	Oil swelling .....	31
2.3.2.3	Oil viscosity .....	32
3	STATEMENT OF THE PROBLEM .....	33
4	METHODOLOGY .....	35
4.1	CMG IMEX and Pseudo-Miscible Model .....	35
4.2	Optimized Properties .....	39
5	NUMERICAL MODELING AND SIMULATIONS .....	41
5.1	Model construction .....	41
5.1.1	Bati Raman field .....	41
5.1.1.1	Model geometry and grid .....	42
5.1.1.2	Reservoir rock and fluid properties .....	44
5.1.1.3	Simulation scenarios .....	48
5.1.1.3.1	Scenario 1 .....	48
5.1.1.3.2	Scenario 2 .....	48
5.1.1.3.3	Scenario 3 .....	49

5.1.1.3.4	Scenario 4 .....	49
5.1.1.3.5	Scenario 5 .....	49
6	RESULTS AND DISCUSSION .....	51
6.1	Scenario 1 .....	51
6.2	Scenario 2 .....	53
6.3	Scenario 3 .....	56
6.4	Scenario 4 .....	60
6.5	Scenario 5 .....	63
6.6	Economical considerations .....	66
7	CONCLUSION .....	69
	REFERENCES .....	73
	APPENDICES	
A.	Scenario 1 Raw Material .....	79
B.	Scenario 2 Raw Material .....	86
C.	Scenario 3 Raw Material .....	92
D.	Scenario 4 Raw Material .....	98
E.	Scenario 5 Raw Material .....	101

## LIST OF TABLES

### TABLES

Table 2.1 Technological uses of CO <sub>2</sub> (Aresta & Dibenedetto, 2010) .....	14
Table 2.2 Characteristics of trapping mechanisms in saline aquifers (Yang et al., 2010).....	22
Table 5.1 Reservoir rock properties .....	44
Table 5.2 WAG Injection Cycles .....	49
Table 6.1 Scenario 1 outcomes.....	52
Table 6.2 Scenario 2 outcomes.....	55
Table 6.3 Scenario 3 outcomes.....	59
Table 6.4 Scenario 4 outcomes.....	62
Table 6.5 Oil Recovery Factors increase for various WAG configurations.....	64
Table 6.6 Change in CO <sub>2</sub> volumes in reservoir for various WAG configurations..	65

## LIST OF FIGURES

### FIGURES

Figure 2.1. Average annual atmospheric CO <sub>2</sub> concentrations from Antarctic ice and firm from 1010–1960 (Bouzalakos, 2010).....	6
Figure 2.2. Average annual atmospheric CO <sub>2</sub> concentrations based on direct measurements at Mauna Loa Observatory (Bouzalakos, 2010) .....	6
Figure 2.3. Temperature vs Solar Activity (NASA, n.d.) .....	7
Figure 2.4. Technical options for CO <sub>2</sub> capture (Rubin et al., 2012) .....	9
Figure 2.5. Simplified schematic of carbon capture in PC power plant (Rubin et al., 2012) .....	10
Figure 2.6. Simplified schematic of an integrated gasification combined cycle (IGCC) coal power plant with pre-combustion CO <sub>2</sub> capture using a water-gas shift reactor and a Selexol CO <sub>2</sub> (Rubin et al., 2012).....	11
Figure 2.7. Simplified schematic of a coal-fired power plant using oxy-combustion technology (Rubin et al., 2012).....	13
Figure 2.8. Carbon sequestration classification (Kambale & Tripathi, 2010) .....	16
Figure 2.9. EOR Methods (Ganzer & Reinicke, 2017).....	25
Figure 2.10. The schematic of the CO <sub>2</sub> (carbon dioxide) miscible process showing the transition zone between the injection and production well (Verma, 2015) .....	27
Figure 2.11. Correlation of Minimum Miscibility Pressure with C <sub>5</sub> + Molecular Weight and reservoir temperature (Mungan, 1981; Verma, 2015).....	28
Figure 2.12. Lasater correlation relating the molecular weight of C <sub>5</sub> + components with oil gravity (Lasater, 1958; Verma, 2015).....	29
Figure 5.1. X-Y view (top) of the model .....	43
Figure 5.2. X-Z view of the model.....	43
Figure 5.3. Solution Gas Oil Ratio and Oil Formation Volume Factor vs Pressure	45
Figure 5.4. Oil and Gas Viscosities vs Pressure .....	45

Figure 5.5. Relative Permeability vs Water Saturation .....	46
Figure 5.6. Capillary Pressure vs Water Saturation .....	46
Figure 5.7. CO <sub>2</sub> Formation Volume Factor vs Pressure .....	47
Figure 5.8. CO <sub>2</sub> Viscosity vs Pressure.....	47
Figure 6.1. Oil Recovery Factor for various injection patterns .....	52
Figure 6.2. CO <sub>2</sub> Volumes in reservoir for various injection patterns .....	53
Figure 6.3. Oil Recovery Factors for various patterns sizes.....	54
Figure 6.4. CO <sub>2</sub> Volumes in reservoir for various pattern sizes.....	55
Figure 6.5. Oil Recovery Factors for various CO <sub>2</sub> injection rates.....	57
Figure 6.6. Rate of oil recovery factor increase vs CO <sub>2</sub> injection rate .....	57
Figure 6.7. Time before CO <sub>2</sub> Breakthrough to production wells .....	58
Figure 6.8. CO <sub>2</sub> Volumes in reservoir for various CO <sub>2</sub> injection rates .....	59
Figure 6.9. Oil Recovery Factors for CO <sub>2</sub> injection into various zones .....	60
Figure 6.10. CO <sub>2</sub> Volumes in reservoir for injection into various zones .....	62
Figure 6.11. Reservoir Pressures for CO <sub>2</sub> injection into various zones .....	63
Figure 6.12. Oil Recovery Factors for various WAG configurations .....	64
Figure 6.13. CO <sub>2</sub> Volumes in reservoir for various WAG configurations .....	66
Figure 7.1. Peripheral injection top view .....	79
Figure 7.2. Directline injection top view .....	79
Figure 7.3. 5-Spot pattern injection top view .....	79
Figure 7.4. 9-Spot pattern injection top view .....	80
Figure 7.5. Inverted 5-Spot pattern injection top view .....	80
Figure 7.6. Inverted 7-Spot pattern injection top view .....	80
Figure 7.7. Inverted 9-Spot pattern injection top view .....	80
Figure 7.8. Directline Injection RF.....	81
Figure 7.9. Directline Injection CO <sub>2</sub> Volumes .....	81
Figure 7.10. Peripheral Injection RF .....	81
Figure 7.11. Peripheral Injection CO <sub>2</sub> Volumes.....	82
Figure 7.12. 5-Spot Pattern Injection RF.....	82
Figure 7.13. 5-Spot Pattern Injection CO <sub>2</sub> Volumes .....	82

Figure 7.14. 9-Spot Pattern Injection RF .....	83
Figure 7.15. 9-Spot Pattern Injection CO <sub>2</sub> Volumes.....	83
Figure 7.16. Inverted 5-Spot Pattern Injection RF.....	83
Figure 7.17. Inverted 5-Spot Pattern Injection CO <sub>2</sub> Volumes .....	84
Figure 7.18. Inverted 7-Spot Pattern Injection RF.....	84
Figure 7.19. Inverted 7-Spot Pattern Injection CO <sub>2</sub> Volumes .....	84
Figure 7.20. Inverted 9-Spot Pattern Injection RF.....	85
Figure 7.21. Inverted 9-Spot Pattern Injection CO <sub>2</sub> Volumes .....	85
Figure 7.22. 75 Acres Pattern Size RF.....	86
Figure 7.23. 75 Acres Pattern Size CO <sub>2</sub> Volumes .....	86
Figure 7.24. 100 Acres Pattern Size RF.....	86
Figure 7.25. 100 Acres Pattern Size CO <sub>2</sub> Volumes .....	87
Figure 7.26. 200 Acres Pattern Size RF.....	87
Figure 7.27. 200 Acres Pattern Size CO <sub>2</sub> Volumes .....	87
Figure 7.28. 215 Acres Pattern Size RF.....	88
Figure 7.29. 215 Acres Pattern Size CO <sub>2</sub> Volumes .....	88
Figure 7.30. 230 Acres Pattern Size RF.....	88
Figure 7.31. 230 Acres Pattern Size CO <sub>2</sub> Volumes .....	89
Figure 7.32. 250 Acres Pattern Size RF.....	89
Figure 7.33. 250 Acres Pattern Size CO <sub>2</sub> Volumes .....	89
Figure 7.34. 400 Acres Pattern Size RF.....	90
Figure 7.35. 400 Acres Pattern Size CO <sub>2</sub> Volumes .....	90
Figure 7.36. 500 Acres Pattern Size RF.....	90
Figure 7.37. 500 Acres Pattern Size CO <sub>2</sub> Volumes .....	91
Figure 7.38. 600 Acres Pattern Size RF.....	91
Figure 7.39. 600 Acres Pattern Size CO <sub>2</sub> Volumes .....	91
Figure 7.40. RF at 10 MMscf injection.....	92
Figure 7.41. CO <sub>2</sub> Volumes at 10 MMscf injection .....	92
Figure 7.42. RF at 20 MMscf injection.....	92
Figure 7.43. CO <sub>2</sub> Volumes at 20 MMscf injection .....	93

Figure 7.44. RF at 30 MMscf injection .....	93
Figure 7.45. CO <sub>2</sub> Volumes at 30 MMscf injection.....	93
Figure 7.46. RF at 50 MMscf injection .....	94
Figure 7.47. CO <sub>2</sub> Volumes at 50 MMscf injection.....	94
Figure 7.48. RF at 100 MMscf injection .....	94
Figure 7.49. CO <sub>2</sub> Volumes at 100 MMscf injection.....	95
Figure 7.50. RF at 150 MMscf injection .....	95
Figure 7.51. CO <sub>2</sub> Volumes at 150 MMscf injection.....	95
Figure 7.52. RF st 200 MMscf injection .....	96
Figure 7.53. CO <sub>2</sub> Volumes at 200 MMscf injection.....	96
Figure 7.54. RF at 250 MMscf injection .....	96
Figure 7.55. CO <sub>2</sub> Volumes at 250 MMscf injection.....	97
Figure 7.56. RF at 500 MMscf injection .....	97
Figure 7.57. CO <sub>2</sub> Volumes at 500 MMscf injection.....	97
Figure 7.58. RF for CO <sub>2</sub> Injection into Oil Zone .....	98
Figure 7.59. CO <sub>2</sub> Volumes for Injection into Oil Zone.....	98
Figure 7.60. Reservoir Pressure While CO <sub>2</sub> Injection into Oil Zone .....	98
Figure 7.61. RF for CO <sub>2</sub> Injection into Water Zone.....	99
Figure 7.62. CO <sub>2</sub> Volumes for Injection into Water Zone .....	99
Figure 7.63. Reservoir Pressure While CO <sub>2</sub> Injection into Water Zone .....	99
Figure 7.64. RF for CO <sub>2</sub> Injection into Both Oil and Water Zones.....	100
Figure 7.65. CO <sub>2</sub> Volumes for Injection into Both Oil and Water Zones.....	100
Figure 7.66. Reservoir Pressure While CO <sub>2</sub> Injection into Both Oil and Water Zones .....	100
Figure 7.67. RF for 1:1 WAG Cycle ( 3 month each ).....	101
Figure 7.68. CO <sub>2</sub> Volume for 1:1 WAG Cycle ( 3 months each ) .....	101
Figure 7.69. RF for 1:2 WAG Cycle ( 3 months H <sub>2</sub> O – 6 months CO <sub>2</sub> ).....	101
Figure 7.70. CO <sub>2</sub> Volume for 1:2 WAG Cycle ( 3 months H <sub>2</sub> O – 6 months CO <sub>2</sub> ) .....	102
Figure 7.71. RF for 2:1 WAG Cycle ( 6 months H <sub>2</sub> O – 3 months CO <sub>2</sub> ).....	102

Figure 7.72. CO<sub>2</sub> Volume for 2:1 WAG Cycle ( 6 months H<sub>2</sub>O – 3 months CO<sub>2</sub> )  
..... 102

Figure 7.73. RF for 1:1 WAG Cycle ( 6 month each ) ..... 103

Figure 7.74. CO<sub>2</sub> Volume for 1:1 WAG Cycle ( 6 month each )..... 103

## LIST OF ABBREVIATIONS AND NOMENCLATURE

### ABBREVIATIONS

ASP	Alcaline-Surfactant-Polymer
ASU	Air Separation Unit
CCO2	Continuous CO2
CCS	Carbon Capture and Storage
CCU	Carbon Capture and Utilization
CCUS	Carbon Capture, Utilization and Storage
CHOPS	Cold Heavy Oil Production with Sand
CMG	Computer Modelling Group
CO2-EOR	CO2 Enhanced Oil Recovery
CO2-WAG	CO2 water-alternating gas
ECBM	Enhance Coalbed Methane
EOR	Enhanced Oil Recovery
FCM	First-Contact Miscible
Gt	Giga ton
HC	Hydrocarbon
IFT	Interfacial Tension
IGCC	Integrated Gasification Combined Cycle
MCM	Multiple-Contact Miscible

MEA	Monoethanolamine
MMP	Minimum Miscible Pressure
NGCC	Natural Gas-Fired Combined Cycle
PC	Pulverised Coal
PCC	Post-Combustion Capture
Pg	Peta gram
RF	Recovery Factor
SAGD	Steam Assisted Gravity Drainage
UNFCCC	United Nations Framework Convention on Climate Change
WAG	Water Alternating Gas

## **NOMENCLATURE**

$\omega$	mixing parameter
F	partitioning function
S	saturation, fraction
B	formation volume factor, RB/STB
k	permeability, md
$k_r$ ( $k_{rp}$ )	relative permeability, fraction
$P_c$	capillary pressure, psi
P	pressure, psi
$\mu$	viscosity, cp

$\rho$	density, mass/volume
$\gamma$	oil specific gravity
T	temperature (F)
MW	oil molecular weight

### **Subscripts**

rp, r	relative
o	oil
w	water
g	gas
sol	solvent (CO <sub>2</sub> )
i	initial
s	saturation
liq	liquefaction

### **Superscripts**

eff	effective
m	miscible
Im	Immiscible
Frac	Fraction

## CHAPTER 1

### INTRODUCTION

Global climate change has been a huge issue for a long time. It is stated, that one of the major causes of this change is increasing amount of greenhouse gases emissions, which include: Carbon Dioxide (CO<sub>2</sub>), Methane (CH<sub>4</sub>), Nitrous Oxide (N<sub>2</sub>O), Hydrofluorocarbons (HFCs), Perfluorocarbons (PFCs) and Sulphur hexafluoride (SF<sub>6</sub>) (United Nations Climate Change, 2019b). These gases are affecting atmosphere insulation which results in the Earth keeping the warmth more than it was before the increase (Ansarizadeh et al., 2015). The concentration of CO<sub>2</sub> has reached 385ppm in 2008 starting with 280ppm in preindustrial era and continues to increase with the rate of 2ppm each year (Bouzalakos, 2010). Major reasons behind this increase are fossil fuel combustion, processes going on in cement plants, and deforestation (Lal, 2010). As the result, the global temperature average has increased for about 0.85 °C between 1880 and 2012 (IPCC, 2014).

Starting with the Kyoto protocol for the two commitment periods, and then continuing with Paris Agreement with one commitment period, countries all over the world are trying to reduce the amount of anthropogenic greenhouse gases in the atmosphere, and to mitigate their effect on climate change (United Nations Climate Change, 2019b, 2019a). Global trend of carbon dioxide management usually relies on three different strategies. The first one, is switching to the low-carbon energy sources, such as alternatives and renewables. The second, developing and applying new technology in order to increase efficiency of conventional energy sources. Finally, third strategy is to apply Carbon Capture, Utilization and Storage (CCUS) techniques to decrease the amount of emitted CO<sub>2</sub> (Bouzalakos, 2010). Since most of world energy sources are fossil fuels, rapid transition to low-carbon energy sources is not technically and economically feasible. So, at the moment, the major

method of CO<sub>2</sub> mitigation is considered to be CCUS (Ansarizadeh et al., 2015). Applying CCUS is the way to enable continuous use of conventional energy sources (fossil fuels), while decreasing the amount of CO<sub>2</sub> in the atmosphere (IRGC, 2008). CCUS consists of several steps applied in the process: Capturing CO<sub>2</sub> from exhaust gases, pressurizing and transporting to the storage or utilization site, and finally sequestration or utilization process (Bouzalakos, 2010). With these technologies approximately 60% of world CO<sub>2</sub> emissions that are being resulted by stationary sources operations can be mitigated (Ansarizadeh et al., 2015).

At the moment, one of the most effective ways for carbon sequestration is storing it in geological formation, which can also be called geosequestration. This also involves the usage of hydrocarbon reservoirs and deep saline aquifers. Unfortunately, cost of CCUS is quite high at the moment. It is estimated, that around 2020 average cost of the project per tonne of CO<sub>2</sub> abated was in the range of 35–50€, which is not economically feasible for most of the companies to implement (Bouzalakos, 2010). On the other hand, there is an established practice of CO<sub>2</sub> usage for enhanced oil recovery (EOR) purposes. New technologies available in EOR operations provide opportunities for combination of the process with carbon dioxide sequestration, thus utilizing CO<sub>2</sub> for enhanced oil recovery and then storing it in oil reservoir (Gaspar Ravagnani et al., 2009). The advantage of this method is that the cost of carbon sequestration decreases due to profit available from additional oil production. Furthermore, field that has already been submitted to EOR applications before, can be even more cost effective, since it already has most of the required infrastructure required for gas injection into the reservoir. There are three ways to implement CO<sub>2</sub>-EOR in combination with carbon storage: conventional, which mainly focuses on EOR, rather than CO<sub>2</sub> storage; advanced, in which operator is trying to utilize and store more carbon dioxide, while increasing oil recovery; and maximum storage case, when CO<sub>2</sub>-EOR is mainly focused on CO<sub>2</sub> sequestration, rather than oil recovery(IEA, 2015). While there has not been a lot of experience in usage of CO<sub>2</sub>-EOR for carbon dioxide storage, the IEAGHG Weyburn-Midale CO<sub>2</sub> Monitoring and Storage Project, which was implemented between 2000 and 2012,

provided evidence, that both EOR and CO<sub>2</sub> sequestration can be co-optimized, and permanent storage of carbon dioxide is achievable in the process(IEA, 2015).

Currently CO<sub>2</sub> is injected either only focusing on EOR, disregarding amount of CO<sub>2</sub> stored, or disregarding oil recovery and only focusing on CO<sub>2</sub> sequestration.

The purpose of this study, is the co-optimization of both EOR and sequestration and finding an optimal way for the process in heavy oil field. The approach includes the implementation of reservoir simulations to this study. The simulations include various cases of CO<sub>2</sub> injection patterns, well spacing, injection rates, zones injected, and feasibility of using Water-Alternating-Gas injection for this purpose. The reservoir modeling is performed by using CMG's IMEX, Builder and Results software.



## CHAPTER 2

### LITERATURE REVIEW

#### 2.1 Greenhouse gases and climate change

According to scientists the global warming trend is attributed to the greenhouse effect, which is the result of Earth heat being trapped by the atmosphere (NASA, n.d.). Major gases, that prevent heat from escaping to space are: Carbon Dioxide (CO<sub>2</sub>), Methane (CH<sub>4</sub>), Nitrous Oxide (N<sub>2</sub>O), Hydrofluorocarbons (HFCs), Perfluorocarbons (PFCs) and Sulphur hexafluoride (SF<sub>6</sub>) (United Nations Climate Change, 2019b). CO<sub>2</sub> is the major forcing element of global warming. Its concentration in the atmosphere has increased by more than 30% since the beginning of industrial revolution (NASA, n.d.). As it can be seen on Figure 2.1 and 2.2, the concentration of CO<sub>2</sub> has reached 385ppm in 2008 starting with 280ppm in preindustrial era and continues to increase with the rate of 2ppmv each year (Bouzalakos, 2010).

The following are considered as the sources of carbon dioxide: naturally induced CO<sub>2</sub> coming from the processes such as volcano eruptions and respiration, and human induced CO<sub>2</sub>, from changes in land usage, producing energy from fossil fuels, and deforestation. It was stated by 1300 experts from different countries, that there is 95% probability, that the increase in global temperature over the past 50 years was caused mainly by human activities, resulting in greenhouse gases emission (IPCC, 2014). Over the past century, concentration of carbon dioxide has increased significantly mainly due to fossil fuel burning processes (NASA, n.d.).

Due to this increase, as it can be seen on the Figure 2.3, the global temperature average has increased for about 0.85 °C between 1880 and 2012 (IPCC, 2014; NASA, n.d.).

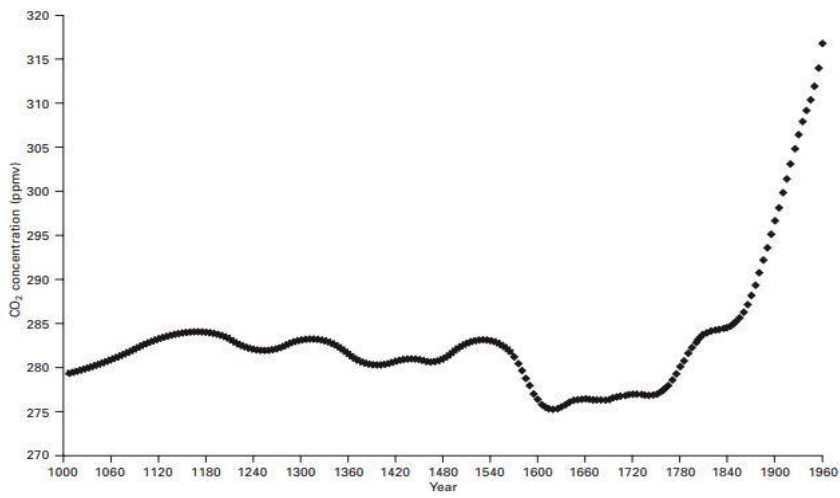


Figure 2.1. Average annual atmospheric CO<sub>2</sub> concentrations from Antarctic ice and firn from 1010–1960 (Bouzalakos, 2010)

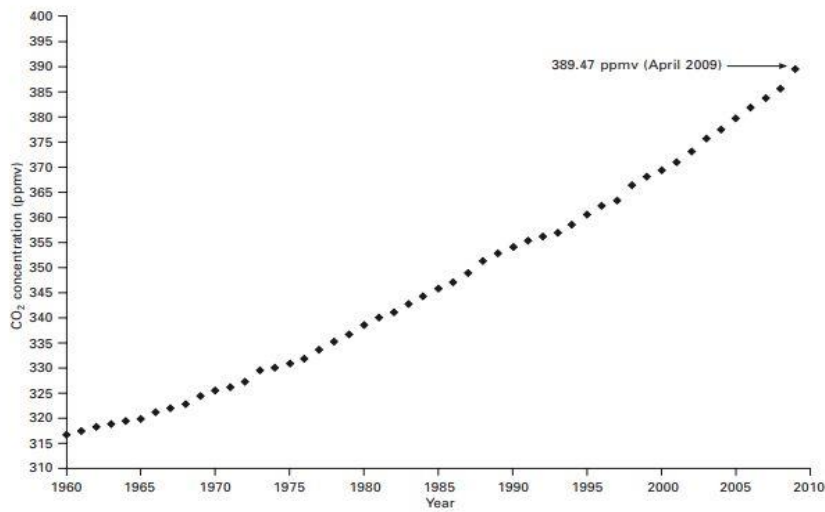


Figure 2.2. Average annual atmospheric CO<sub>2</sub> concentrations based on direct measurements at Mauna Loa Observatory (Bouzalakos, 2010)

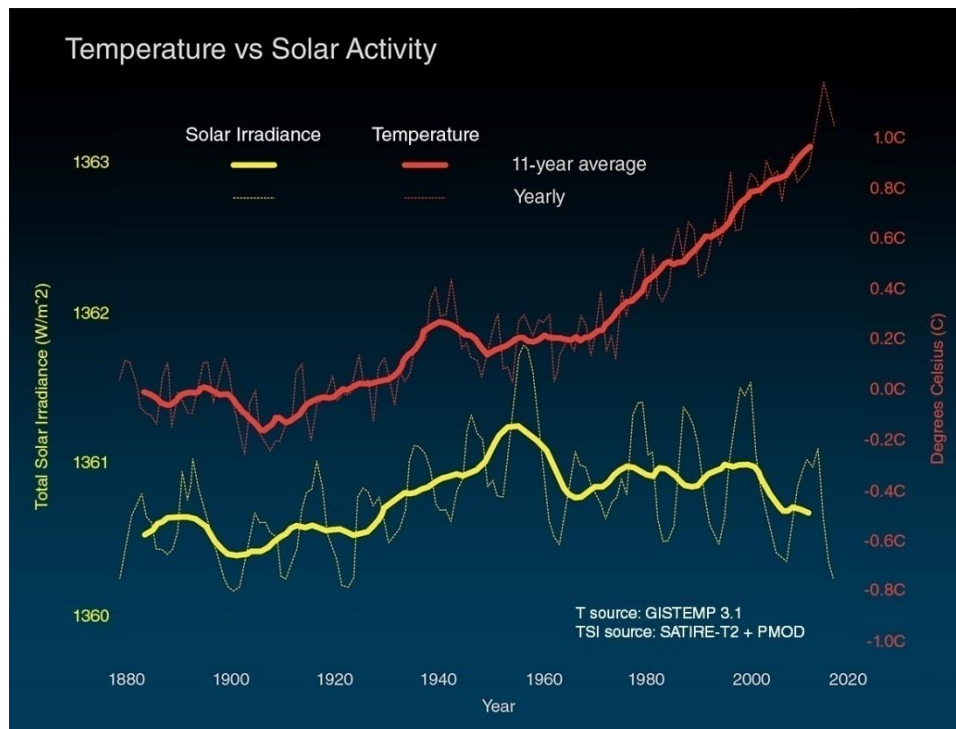


Figure 2.3. Temperature vs Solar Activity (NASA, n.d.)

## 2.2 Carbon capture, utilization and storage (CCUS)

Carbon capture and storage (CCS) is the name for the process of carbon dioxide isolation from atmosphere and gas streams in industrial and energy plants, its transportation to the sequestration facility and long-term storage in that facility (Metz et al., 2005). On the other hand, Carbon Capture and Utilization (CCU) is the process in which you utilize the captured carbon, rather than just storing it. Together both these processes are called Carbon Capture, Utilization and Storage (CCUS). CCUS is one of the most recognized methods used for the purpose of reduction in carbon dioxide emissions in the atmosphere, which is one of the main causes of climate change (Rubin et al., 2012). The process of carbon capture and storage, can also be referred as carbon sequestration, according to The United Nations Framework Convention on Climate Change (UNFCCC) (Nair, 2012). There are three main factors that trigger the interest and development in this technology. First is

realization that to prevent serious impact on global climate, significant reductions in CO<sub>2</sub> emissions are required. Second is becoming aware that just reducing the energy consumption and transferring from fossil fuels to alternative energy sources is not enough for required atmospheric CO<sub>2</sub> reductions, since 85% of world's energy supply is coming from conventional energy sources. Applying CCUS is the way to enable continuous use of conventional energy sources (fossil fuels), while decreasing the amount of CO<sub>2</sub> in the atmosphere. Third is that implementing CCUS greatly reduces the cost of climate change mitigation (IRGC, 2008; Rubin et al., 2012).

CCUS consists of several steps applied in the process: Capturing CO<sub>2</sub> from exhaust gases, pressurizing and transporting to the storage or utilization site, and finally sequestration or utilization process (Bouzalakos, 2010).

### **2.2.1 Carbon capture**

The aim of carbon capture is to produce a stream of CO<sub>2</sub> with high purity levels, which can be transported and sequestered (Jain et al., 2012; Rubin et al., 2012).

There are several technologies available for this purpose nowadays. Typically, they are presented as a purification step in processes required for obtaining useful products, such as electricity, fuels, chemicals and etc (Rubin et al., 2012). There are various approaches for CO<sub>2</sub> separation and capture, which are illustrated on Figure 2.4.

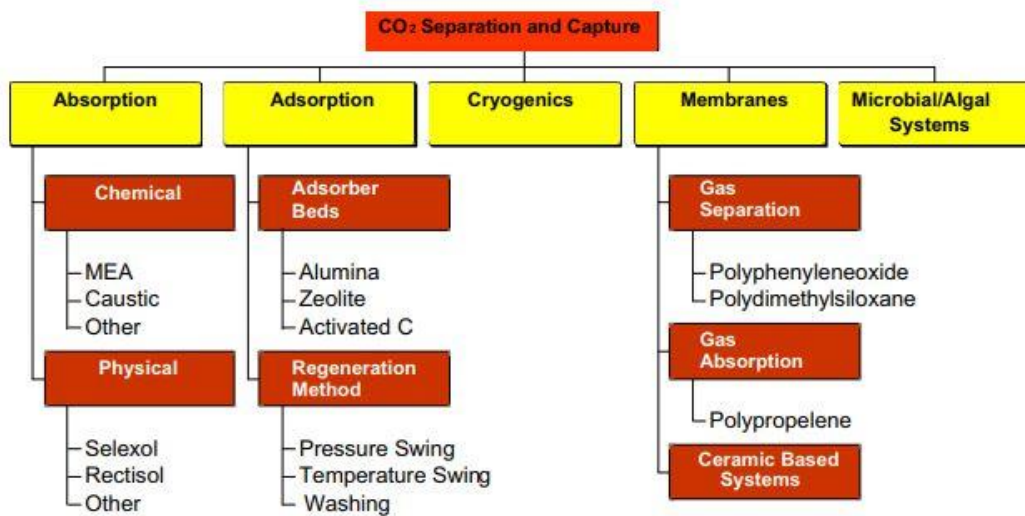


Figure 2.4. Technical options for CO<sub>2</sub> capture (Rubin et al., 2012)

Most of the CO<sub>2</sub> obtained during industrial processes is obtained as a byproduct of fossil fuel combustion, therefore it is usually classified as pre-combustion and post-combustion systems, which depends on whether the CO<sub>2</sub> is separated before or after the combustion process. Another alternative is oxy-combustion (oxyfuel) carbon capture technology, which does not require a special capture device (Rubin et al., 2012).

### 2.2.1.1 Post-combustion capture (PCC)

In the post-combustion system, the carbon dioxide is captured from the flue gases which are a by-product of fossil fuels burning process. There are several techniques that can be used for the purpose: distillation, membranes, adsorption, physical and chemical absorption (C. Soares, 2015). In coal power plant the mixture of pulverized coal (PC) and air is burned by using a furnace or boiler. Then steam generated by heat from the process above drives a turbine. The removal of the air pollutants as well as some other compounds has to be removed from the gas for further processing and carbon capture (Rubin et al., 2012).

Nowadays, post-combustion capture with implementation of amines is considered the most cost-effective method for capturing carbon dioxide of high purity with the most common method for use in coal powered power plants is using monoethanolamine (MEA), an organic solvent of amine compounds (Rubin et al., 2012; C. Soares, 2015). In absorber the chemical reaction between amine solution and flue gas is going on, which capture efficiency of up to 90%. Then, in regenerator, which is also called stripper, CO<sub>2</sub> is released from the resulting mixture, by application of required heat. Similar capture technology can also be implemented to the natural gas-fired combined cycle (NGCC) power plant (Rubin et al., 2012). This post-combustion technology based on amine capture is used in one of the biggest CCS plants in the world, namely Boundary Dam coal CCS project, based in Saskatchewan, Canada, with 1 Mt/yr capture capacity (Evans, 2014; MIT, n.d.-a).

A simplified schematic of carbon capture in PC power plant is illustrated in Figure 2.5.

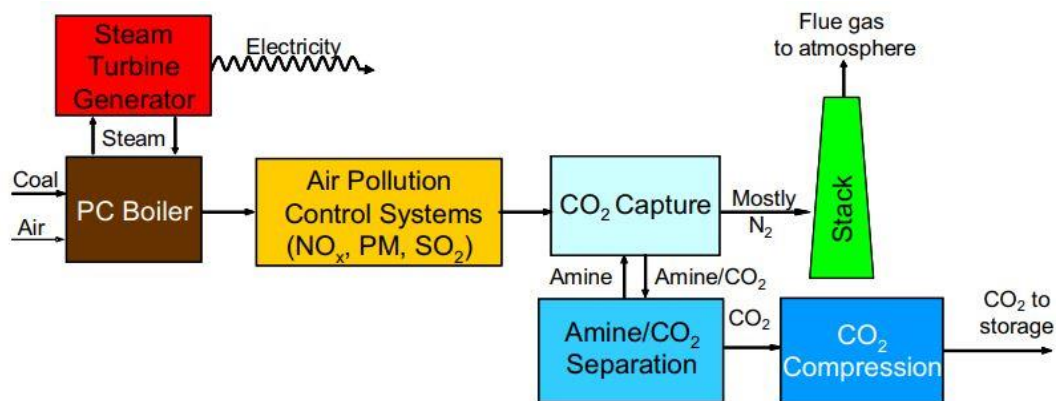


Figure 2.5. Simplified schematic of carbon capture in PC power plant (Rubin et al., 2012)

### 2.2.1.2 Pre-combustion

The removal of CO<sub>2</sub> from fuel before the process of combustion requires conversion of this fuel to the form that is suitable for carbon capture. The process used for this purpose in coal fired plants is called partial oxidation or gasification. This is done by reacting coal with steam and oxygen in high temperature and pressure conditions, where at the end synthesis gas, also called syngas - a gaseous mixture of carbon monoxide and hydrogen - is obtained. This mixture can be burned for power generation, and this method is called integrated gasification combined cycle (IGCC). Afterwards, by reacting it with steam, a two stage shift reactor converts CO to carbon dioxide, resulting in mixture of CO<sub>2</sub> and hydrogen. By utilizing a chemical solvent, CO<sub>2</sub> is captured, and the steam of hydrogen is burned for power generation (Rubin et al., 2012). The technique described is valued for the much smaller amount of fluid to be treated compared to PCC. Thus, while in post-combustion system whole flue gas at the end of the combustion has to be processed, in by implementing IGCC only the syngas is required to go through the process (C. Soares, 2015). An example for use of pre-combustion IGCC is Kemper County coal CCS project, based in Mississippi, USA, with around 3 Mt/yr capture capacity (Evans, 2014; MIT, n.d.-b). A simplified schematic of this process is shown on Figure 2.6.

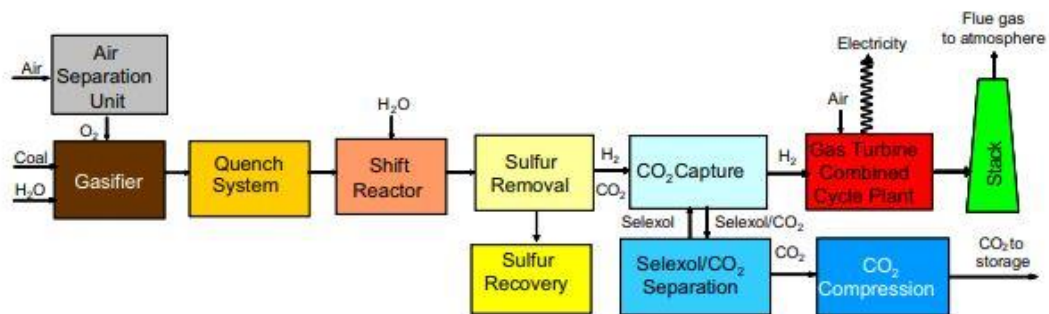


Figure 2.6. Simplified schematic of an integrated gasification combined cycle (IGCC) coal power plant with pre-combustion CO<sub>2</sub> capture using a water-gas shift reactor and a Selexol CO<sub>2</sub> (Rubin et al., 2012)

Power plants using natural gas as fuel can also use pre-combustion capture method. The process is similar to coal fired power plants. First step is to convert natural gas to syngas by reacting it with steam and oxygen, which is called reforming. Then, same as with coal, CO is converted to carbon dioxide, which is then separated from H<sub>2</sub> and captured (Rubin et al., 2012).

For coal power plants, this pre-combustion carbon capture technique, with the conversion process before combustion, is cheaper than post-combustion. On the other hand, same cannot be said for natural gas power plants (Rubin et al., 2012).

### **2.2.1.3 Oxy-combustion**

Oxy-combustion system, which is often referred as oxyfuel system, was first developed as an alternative to post-combustion capture method in coal-fired power plants. In this technique, rather than air, pure oxygen is used in combustion process. At the end of the process, resultant mixture consists of CO<sub>2</sub>, water vapor and small amounts of other pollutants. After the removal of water vapor by cooling and compressing the gas mixture, and further removal of pollutants, carbon dioxide is ready to be sent to storage facility (Rubin et al., 2012). One of the examples for oxy-combustion CCS project is White Rose (formerly UK Oxy CCS project) based in North Yorkshire, UK, with 2 Mt/yr capture capacity (90% carbon capture) (MIT, n.d.-c). A simplified schematic of this process is shown on Figure 2.7.

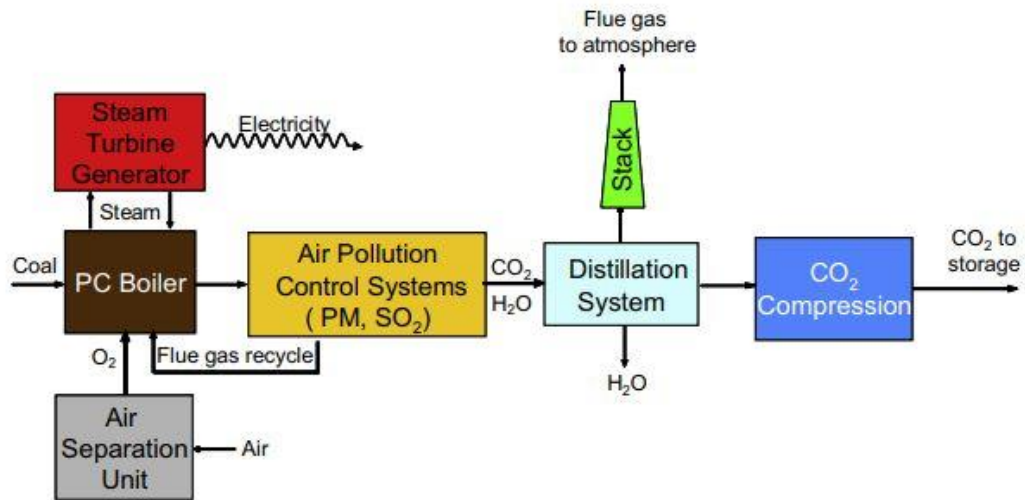


Figure 2.7. Simplified schematic of a coal-fired power plant using oxy-combustion technology (Rubin et al., 2012)

The advantage of oxyfuel system over post-combustion, is that it does not require an expensive capture technology. On the other hand, approximately three times more oxygen is required for oxy-combustion system, so, a costly air separation unit (ASU) has to be used (Rubin et al., 2012). As ASU consumes significant amount of electricity, new energy-efficient O<sub>2</sub> isolation technologies are in the development process (C. Soares, 2015). There are also some other requirements, such as additional flue gas processing to reduce conventional air pollutants amount, recycling of a portion of inert flue gas back to boiler for the purpose of maintaining operating temperatures, and proper sealing of the system in order to prevent air leakage into the flue gas (Rubin et al., 2012).

Theoretically, oxyfuel capture system can be implemented in the natural gas fired power plants, but practically, it will require a lot of modifications to the current power generation technology (Rubin et al., 2012).

## 2.2.2 Carbon utilization

Nowadays carbon dioxide utilization becomes more and more recognized with each day, since it not only reduces the amount of anthropogenic CO<sub>2</sub> in the atmosphere, but also is capable of creating economic value (Huang Chung-Sung, 2014).

Commercial benefits of CO<sub>2</sub> can be obtained either by direct use, or by conversion it into chemicals or fuels (Cuéllar-Franca & Azapagic, 2015). Direct utilization may include usage of carbon dioxide in food and drinking industry as carbonating agent, preservative and packaging gas, as physical solvent, as respiratory stimulant, and one of the most valuable uses of carbon dioxide in terms of amount, enhanced oil recovery (Alper & Yuksel Orhan, 2017; Cuéllar-Franca & Azapagic, 2015). Table 2.1 lists some of the technological (direct) uses of CO<sub>2</sub> in different industries.

Table 2.1 Technological uses of CO<sub>2</sub> (Aresta & Dibenedetto, 2010)

Technology	Application
Food industry	Additive to beverages Food packaging, dry-ice Extraction of aromas, caffeine ...
Fumigant	Antibacterial agent for cereals
Antifire	Extinguishers
Mechanical industry	Moulding, cutting, soldering
Electronics	Cleaning fluid
Dry washing	Cleaning fluid
Fluid in circuits	Air conditioning
Water treatment	pH control of process waters
Extraction	Enhanced oil recovery (EOR) Extraction of bio-oil from biomass

Another way to utilize CO<sub>2</sub> is conversion into chemicals and fuels. Carboxylation reactions can be used to produce organic compounds such as carbonates, acrylates and polymers. On the other hand, chemicals such as methane, methanol, syngas, urea and formic acid can be produced through reduction reactions. Carbon dioxide can be

also used for fuels generation by implementing various processes, such as Fischer–Tropsch process. Still, most of these processes are not suitable for long time decrease in CO<sub>2</sub> amounts, since these chemicals and fuels have short life span, and in the end used carbon dioxide is still emitted into the atmosphere. This is the precursor for further research in using CO<sub>2</sub> for synthesis of materials with longer lifespan, such as mineral carbonates, obtained through the process also called mineral carbonation (Cuéllar-Franca & Azapagic, 2015).

Mineral carbonation is the process carbonates are formed by reaction of carbon dioxide with metal oxides. Carbonates that are formed through this process can be used in construction and provide long time storage of CO<sub>2</sub> used in the process. However, this technology requires further development, since the cost of the process is high, and makes it not economically feasible (Cuéllar-Franca & Azapagic, 2015).

Using carbon dioxide for microalgae cultivation, which is being used in biofuels production, is another utilization method, that is worth mentioning. Microalgae are able to take CO<sub>2</sub> and nitrogen directly from waste streams. Unfortunately, large-scale usage of microalgae for biofuels production is not economically feasible, due to high production costs and energy requirements (Cuéllar-Franca & Azapagic, 2015).

### **2.2.3 Carbon storage**

Carbon sequestration can be described as long-term storage of CO<sub>2</sub> (Kambale & Tripathi, 2010). Various options for carbon dioxide storage are currently available. Major global pools for carbon sequestration are: geologic, terrestrial, biosphere and oceanic (Bouzalakos, 2010; Kambale & Tripathi, 2010).

There are several major properties that should be considered before CO<sub>2</sub> storage (Kambale & Tripathi, 2010):

- The storage period should be long enough for efficient reduction in carbon dioxide concentration in the atmosphere
- The overall sequestration process should be economically feasible, that is its cost should be minimized
- All precautions should be taken to minimize risk of any kind of accident
- There should be no or minimal impact on environment
- No national or international laws and regulations should be violated by the process

Basically carbon sequestration can be divided into two major groups: biotic and abiotic (Kambale & Tripathi, 2010). Figure 2.8 illustrates major classification of carbon sequestration.

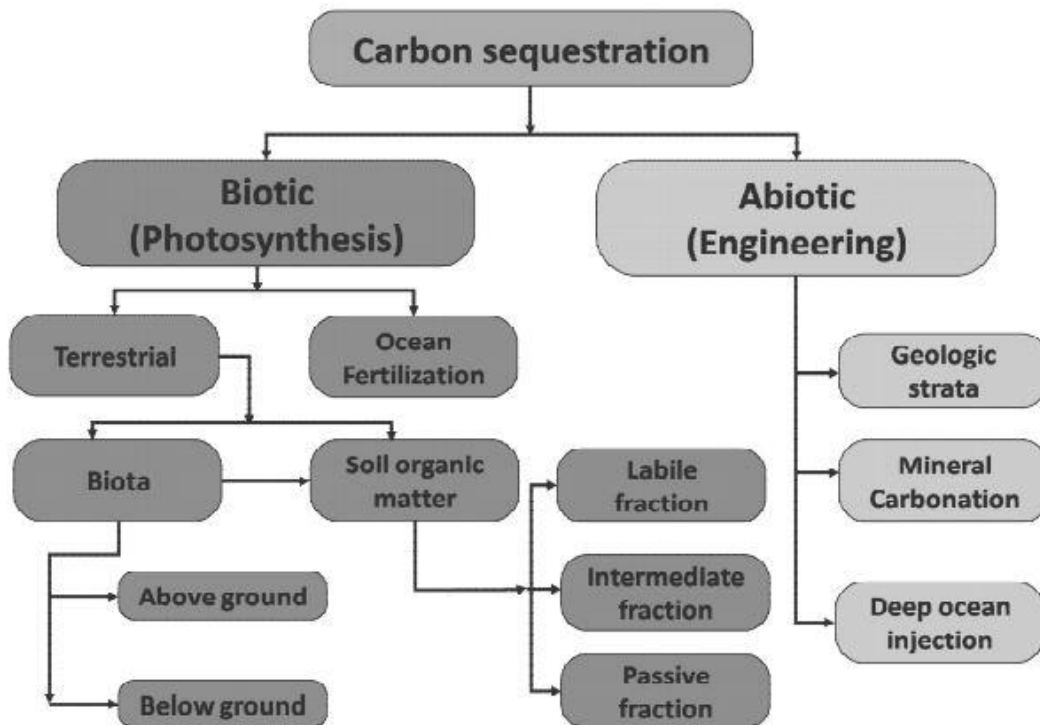


Figure 2.8. Carbon sequestration classification (Kambale & Tripathi, 2010)

Biotic carbon sequestration is based on converting carbon dioxide into sugars, carbohydrates, celluloses and lignins by the process called photosynthesis. Basically, CO<sub>2</sub> in atmosphere is sequestered in terrestrial and aquatic carbon pools (Bouzalakos, 2010). As it can be seen from the Figure 2.8, biotic sequestration can be further divided into terrestrial and ocean sequestrations, with terrestrial including its own smaller subgroups.

Abiotic carbon sequestration is CO<sub>2</sub> without any kind of biological activity involved. It includes sequestration in geological formations (geosequestration), ocean, and by mineral carbonation, which was discussed in chapter 2.2.2.

### **2.2.3.1 Terrestrial sequestration**

Terrestrial sequestration can be described as carbon storage in biomass both aboveground and belowground, and in soil carbon as soil/organic matter and inorganic carbon. These methods have the capability of storing carbon dioxide in forests and soils for centuries (Post et al., 2009). Terrestrial carbon pool is the third largest global carbon dioxide pool. It is estimated, that terrestrial pool to contain about 2850 Pg of carbon. Theoretically sequestration potential in terrestrial pool can be estimated as 6-10 Pg C/year, while the widely accepted technical potential is 3 Pg C/year (Lal, 2010).

The sequestration system described above has numerous benefits when considering ecosystem services. These can be: agronomic productivity increase, food security and water quality improvement, and biodiversity enrichment. Considering all these benefits, terrestrial carbon sequestration can be considered as a win-win method as it helps to reduce anthropogenic CO<sub>2</sub> in the atmosphere and improve the ecosystem simultaneously (Lal, 2010).

### **2.2.3.2 Ocean sequestration**

Ocean carbon pool is the largest among global pool of carbon with approximately 40,000 Pg of carbon. It is stated, that deep ocean is unsaturated when considering CO<sub>2</sub>. It has been estimated, that injecting all anthropogenic carbon dioxide, that would double the concentration in the atmosphere will increase the concentration of carbon in ocean by just 2%. It should be also noted; that ocean is not isolated from the atmosphere. Considering long time period, 1000s of years, 80% of today's anthropogenic carbon dioxide will eventually be naturally sequestered in the ocean. Implementing ocean sequestration methods will just accelerate the natural process, which will be beneficial for climate and environment (Kambale & Tripathi, 2010).

There are both biotic and abiotic methods for ocean carbon sequestration.

Biotic method is ocean fertilization with some nutrients, such as iron, to stimulate the growth of marine phytoplankton, which in result will increase the uptake of atmospheric carbon. It is assumed, what the carbon will remain in the ocean with the phytoplankton eventually sinking to the deep ocean. The experiments conducted in the ocean show, that addition of iron to the ocean increases phytoplankton biomass significantly. However, the effectiveness of this sequestration method is not proved. For effective sequestration, the carbon has to be transported to the deep ocean. Until now no experiments have been conducted to determine this transfer efficiency (Kambale & Tripathi, 2010).

Abiotic method is focused on direct injection of CO<sub>2</sub> into deep ocean. The injection depth should be at least 500 m, which corresponds to 5 MPa hydrostatic pressure and 4 °C temperature. At these conditions carbon dioxide is in liquid phase. At the depth less than 500 m, the CO<sub>2</sub> will vaporize and escape the ocean (Golomb & Pennell, 2010). At the depth between 500m and 3000 m, the density of carbon dioxide is less than the one of the seawater, which results in CO<sub>2</sub> being ascended by the buoyancy. At any depth greater than 3000 m, the carbon dioxide becomes heavier than seawater,

resulting in its dropping to the bottom of the ocean and forming a, so called, "CO<sub>2</sub> lake" (Kambale & Tripathi, 2010).

Even though there is great potential for oceanic carbon sequestration, there is strong opposition of this method by marine biologists and environmental groups. The main concern is possible acidification of large volumes of seawater because of the formation of carbonic and bicarbonic acid. Another constraint for this method are international regulations which prohibit dumping of industrial waste into the ocean, which may also include anthropogenic CO<sub>2</sub>. Several proposals have been made that could result in minimizing of acidification. However, further studies are required to determine their feasibilities (Golomb & Pennell, 2010).

### **2.2.3.3 Geosequestration**

Geosequestration, or geological sequestration, can be described as capture, transportation, and injection of carbon dioxide to underground deep rock formations for long-time storage (Metz et al., 2005). Geologic carbon pool is the second largest among global carbon sinks, with up to 10000 Pg carbon (Lal, 2010). The process of CO<sub>2</sub> storage in geological formation has been naturally going for hundreds of millions years. CO<sub>2</sub> that is produced by biological and igneous activities, and some chemical reactions is accumulated in natural underground formations in various forms (Metz et al., 2005).

There are several potential sinks for underground carbon dioxide storage: deep saline formations and aquifers, oil and gas reservoirs, and deep unmineable coal seams. At the moment, deep saline aquifers are considered to have the highest potential for sequestration, however their capacity and suitability of properties is still under discussion (Bouzalakos, 2010). On the other hand, oil and gas reservoirs are considered as the first choice for carbon dioxide injection due to the advantage provided by the possibility of combining storage with CO<sub>2</sub> enhanced oil recovery (CO<sub>2</sub>-EOR). This will result in increase in overall storage capacity and decrease in

cost of sequestration due to additional oil production (Bachu, 2010; Bouzalakos, 2010). As for the coal seams, there is potential for storage combined with enhanced methane production, but further studies of this subject are required (Bouzalakos, 2010). It should also be noted, that continental shelf and some adjacent deep-marine sedimentary basins can be considered as potential carbon storage formation, however most of these sediments are too thin and impermeable for the sequestration. There has also been some considerations of using salt caverns, basalt and shales (organic rich) for the storage (Metz et al., 2005).

#### **2.2.3.3.1 Coal seams**

Coal seams can be characterized as fractured porous media, with large internal surface area. Methane (CH<sub>4</sub>) is generated and retained in the coal formation during some geological processes are going on, in the formation of coal seams, through the process called coalification. In coal seams, gas not only fills fractures and pores, but also is adsorbed to the coal surface, and absorbed into its structure. Since adsorbed methane is of a much higher density than gas, reservoir rock has better capacity for CO<sub>2</sub> storage (Mazzotti et al., 2010).

Storage capacity of coal seams is relatively smaller compared to other geological storage pools. Still, formations promising economically feasible mining potential have been considered as possible storage sinks for carbon dioxide. Even though the worst case scenario suggests that storage potential of these reservoirs are much smaller than the one of other geological formations, compared to the current rate of anthropogenic emissions, which is approximately 30 Gt CO<sub>2</sub> /year, these amounts should still be taken into consideration as means of greenhouse effect mitigation (Mazzotti et al., 2010).

The trapping mechanisms, that are containing carbon dioxide inside the coal seams are: first, stratigraphic and structural, which is basically free phase in fractures and pores; second, hydrodynamic, which is CO<sub>2</sub> dissolved in water; and third, adsorption

on the coal surface, which is dominant during storage (Ibrahim & Nasr-El-Din, 2015).

At the moment, main approach of carbon sequestration in coal seams is enhance coalbed methane (ECBM) recovery, which results in economically profitable production from coal seams. This can be achieved by carbon dioxide injection at supercritical conditions. The method is currently being studied to improve the understanding of sorption and displacement processes. The pilot tests that were conducted have demonstrated technical feasibility of carbon dioxide injection into the coal seams, for simultaneous CH<sub>4</sub> recovery and CO<sub>2</sub> storage. However, further research is required for full realization of storage potential (Mazzotti et al., 2010).

#### **2.2.3.3.2 Deep saline aquifers**

Deep saline aquifers can be defined as underground formations filled with water. They are very important in terms of carbon sequestration, since they are widely distributed across the globe, commonly have high volumes, and are capable of storing CO<sub>2</sub> for long time periods. Due to usual high permeability values, these storage sites are capable of producing and injecting fluids at high rates. Even though, that storage capacity is often accepted as very large, there are a lot of uncertainties related to properties of the reservoir, and flow regimes (Rosenbauer & Thomas, 2010).

To evaluate potential of deep saline aquifers for storage, several factors, such as: total capacity, ease of injection, and environmental and human health risks; should be considered. Furthermore, to calculate net pore volume of the formation, create groundwater and carbon dioxide flow maps, and calculate hydrostatic potential, some physical and chemical properties have to be evaluated. Among these are: temperature and depth with regards to depth, mineralogy, grainsize, porosity and permeability, reservoir structure and thickness, composition of fluid in place, and confinement of the reservoir (Rosenbauer & Thomas, 2010).

Preferable saline formations for carbon storage are required to have a low permeability cap rock above the reservoir. It is essential, since the cap rock prevents the migration of injected CO<sub>2</sub> back to the atmosphere. Another preferable parameter is the depth that should vary between 800 m and 3000 m, where geologic parameter are most favorable for carbon dioxide storage (De Silva et al., 2015).

There are several trapping mechanisms for carbon storage in deep saline aquifers. These mechanisms can be classified into three major groups: geological trapping, geochemical trapping, and hydrodynamic trapping. Each of these groups has several trap mechanisms described in Table 2.2 (Yang et al., 2010).

Considering the future of deep saline sequestration, pilot and commercial sequestration projects, such as Snohvit, Sleipner, In Salah, Gorgon, proved that this method is technologically feasible. Still, there are several aspects, such as costs, environment, legal framework, and acceptance by people, that should be taken into account (Michael et al., 2010; Rosenbauer & Thomas, 2010).

Table 2.2 Characteristics of trapping mechanisms in saline aquifers (Yang et al., 2010)

Trapping mechanism		Characteristics		
		Nature of trapping	Capacity limitation/benefits	Potential size
Geological trapping Reservoir scale (km)	Structural and stratigraphic trapping	Buoyancy within anticline, fold, fault block, pinch-out. CO <sub>2</sub> remains below physical trap	Without hydraulic system, limited by compression of reservoir fluid. With hydraulic system, displace formation fluid	Significant
	Residual gas trapping	CO <sub>2</sub> fills interstices between pores of rock grains	Can equal 15%-20% of reservoir volume. Eventually dissolves into formation water	Very large
Geochemical trapping Well scale (cm to m)	Solubility and ionic trapping (Dissolution)	CO <sub>2</sub> migrates through reservoir beneath seal and eventually dissolves into formation water	CO <sub>2</sub> saturated water may migrate towards the basin center. Limited by CO <sub>2</sub> -water contact and favor highly permeable (vertical) and thick reservoirs	Very large
	Mineral trapping	CO <sub>2</sub> reacts with existing rock to form new stable minerals	Reaction rate is slow. Precipitation could reduce injectivity. Approaches 'permanent' trapping.	Significant trapping.
Hydrodynamic trapping Basin scale (100km)	Migration trapping	CO <sub>2</sub> migrates through reservoir beneath seal, moving with the regional flow system while other trapping mechanisms work	No physical trap may exist; totally reliant on slow transport mechanism and chemical processes. Can include all other trapping mechanisms along the migration pathway	Very large

### **2.2.3.3.3 Oil and gas reservoirs**

Currently oil and gas reservoir are main candidates for geosequestration and there are several reasons for that. First, it is known, that hydrocarbon reservoirs are capable of containing large volumes of fluids for long time periods. Second, most of the reservoirs have already been well characterized both in terms of formation rock and formation fluids. Third, the facilities and equipment that were used for hydrocarbon production can be converted to CO<sub>2</sub> injection needs, which will significantly decrease overall cost of the project. Finally, if the field is still in production phase, carbon storage can be combined with EOR applications, which will make the project even more (economically) feasible, due to additional oil production (Bachu, 2010; Le Gallo et al., 2002). It is also worth mentioning that the surface facilities created for CO<sub>2</sub>-EOR or carbon storage in hydrocarbon reservoir can be further used for later saline aquifers sequestration (Vega & Kavscek, 2010).

It is usually stated, that 800 m is the minimum required depth for CO<sub>2</sub> injection and storage in the underground geological formations. While it is true for most of the cases, shallower reservoir should not be rejected right away if other requirements, such as capacity, confinement, risks for environment and health, and social acceptance are met. While selecting storage site another important parameter that should be considered is time of availability. Some reservoirs are not suitable for carbon sequestration during the production period. Absence of strong aquifer is another criterion, that can be an advantage for the storage project. If strong aquifer support exists in the system, water will migrate to the hydrocarbon reservoir, as oil and gas are produced, consequently reducing the overall storage capacity of the pool. Same is also suitable for fields that had undergone major water and gas flooding (Bachu, 2010).

CO<sub>2</sub> has been injected into the oil reservoirs for a long time now. Even though depleted oil reservoir provides great potential for carbon storage in terms of capacity, combination of CO<sub>2</sub>-EOR and sequestration is preferred for economical reasons.

There are several aspects that should be considered before simultaneous CO<sub>2</sub>-EOR and storage. First, it is reservoir seals' integrity. Overpressurization of pore fluid may result in damage to the reservoir barriers. Some other risks are related to the integrity of old wells' barriers such as casings and cement plugs. Studies should be conducted prior to injection to prevent leakage through fractures in the barriers (Vega & Kovscek, 2010).

Common practice for CO<sub>2</sub>-EOR is water alternating gas (WAG) injection, which alternated water and carbon dioxide injection in sequential way. However, this method is not suitable for EOR-storage co-optimization, since large water volume injection significantly reduces the capacity of the reservoir. For proper co-optimization of these processes it is required to reduce injected water amount as much as possible and establish high quality well control to prevent back production of injected gas. Simulation conducted by Kovscek and Cakici (2005) shows that in terms of oil recovery both immiscible CO<sub>2</sub>-EOR and WAG are similar. However, the capacity for storage is much higher with immiscible carbon dioxide injection. They have also shown that miscible CO<sub>2</sub> injection can provide same storage volume as immiscible (Vega & Kovscek, 2010).

As for natural gas reservoirs, there have not been any significant CO<sub>2</sub> injections. However, studies show that production acceleration can be achieved by reservoir re-pressurization while carbon dioxide injection. The advantage of carbon dioxide flooding in natural gas reservoirs, is that injected gas is denser and more viscous than the fluid in place, enabling uniform sweeping (Vega & Kovscek, 2010).

Carbon sequestration in unconventional oil and gas reservoirs is a point of interest for current sequestration studies. Conducted laboratory tests show that immiscible CO<sub>2</sub> injection into the unconventional shale rock formation is technically feasible to be used as enhanced oil production tool, which leads us to possible future storage sites (Vega & Kovscek, 2010).

### 2.3 CO<sub>2</sub>-EOR

Enhanced oil recovery (EOR) can be defined as additional oil production due to injection of materials that are not initially present in the hydrocarbon reservoir. Major EOR methods can be classified into four groups: chemical, gas injection, thermal, and other, relatively new, EOR techniques (Ganzer & Reinicke, 2017). Figure 2.9 displays classification of commonly used EOR methods.

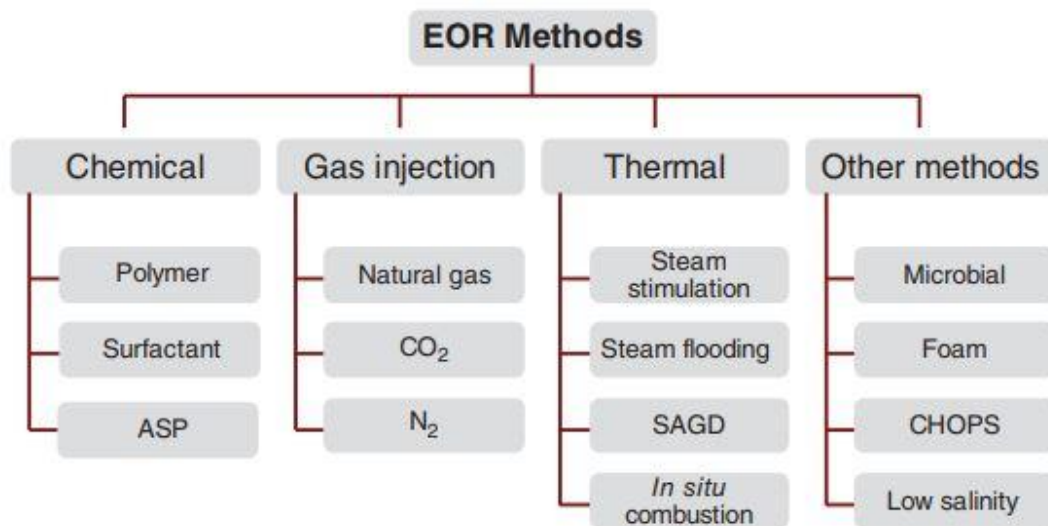


Figure 2.9. EOR Methods (Ganzer & Reinicke, 2017)

Gas injection methods are widespread as means of oil recovery improvement. One of the most popular gas used in this process is carbon dioxide. The reasons for increased interest in usage of this gas are (Ganzer & Reinicke, 2017):

- CO<sub>2</sub> is very advantageous in terms of miscibility
- CO<sub>2</sub> demonstrates advantageous phase properties compared to other gases
- CO<sub>2</sub> injection can be used as climate change mitigation method

Carbon dioxide flooding can be included in both secondary and tertiary recovery phases of oil production, with immiscible and miscible flooding respectively (Hamouda & Chughtai, 2018).

### **2.3.1 Miscible CO<sub>2</sub>-EOR**

When miscible fluids mix, they become indistinguishable. There is no interfacial tension between two fluids, the mixture is not affected by rock wettability or relative permeability. Usually miscible flooding can achieve almost 100% microscopic recovery efficiency in case when there is no water (Vega & Kavscek, 2010).

During miscible flooding, usage of CO<sub>2</sub> is far more advantageous comparing to other gases due to its low minimal miscible pressure (MMP), which enables CO<sub>2</sub>-oil miscibility development to be dynamic at relatively low pressures. Thanks to high density, low viscosity properties of carbon dioxide in reservoir conditions, which is called supercritical, injection of the gas is easy, while the capacity to extract hydrocarbons from oil phase remains high (Ganzer & Reinicke, 2017).

There are two miscible displacement processes available for miscible system (Vega & Kavscek, 2010):

1. First-contact miscible (FCM) displacement - CO<sub>2</sub> forms a single phase with formation fluid at first contact.
2. Multiple-contact miscible (MCM) displacement - Miscibility developed in reservoir formation due to changes in composition in both gas phase and reservoir oil while the move through the reservoir.

Usually miscibility during carbon dioxide flooding is developed by MCM displacement (Vega & Kavscek, 2010). There are several processes going on in the reservoir during the miscible displacement. First, injected carbon dioxide is vaporizing intermediate and higher molecular weight hydrocarbons (vaporization gas-drive process), then some part of the injected gas dissolves in the reservoir fluid

(condensation gas-drive process). This transfer between CO<sub>2</sub> and oil molecules helps oil and gas become completely miscible and creates a transition zone along the flow path (Verma, 2015). Figure 2.10 illustrated the process described above.

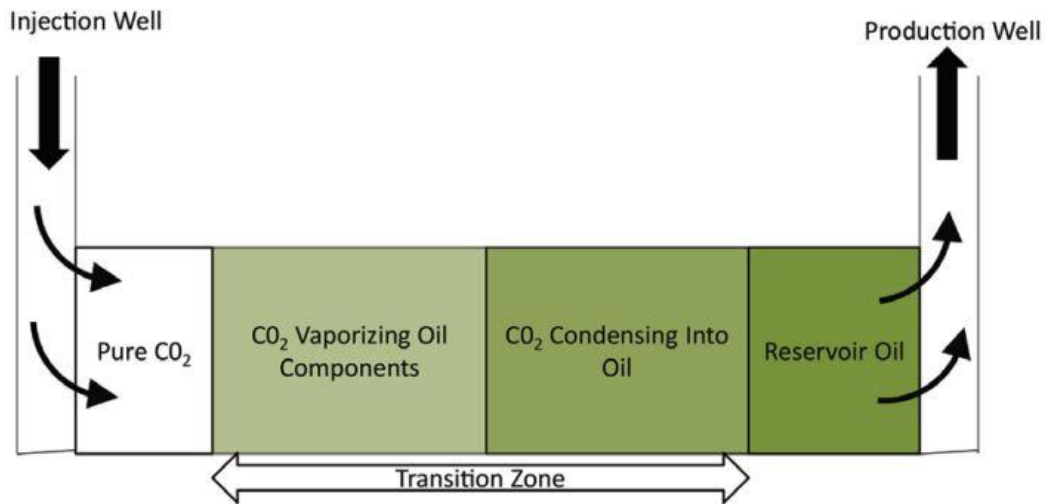


Figure 2.10. The schematic of the CO<sub>2</sub> (carbon dioxide) miscible process showing the transition zone between the injection and production well (Verma, 2015)

Two main strategies for miscible flooding optimization are commonly used: 1) continuous CO<sub>2</sub> injection (CCO<sub>2</sub>); 2) CO<sub>2</sub> water-alternating gas (CO<sub>2</sub>-WAG). Several studies have been conducted in order to determine which of these two strategies is more feasible. It was concluded, that CO<sub>2</sub>-WAG is far more efficient in terms of oil recovery compared to CCO<sub>2</sub> (Bhatti et al., 2019).

There is one problem associated with miscible CO<sub>2</sub> flooding, which is asphaltene precipitation. Even in low amounts it is capable of hindering fluid flow and reducing mobility. It is more common for light oil reservoirs. It starts with solid particles coming out of solution, after which these particles join, grow, which finally may lead to formation damage by blocking flow paths (Perera et al., 2016).

### 2.3.1.1 Minimum Miscible Pressure

There are various methods to determine minimum miscibility pressures. The most precise and reliable is considered to be slim-tube tests. However, these tests, performed in a laboratory, are often considered expensive, that is why mathematical models and correlations are often used as alternatives (Verma, 2015). As for the difference between these two alternatives, correlations are easy to perform, however, compared to mathematical models, they provide worse results and are less precise (Verma, 2015).

One of the correlations, that can be used for this specific task, was derived by Holm and Josendal (Holm & Josendal, 1974). By using it with extensions by Mungan (Mungan, 1981) or correlations by Lasater (Lasater, 1958) which are used to determine C5+ components' molecular weight, MMP can be determined with a high precision for a correlation (Verma, 2015).

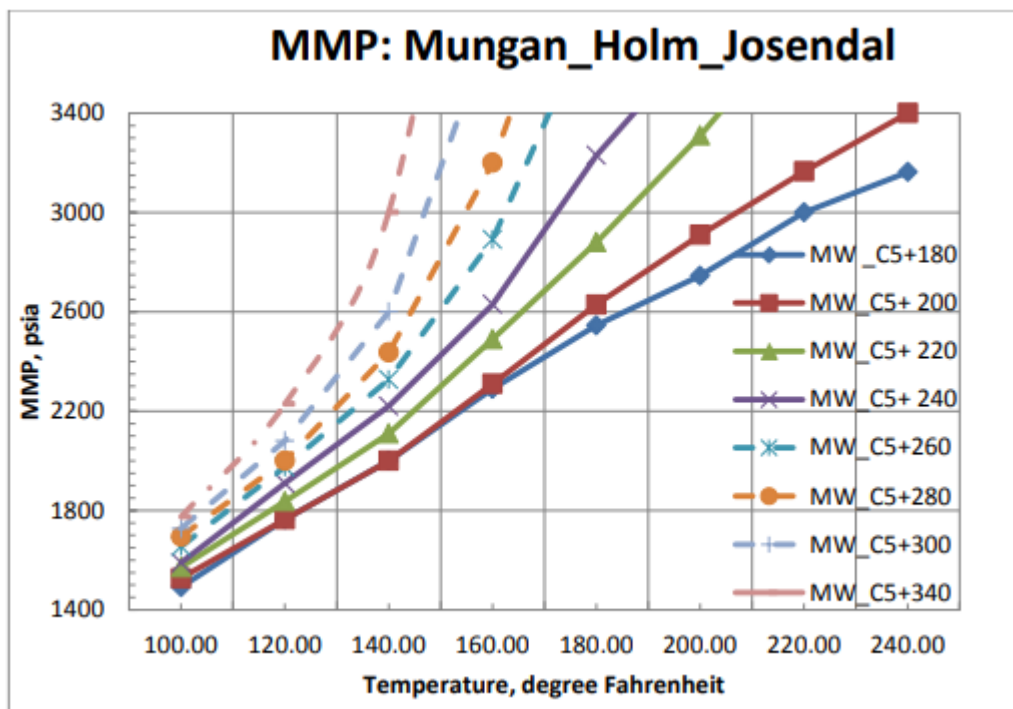


Figure 2.11. Correlation of Minimum Miscibility Pressure with C5+ Molecular Weight and reservoir temperature (Mungan, 1981; Verma, 2015).

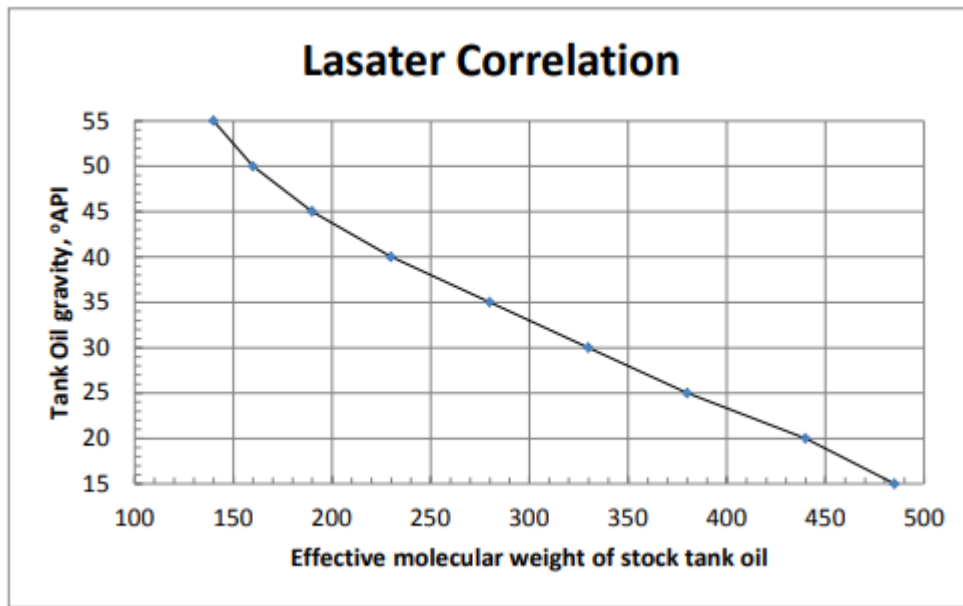


Figure 2.12. Lasater correlation relating the molecular weight of C5+ components with oil gravity (Lasater, 1958; Verma, 2015).

### 2.3.2 Immiscible CO<sub>2</sub>-EOR

Even though miscible CO<sub>2</sub> flooding is considered very effective, there are some limitations to its application, such as high pressure requirements for miscibility of oil and CO<sub>2</sub>, high geological dip for displacement front stabilization, and requirement for reservoir fluid to be light, which is high API gravity and low viscosity. These limitations are precursors for immiscible carbon dioxide flood studies, since it is not affected much by these restrictions (Al-Bayati et al., 2018).

In immiscible flooding there is sharp interface between all the phases in the formation, which makes their presence clearly evident. Two major factors that should be considered during immiscible CO<sub>2</sub> injection are interfacial tension (IFT) between phases and wettability of the reservoir rock (Vega & Kovscek, 2010). In this method the increase in oil recovery is mainly governed by low IFT values between two phases. Low IFT values lead to decrease in capillary forces which are

responsible for trapping of oil phase. Rock wettability, which is another factor in immiscible flooding, in combination with pore size distribution in the formation are also controlling factors for capillary forces (Al-Bayati et al., 2018). Fluid flow during this process is mainly dominated by the balance of capillary and gravity forces. The limiting factors for oil ultimate recovery in immiscible carbon dioxide flooding are volumetric sweep, displacement efficiency, and solubility of CO<sub>2</sub> in formation fluid, which is responsible for reduction in oil viscosity and density. There are several problems that have a possibility of being encountered and affect the factors mentioned above. For example, reservoir heterogeneity may lead to poor sweep efficiency by causing gravity override; viscous fingering, which is also affected by mobility ratios, and can cause bypassing the oil and early gas breakthrough; and unstable pressure distribution (Al-Bayati et al., 2018; Vega & Kavscek, 2010).

Some immiscible tests on cores have been conducted, which showed 0-10% of incremental oil recovery during countercurrent injection of CO<sub>2</sub> and around 18-35% for concurrent injection. The results of these tests show that regardless of the possible problems and limitations of immiscible flood discussed in this chapter, this method is able to be technically feasible, and to be used for carbon geosequestration (Vega & Kavscek, 2010).

### **2.3.2.1 CO<sub>2</sub> solubility in oil**

There are several major factors influencing solubility of carbon dioxide in oil. So, as rule of thumb, solubility of CO<sub>2</sub> increases with increasing pressure and API gravity, while decreases with temperature. Furthermore, if reservoir temperature is less than critical carbon dioxide temperature (T<sub>c</sub>, CO<sub>2</sub> = 88°F) oil composition and liquefaction pressure also have effect on solubility (Emera & Sarma, 2007). As with increasing solubility of carbon dioxide oil viscosity drops, CO<sub>2</sub> injection in super-critical conditions are more efficient than below critical temperature condition (Perera et al., 2016).

There are correlations for determining carbon dioxide solubility, oil swelling and oil viscosity, developed by Emera and Sarma (Perera et al., 2016).

So, for super-critical conditions, the CO<sub>2</sub> solubility can be determined using the following correlation:

$$\text{CO}_2 \text{ Solubility } \left( \frac{\text{mol}}{\text{mol}} \right) = 2.238 - 0.33y + 3.23y^{0.6474} - 4.8y^{0.25656} \quad (2.1)$$

$$\text{With } y = \gamma \left( \frac{T^{0.8}}{P_s} \right) \exp \left( \frac{1}{MW} \right) \quad (2.2)$$

As for the sub-critical conditions, the correlation is as follows:

$$\text{CO}_2 \text{ Solubility } \left( \frac{\text{mol}}{\text{mol}} \right) = 0.033 - 1.14y - 0.7716y^2 + 0.217y^3 - 0.02183y^4 \quad (2.3)$$

$$\text{With } y = \gamma \left( \frac{P_s}{P_{\text{liq}}} \right) \exp \left( \frac{1}{MW} \right) \quad (2.4)$$

$\gamma$  is the oil specific gravity (oil density at 15.6 °C), T is the temperature (F), P<sub>s</sub> is the saturation pressure (psi), P<sub>liq</sub> is the CO<sub>2</sub> liquefaction pressure at the specified temperature (psi), MW is the oil molecular weight, and  $\mu_i$  is the initial dead oil viscosity at the specified temperature (cp).

### 2.3.2.2 Oil swelling

Usually oil swelling is determined by using the following equation:

$$\text{Oil swelling factor} = \left( \frac{\text{Saturated CO}_2 \text{ volume at current T}}{\text{Oil volume at current T}} \right) \quad (2.5)$$

In addition to carbon dioxide solubility, oil molecules' size has effect on oil swelling (Perera et al., 2016).

Apart from equation 2.5, following correlations can be used to determine oil swelling factor (Emera & Sarma, 2007):

Molecular weight of hydrocarbon higher or equal to 300:

$$\text{Swelling factor} = 1 + 0.3302y - 0.8417y^2 + 1.5804y^3 - 1.074y^4 + 0.0318y^5 - 0.21755y^6 \quad (2.6)$$

Molecular weight of hydrocarbon lower than 300:

$$\text{Swelling factor} = 1 + 0.48411y - 0.9928y^2 + 1.6019y^3 - 1.2773y^4 + 0.48267y^5 - 0.06671y^6 \quad (2.7)$$

$$\text{With } y = 1000 \left\{ \left( \frac{\gamma}{MW} \right) [\text{CO}_2 \text{ solubility}]^2 \right\}^{\exp\left(\frac{\gamma}{MW}\right)} \quad (2.8)$$

$\gamma$  is the oil specific gravity (oil density at 15.6 °C) and MW is the oil molecular weight.

### 2.3.2.3 Oil viscosity

In addition to carbon dioxide solubility, oil viscosity during Immiscible-CO<sub>2</sub> EOR is dependent on pressure. So, as saturation pressure increases, viscosity decreases until the pressure reaches liquefaction value, after which it starts to rise as the result of pressure and oil compressibility (Emera & Sarma, 2007).

Following equation can be used to determine oil viscosity during Immiscible-CO<sub>2</sub> EOR:

$$\text{Oil viscosity} = y\mu_i - 10.8 \left( \frac{\text{CO}_2 \text{ solubility}}{\mu_i} \right) \quad (2.9)$$

$$\text{With } y = x^{-0.74} \text{ and } x = \left[ \mu_i \left( \frac{P_s}{\mu_i} \right)^{0.2} \right]^{\frac{\gamma}{\text{CO}_2 \text{ solubility}}} \quad (2.10)$$

$P_s$  is the saturation pressure (psi), and  $\mu_i$  is the initial dead oil viscosity at the specified temperature (cp).

## CHAPTER 3

### STATEMENT OF THE PROBLEM

The concentration of CO<sub>2</sub> in the atmosphere has been increasing rapidly for the past century due to high anthropogenic gas emissions. This increase has an adverse effect on environment and leads to global warming. One way of climate change mitigation is carbon sequestration in geological formations, particularly in oil reservoirs.

History of carbon dioxide injection into oil reservoirs lasts for several decades. However, the operations in petroleum sector are being carried out in a way to maximize the recovered oil while keeping the amount of CO<sub>2</sub> injected at its minimum due to the cost of purchase of carbon dioxide. On the other hand, full scale implementation of carbon storage is expensive, which leads to economic restrictions in the implementation phase. To overcome this problem, and make carbon sequestration more appealing, it is necessary to change the way operations are conducted in petroleum sector, by simultaneously maximizing economic oil recovery and the volumes of CO<sub>2</sub> injected and stored in oil reservoirs by using an engineering approach. This process is named as co-optimization.

This study is focused on evaluation of different methodologies that can be applied to recover as much oil as possible while increasing injected CO<sub>2</sub> amounts at the same time. So, parameters, such as injection well pattern, pattern area, CO<sub>2</sub> injection rate, injection zone, and evaluating WAG injection, their effects on both hydrocarbon recovery and CO<sub>2</sub> storage have been observed and analyzed. Reservoir simulation studies have been performed with different scenarios in order to find the co-optimized processes in heavy oil fields. CMG's IMEX in combination with Builder and Results is used to carry out modeling and simulation.



## CHAPTER 4

### METHODOLOGY

This study uses numerical modeling to understand how various reservoir development and carbon sequestration strategies affect both HC production and CO<sub>2</sub> deposition and to conclude which ones are more suitable for production, sequestration or technical optimum between the two. The reservoir modeling and development simulations are done using CMG's Black Oil and Unconventional Simulator called IMEX.

#### 4.1 CMG IMEX and Pseudo-Miscible Model

IMEX is CMG's, black oil simulator. It is capable of modeling reservoirs of various structural complexity, different grid sizes and types, and various fluid types. It is able to use either combination of implicit and explicit calculating methods or just implicit for faster calculations. In combination with Builder, it is a user friendly modeling/simulating software which is often used for simulating unconventional reservoirs, and both secondary and tertiary recovery of hydrocarbons. (CMG, 2019).

One of the precursors for using IMEX black oil simulator in this study, is its ability to simulate pseudo-miscible solvent injection, which in our case is CO<sub>2</sub>. Main advantage of this option is no requirement for chemical analysis of reservoir fluids in terms of composition(Computer Modelling Group, 2018) thus making this method faster and more efficient than compositional simulations (Hughes, 2010). This simulating method was developed by Todd and Longstaff in 1972 to simulate miscible displacement by using black oil model without requirement for detailed compositional analysis of the fluids. The mixing parameter ( $\omega$ ) which represents the mixing of fluids with 0 being fully immiscible and 1 fully miscible(Todd & Longstaff, 1972).

Using pseudo-miscible model requires modifications to several equations which include: relative permeability, viscosity, density, capillary pressure.

$$k_{rp}^{eff} = \frac{\omega_{o(P)}}{\omega_{o\ max}} k_{rp}^m + \left(1 - \frac{\omega_{o(P)}}{\omega_{o\ max}}\right) k_{rp}^{Im} \quad (4.1)$$

Where:

p = oil, solvent, gas

$$\text{Miscible portion of effective relative permeability: } k_{rp}^m = F_p^m k_{row}(S_w) \quad (4.2)$$

With  $F_p^m$  being a partitioning function for  $k_{row}(S_w)$  based on each hydrocarbon's phase weighted saturation.

Immiscible portion of effective relative permeability:

$$k_{rp}^{Im} = k_{ro}(S_w, S_L) \quad (4.3)$$

With  $S_L = S_o + S_w$ ,  $k_{ro}$  = immiscible three phase relative permeability and p = oil.

$$k_{rp}^{Im} = F_p^{Im} k_{rg}(S_g + S_{sol}) \quad (4.4)$$

With  $F_p^{Im}$  being a partitioning function for  $k_{rg}(S_g + S_{sol})$  based on gas and solvent's saturations

As for the Miscible and Immiscible Partitioning Functions ( $F_p^m$  and  $F_p^{Im}$  accordingly), they are calculated as follows:

$$F_o^m = \frac{\omega_o^{frac} S_o^*}{\omega_o^{frac} S_o^* + \omega_g^{frac} S_g + \omega_{sal}^{frac} S_{sol}} \quad (4.5)$$

$$S_o^* = S_o - S_{orm}(S_w) \quad (4.6)$$

$$F_g^m = \frac{\omega_g^{frac} S_g}{\omega_o^{frac} S_o^* + \omega_g^{frac} S_g + \omega_{sal}^{frac} S_{sol}} \quad (4.7)$$

$$F_{sol}^m = 1 - F_o^m - F_g^m \quad (4.8)$$

Where p = solvent, gas, oil

$$\omega_p^{frac} = \frac{\omega_p}{\omega_p \max} \quad (4.9)$$

( $\omega_o$  depends on pressure and  $\omega_p \max$  is maximum value of  $\omega_p$ )

$\omega_{sol}^{frac}$  is a function of several gas/oil parameters and is calculated as follows:

$$\omega_{sol}^{frac} = \left( \frac{\omega_o^{frac} S_o^*}{\omega_o^{frac} S_o^* + \omega_g^{frac} S_g} \right) \omega_o^{frac} + \left( \frac{\omega_g^{frac} S_g}{\omega_o^{frac} S_o^* + \omega_g^{frac} S_g} \right) \omega_g^{frac} \quad (4.10)$$

$$F_g^{lm} = \left( \frac{S_g}{S_g + S_{sol}} \right) \quad (4.11)$$

$$F_{sol}^{lm} = 1.0 - F_g^{lm} \quad (4.12)$$

Oil and gas capillary pressure equations is modified as follows:

$$P_{cog}^{eff} = \frac{\omega_o}{\omega_o \max} P_{cog}(S_g) + \left( 1 - \frac{\omega_o}{\omega_o \max} \right) P_{cog}(S_g + S_{sol}) \quad (4.13)$$

The modified equations for mixture densities, which are based on pure component densities are as follows:

$$\rho_p^{eff} = \omega_p \rho_p^m + (1 - \omega_p) \rho_p^{lm} \quad (4.14)$$

p = gas, oil, solvent

$$\rho_o^m = \left( \frac{S_o^*}{S_o^* + S_{sol}} \right) \rho_o + \left( \frac{S_{sol}}{S_o^* + S_{sol}} \right) \rho_{sol} \quad (4.15)$$

$$\rho_g^m = \left( \frac{S_g}{S_g + S_{sol}} \right) \rho_g + \left( \frac{S_{sol}}{S_g + S_{sol}} \right) \rho_{sol} \quad (4.16)$$

$$\rho_{sol}^m = \left( \frac{\omega_o S_o^*}{\omega_o S_o^* + \omega_g S_g + \omega_{sol} S_{sol}} \right) \rho_o + \left( \frac{\omega_g S_g}{\omega_o S_o^* + \omega_g S_g + \omega_{sol} S_{sol}} \right) \rho_g + \left( \frac{\omega_{sol} S_{sol}}{\omega_o S_o^* + \omega_g S_g + \omega_{sol} S_{sol}} \right) \rho_{sol} \quad (4.17)$$

$$\omega_{sol} = \left( \frac{\omega_o S_o^*}{\omega_o S_o^* + \omega_g S_g} \right) \omega_o + \left( \frac{\omega_g}{\omega_o S_o^* + \omega_g S_g} \right) \omega_g \quad (4.18)$$

$\rho_p^{Im}$  = pure component densities with  $S_o^* = S_o - S_{orm}(S_w)$

The modified equations for mixture viscosities, which are based on  $1/4$  power fluid mixing rule are as follows:

$$\mu_p^{eff} = (\mu_p^m)^{\omega_p} x (\mu_p^{Im})^{(1-\omega_p)} \quad (4.19)$$

With p = solvent, oil or gas

$$\mu_o^m = \& \frac{\mu_o \mu_{sol}}{\left( \left( \frac{S_o^*}{S_o^* + S_{sol}} \right) \mu_{sol}^{1/4} + \left( \frac{S_{sol}}{S_o^* + S_{sol}} \right) \mu_o^{1/4} \right)^4} \quad (4.20)$$

$$\mu_g^m = \& \frac{\mu_g \mu_{sol}}{\left( \left( \frac{S_g}{S_g + S_{sol}} \right) \mu_{sol}^{1/4} + \left( \frac{S_{sol}}{S_g + S_{sol}} \right) \mu_g^{1/4} \right)^4} \quad (4.21)$$

$$\mu_{sol}^m \& = \frac{\mu_g \mu_{sol} \mu_o}{\left( \frac{\omega_o S_o^*}{S_n} \right) \mu_{sol}^{1/4} \mu_g^{1/4} + \left( \frac{\omega_g S_g}{S_n} \right) \mu_o^{1/4} \mu_{sol}^{1/4} + \left( \frac{\omega_{sol} S_{sol}}{S_n} \right) \mu_o^{1/4} \mu_g^{1/4}} \quad (4.22)$$

With:

$$\omega_{sol} = \left( \frac{\omega_o S_o^*}{\omega_o S_o^* + \omega_g S_g} \right) \omega_o + \left( \frac{\omega_g S_g}{\omega_o S_o^* + \omega_g S_g} \right) \omega_g \quad (4.23)$$

$$S_n = \omega_o S_o^* + \omega_g S_g + \omega_{sol} S_{sol} \quad (4.24)$$

$$S_o^* = S_o - S_{orm}(S_w) \quad (4.25)$$

$\mu_p^{Im}$  = pure component viscosities.

For Mixing Parameter estimation above Minimum Miscibility Pressure (MMP) Computer Modelling Group Recommends using Koval formula, which will represent realistic peak value for  $\omega_o$ :

$$\omega_o = 1 - 4 \log(0.78 + 0.22 M^{1/4}) / \log(M) \quad (4.26)$$

$$\text{At reservoir conditions: } M = \mu_{oil} / \mu_{sol} \quad (4.27)$$

For the gas mixing parameter, it is recommended to use  $\omega_g$  equal or greater than oil mixing parameter. Same equation can be used for calculation with  $M = \mu_{sol} / \mu_{gas}$ .

## 4.2 Optimized Properties

Several properties were selected to be optimized in the study conducted.

Firstly, the well pattern was selected. This influenced the ratio of production vs injection wells and how they are positioned relative to each other. This parameter has effect on the sweep efficiency of the injected fluid and thus overall recovery factor of the field.

Second parameter to be optimized was well pattern area, which is the area covering all the wells in the pattern. When implemented to the whole field, pattern area influences the distance and overall number of wells used for the field development. These parameters have significant impact on CO<sub>2</sub> breakthrough to the production wells, thus influencing the amount of carbon dioxide stored at the end of simulation period.

Another parameter to be optimized was injection rate. This is a critical parameter for the study, since it not only influences the amount of carbon dioxide sequestered, but also oil recovery, as the amount of CO<sub>2</sub> affects its sweep efficiency.

Injection into different fluid bearing zones was also considered as injection into oil or water zones can have different effects on both parameters to be co-optimized in this study.

Finally, WAG injection method was analyzed for the purpose of co-optimization. Intermittent water injection can have effect on overall CO<sub>2</sub> amount stored, since water slugs can prevent early breakthrough of the carbon dioxide. These slugs can also influence the sweep efficiency, thus analyzing WAG effect can be critical for CO<sub>2</sub> sequestration and EOR co-optimization.



## CHAPTER 5

### NUMERICAL MODELING AND SIMULATIONS

#### 5.1 Model construction

CMG IMEX was used to simulate CO<sub>2</sub> sequestration in heavy oil field. Bati Raman field's properties were used as base for the model. All the publically available information was used for model construction, with some assumptions being made, when no data was available. It should be noted, that the simulations described in this work do not represent actual simulation for Bati Raman or any other specific field, and just used for study of CO<sub>2</sub> sequestration in general heavy oil field.

##### 5.1.1 Bati Raman field

Containing 1.85MMM bbl of original oil in place, Bati Raman field is considered to be the biggest oil field in the Republic of Turkey, which was discovered in 1961(Babadagli et al., 2008).

Dominant producing formation is a very heterogeneous limestone of Cretaceous age with gross thickness of 64m. The size of the field is around 17km long and 2-4 km wide, with structural trap asymmetric anticline. Porosity of the field is indicated as 18% average. Bati Raman is a dual permeability formation, with primary permeability ranging between 10mD and 100mD, and secondary permeability going as high as 2 Darcies, which is indicated by well testing(Babadagli et al., 2008; Sahin et al., 2012).

Bati Raman oil is considered to be extremely heavy and viscous with API gravities ranging from 9° to 15° and viscosity from 450 to 1000cp in some parts of the field. Due to low solution gas-oil ratio the bubble point pressure is also very low (160psi).

Original reservoir pressure and temperatures were 1800psi at 2067ft and 150° F at 1640ft respectively(Sahin et al., 2012).

Primary recovery of the reservoir resulted in just about 1.7% of initial oil in place being produced. As a result EOR methods have been implemented. Between 1971 and 1978 waterflooding was performed in the field. Even though there was a significant increase in recovery factor, it was calculated that overall recovery will be increased to a maximum value of 5% with this technique (Babadagli et al., 2008).

After extensive studies for finding the most efficient method for oil recovery in Bati Ramant field, immiscible CO<sub>2</sub> injection started in 1986 and continued for several decades. Due to very high MMP compared to reservoir pressure, as injection continued, RF was increasing only due to oil swelling, viscosity reduction, gas diffusion into oil, interfacial tension reduction, and overall pressure support to the reservoir. As the result of the full scale CO<sub>2</sub> injection, the production rate of 14000 bbl/d was achieved, with overall 352.8 Bscf of carbon dioxide injected (Sahin et al., 2012).

#### **5.1.1.1 Model geometry and grid**

A simple three-dimensional Cartesian model was created using dimensions from Bati Raman as reference. Due to educational license limitation of CMG IMEX, number of total grid blocks in model was limited by 50000. Considering this limitation, the model created has total of 49560 blocks with distribution of 118 x 21 x 20 per X, Y and Z axis respectively. The grid dimensions are as following: 473 ft per grid block in X direction, 469 ft in Y direction, and 21 ft per grid block in Z direction. Overall grid dimensions are 55774 ft x 9843 ft x 420 ft.

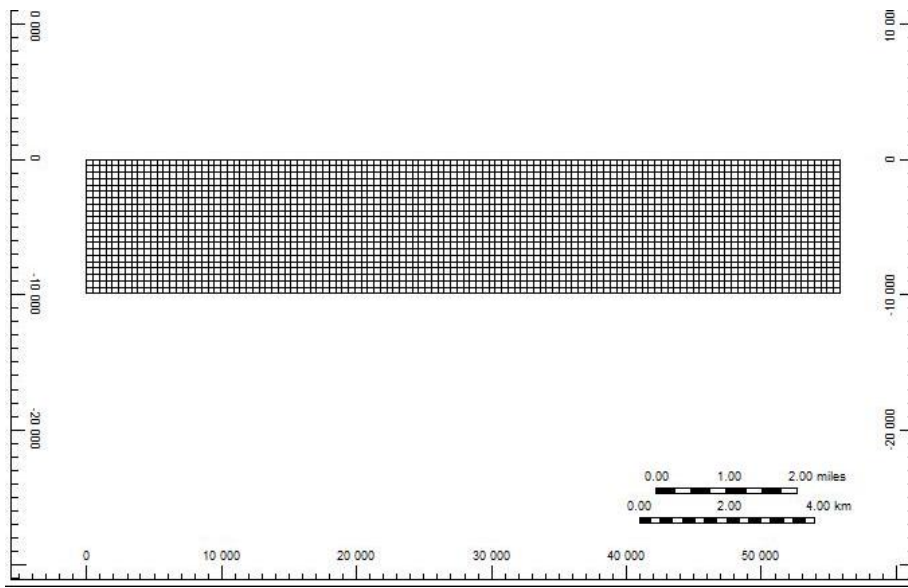


Figure 5.1. X-Y view (top) of the model

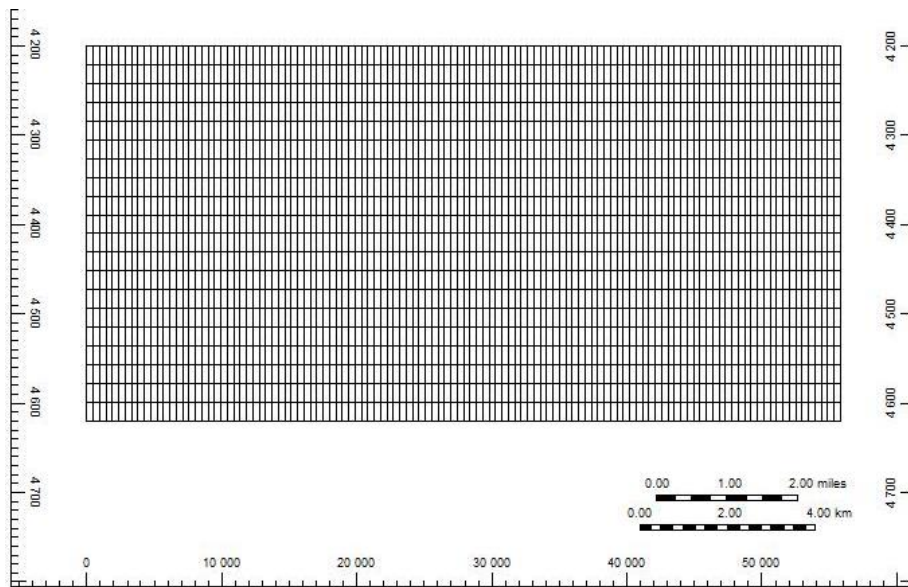


Figure 5.2. X-Z view of the model

### 5.1.1.2 Reservoir rock and fluid properties

Reservoir rock properties used for the simulation are shown in the Table 5.1:

Table 5.1 Reservoir rock properties

Parameter	Value
Porosity (%)	18
Matrix Permeability in X direction (mD)	60
Matrix Permeability in Y direction (mD)	60
Matrix Permeability in Z direction (mD)	6
Net Pay Thickness per grid block (ft)	16.5
Bubble point pressure (psi)	174.7
Oil Saturation (%)	79
Initial Pressure (psi)	1864.7
Water Saturation (%)	21
Rock Compressibility (1/psi)	0.00000381
Temperature (F)	160

By using Bati Raman oil density of 61.4963 lb/ft<sup>3</sup> solubility, viscosities, relative permeability, and capillary pressures were generated using correlations by CMG IMEX and are represented in the Figures 5.3, 5.4, 5.5 and 5.6:

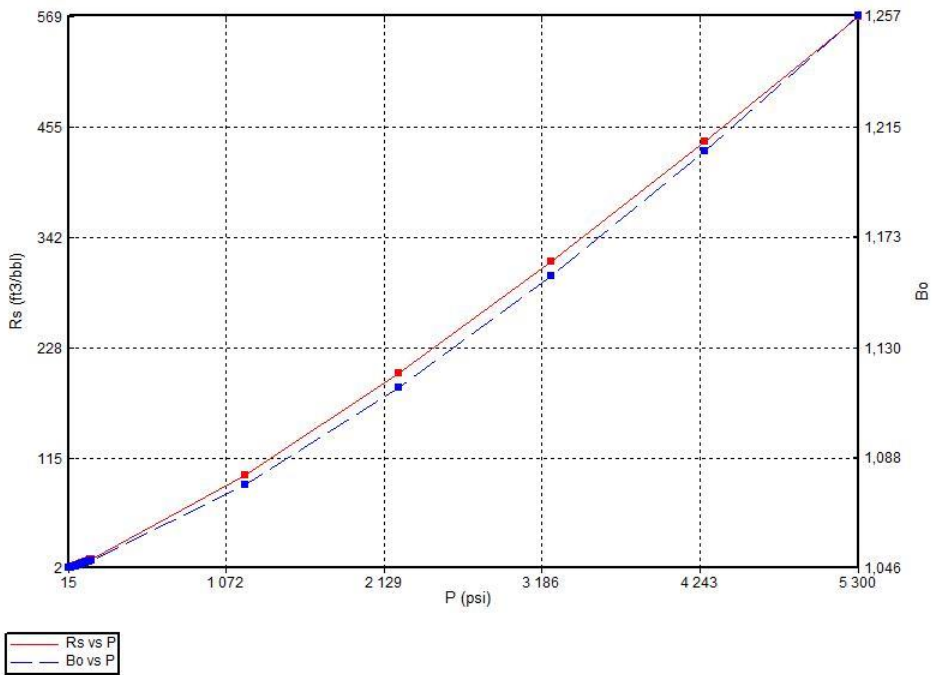


Figure 5.3. Solution Gas Oil Ratio and Oil Formation Volume Factor vs Pressure

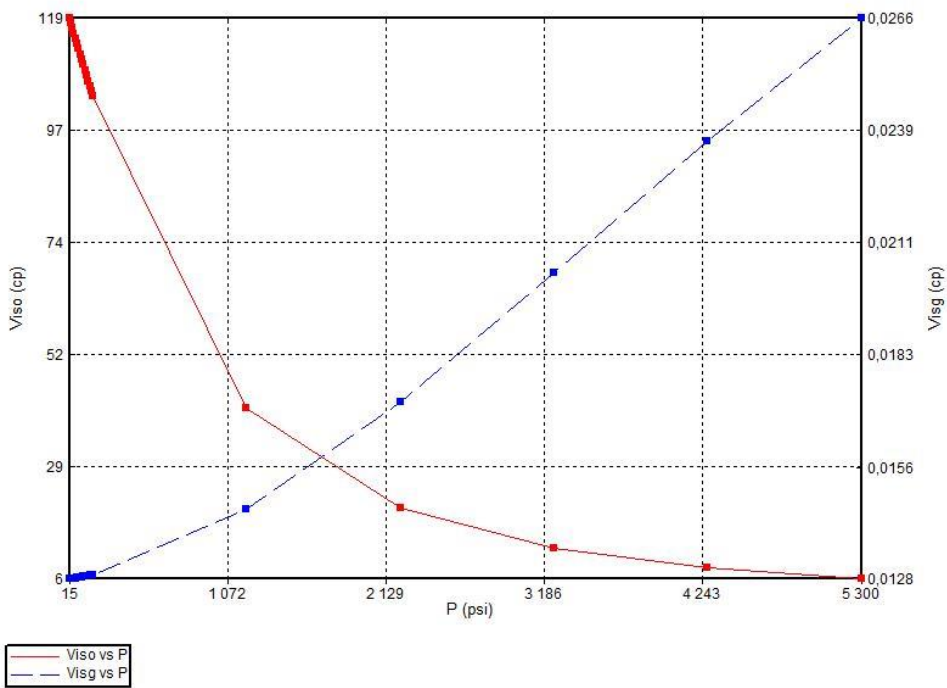


Figure 5.4. Oil and Gas Viscosities vs Pressure

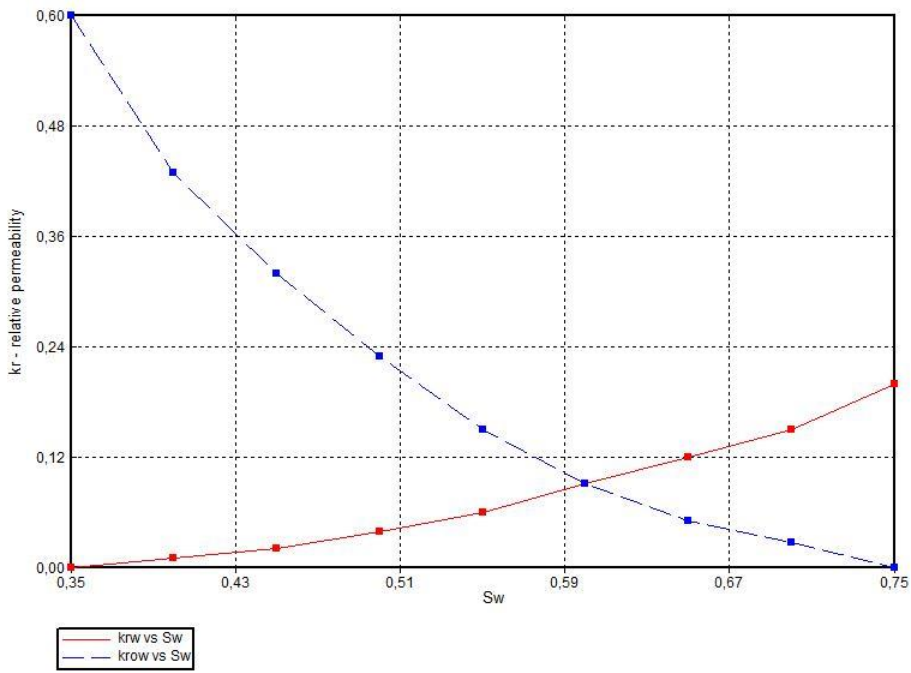


Figure 5.5. Relative Permeability vs Water Saturation

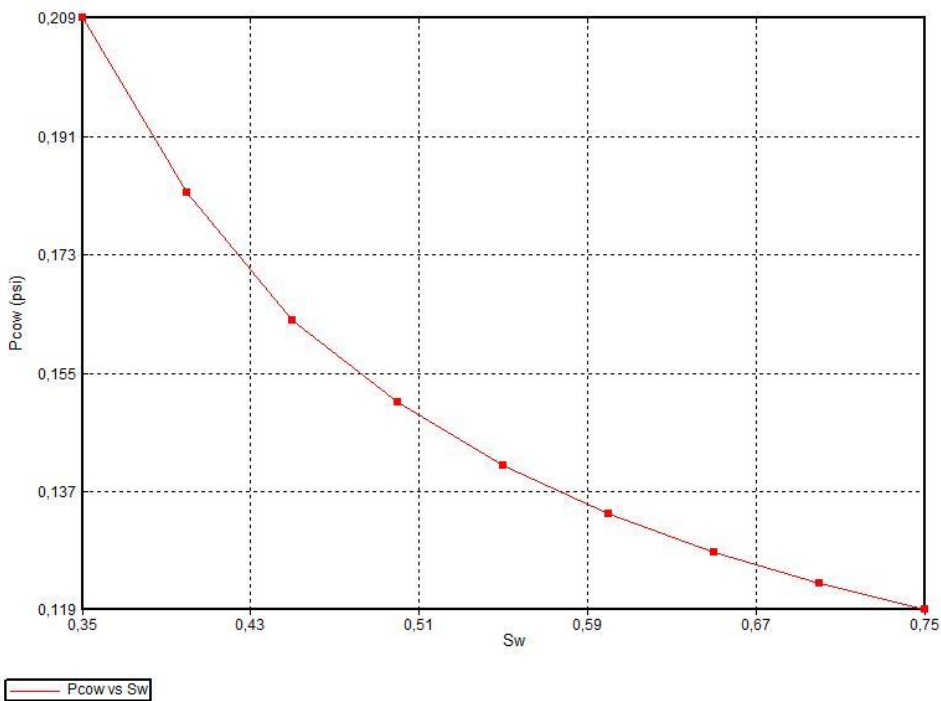


Figure 5.6. Capillary Pressure vs Water Saturation

CO<sub>2</sub> properties used for simulations are represented in the Figures 5.7 and 5.8:

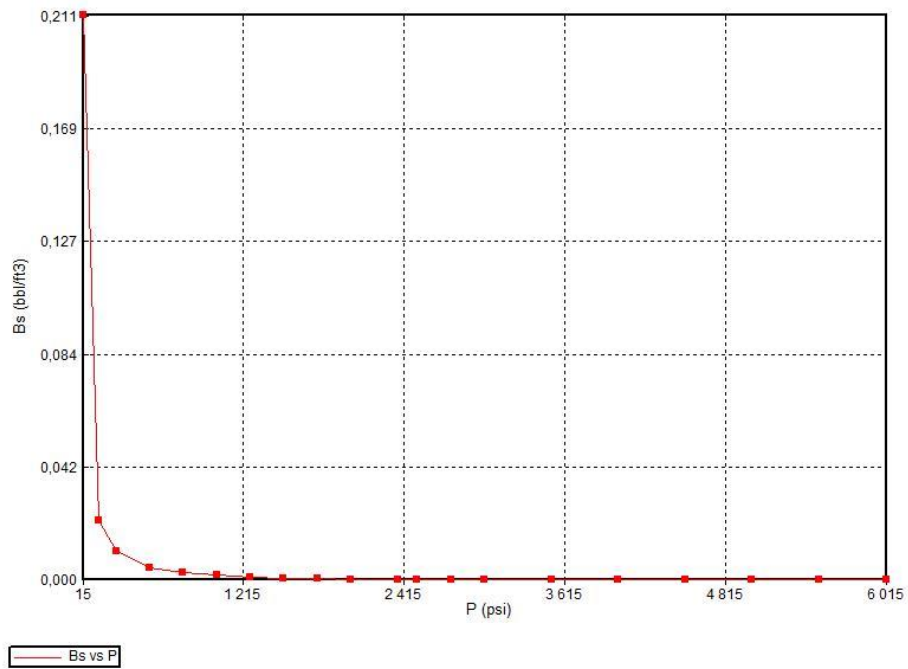


Figure 5.7. CO<sub>2</sub> Formation Volume Factor vs Pressure

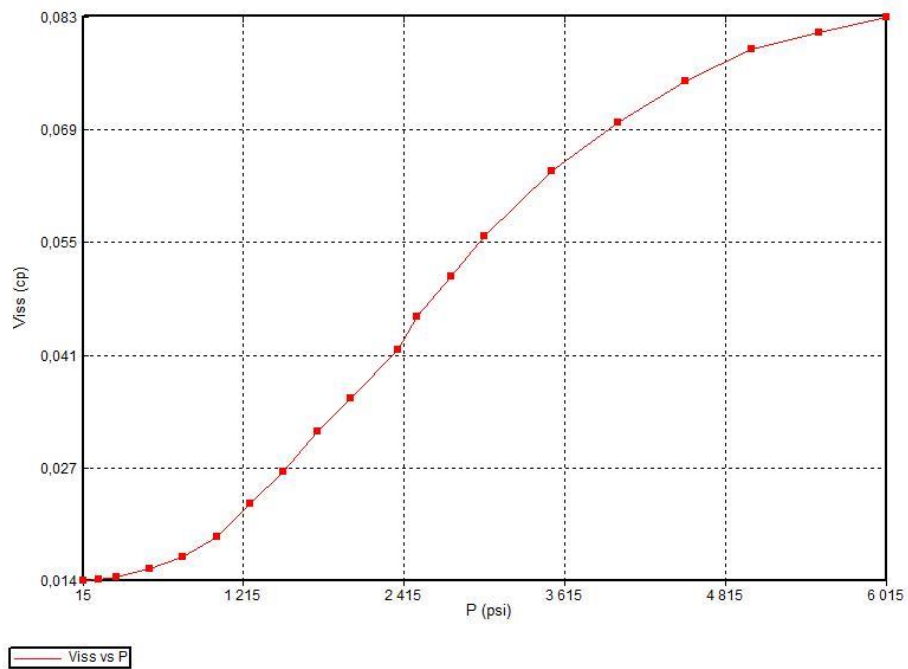


Figure 5.8. CO<sub>2</sub> Viscosity vs Pressure

Carbon dioxide density used is 0.1148 lb/ft<sup>3</sup>. Considering fully immiscible displacement, mixing parameter ( $\omega$ ) was assumed to be 0 at all pressures.

### **5.1.1.3 Simulation scenarios**

Several simulation scenarios were run for the model described above to identify the effect of different parameters on oil recovery factor and CO<sub>2</sub> sequestration.

#### **5.1.1.3.1 Scenario 1**

For the first scenario different well patterns for production and injection wells were used, to identify the most effective one for oil production and carbon dioxide sequestration co-optimisation. The patterns used for simulations are: peripheral, directline, 5 spot, 9 spot, inverted 5 spot, inverted 7 spot, and inverted 9 spot. Top views for the described injection patterns are shown in Appendix A. Cumulative injection rate for each case in this scenario was 30 MM ft<sup>3</sup>/day. For consistency, pattern area was set to be 500 Acres. The model was set to simulate 50 years of operations. Aquifer was assumed to be inactive.

#### **5.1.1.3.2 Scenario 2**

In the second scenario pattern area, which is the area covering all the wells in the pattern, was selected as variable for optimization. Cumulative injection rate was selected to be the same as in Scenario 1, which was 30 MM ft<sup>3</sup>/day. As for the pattern itself, inverted 5 spot was selected for this scenario. Pattern area was variable in the range from 50 Acres up to 600 Acres. Aquifer was assumed to be inactive. The simulations were run for the whole field development study.

### 5.1.1.3.3 Scenario 3

Variable parameter for the third scenario was cumulative injection rate, ranging from 10 MM to 1000 MM ft<sup>3</sup>/day. As for the pattern, inverted 5 spot with area of 75 Acres was selected for these cases. Aquifer was assumed to be inactive.

### 5.1.1.3.4 Scenario 4

For scenario 4, injection into different zones, such as aquifer, oil bearing zone, or combined were simulated. Here it was assumed that there is an active aquifer below the oil zone. The pattern was selected to be inverted 5 spot with 110 acres pattern area. Cumulative flow rate of 300 MM ft<sup>3</sup>/day was used.

### 5.1.1.3.5 Scenario 5

Scenario 5 was used to simulate Water alternating gas injection and understand its effects of oil production and carbon dioxide deposition. Inverted 5 spot with 110 acres pattern area was again used for this scenario. Cumulative injection rate was 300 MM ft<sup>3</sup>/day for CO<sub>2</sub> injection periods and 10000 bbl/day for periods of water injection. For this scenario, duration of each fluid injection was changed from case to case. Thus, there have been run four simulations with the following cycle durations:

Table 5.2 WAG Injection Cycles

CO <sub>2</sub> Injection (months)	H <sub>2</sub> O Injection (months)
3	3
3	6
6	3
6	6



## CHAPTER 6

### RESULTS AND DISCUSSION

#### 6.1 Scenario 1

As it has been mentioned in chapter 5.1.1.3.1, several well patterns have been tested in Scenario 1 for the purpose of determining the optimum one for both CO<sub>2</sub> sequestration and oil recovery. Simulations indicate that the well pattern resulting in the most oil recovery factor is inverted 9 spot, with RF being 3.72 at the end of 50-year simulation. The worst pattern in terms of oil production was observed from directline pattern resulting in just 0.87 recovery factor.

As for the CO<sub>2</sub> deposition at the end of 50 year operations, results indicate that the least efficient pattern is the inverted 9 spot with just 7.05E+10 standard conditions ft<sup>3</sup>. This is the result of carbon dioxide bypass to the production wells and higher CO<sub>2</sub> production compared to the other wells. As for the most efficient pattern in this case, it is 5 spot with 3.91E+11 standard cuft.

As it can be seen from the Figures 6.1 and 6.2, inverted 5 spot pattern result in RFs and CO<sub>2</sub> volumes stored being above average values. Its oil recovery factor and carbon dioxide maximum deposited volumes are 2.10 after 50 years and 2.78E+11 after almost 35.5 years of operations respectively. Considering the fact, that this pattern is second best both in terms of oil production and CO<sub>2</sub> deposition, and the fact that it is the only pattern with oil recovery and CO<sub>2</sub> amounts stored above average, we can conclude that it represents optimum pattern for carbon dioxide sequestration and EOR co-optimisation in heavy oil fields.

Table 6.1 Scenario 1 outcomes

Type of Pattern	<i>Max CO<sub>2</sub> Deposited</i>	
	<i>RF</i>	<i>(scf)</i>
Peripheral	1.55	1.72E+11
Directline	0.87	2.76E+11
5 Spot	1.09	3.97E+11
9 Spot	0.94	2.59E+11
Inverted 5 Spot	2.10	2.78E+11
Inverted 7 Spot	3.56	1.67E+11
Inverted 9 Spot	3.75	1.04E+11

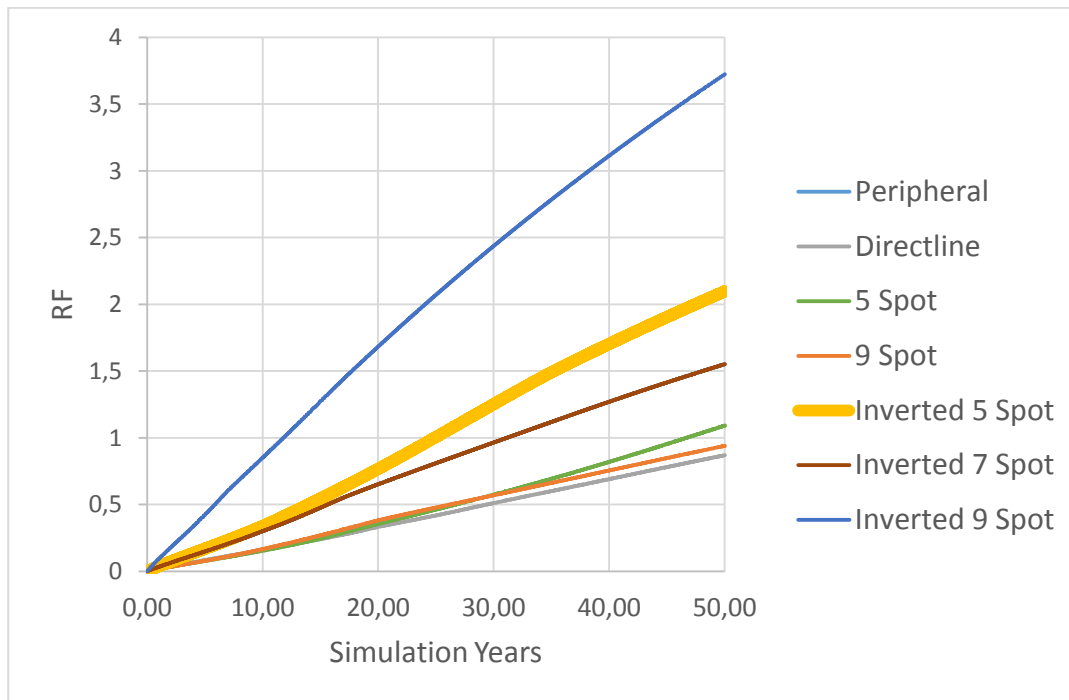


Figure 6.1. Oil Recovery Factor for various injection patterns

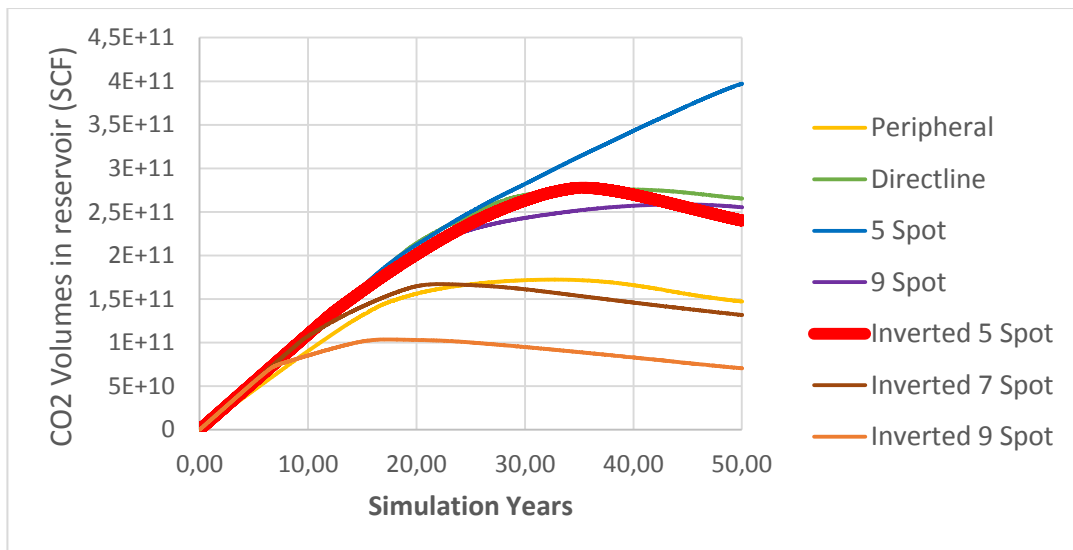


Figure 6.2. CO<sub>2</sub> Volumes in reservoir for various injection patterns

## 6.2 Scenario 2

The aim of the simulations in this scenario was to determine the effect of well pattern area on both CO<sub>2</sub> sequestration and oil recovery. Scenario 2 simulations indicate, that with decreasing pattern area there is a significant increase in oil recovery factor. So, among 9 simulations conducted, 75-acre pattern show the highest recovery of 9.66. On the contrary, the biggest pattern of 600 acres show the smallest recovery of 1.76. However, it should be also noted, that these simulations correspond to the number of patterns of 185 and 9 respectively. As it can be seen on the Figure 6.3, the graphs of 230 and 250 acre simulations overlap, with both having same number of patterns, which is 30. This indicate, that oil recovery factor is mostly dependent on number of wells, rather than size of the pattern.

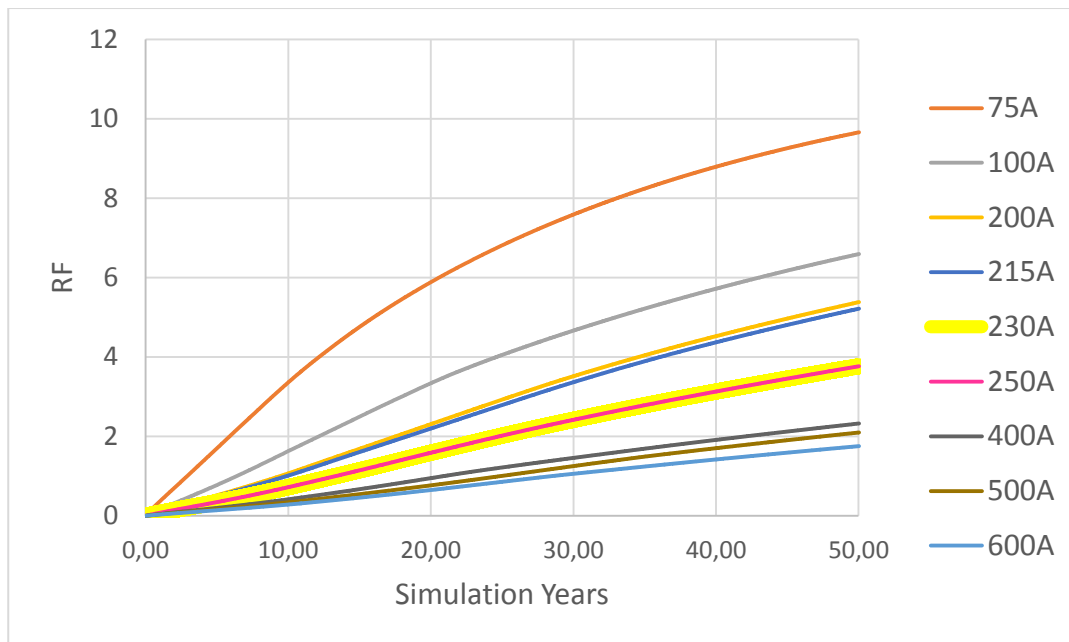


Figure 6.3. Oil Recovery Factors for various patterns sizes

Figure 6.4 represents CO<sub>2</sub> deposition in the reservoir for each simulation in this scenario. It can be clearly seen that with decreasing pattern size, the amount of carbon dioxide deposited decreases. This is due to earlier CO<sub>2</sub> breakthrough as the production and injection wells are getting closer to each other. So, the breakthrough for 75-acre pattern is simulated to be after just 11 years of injection, while for bigger patterns it was after around 35 years. After the breakthrough the amount of carbon dioxide starts decreasing in each case, as the production rate for it gets bigger than injection.

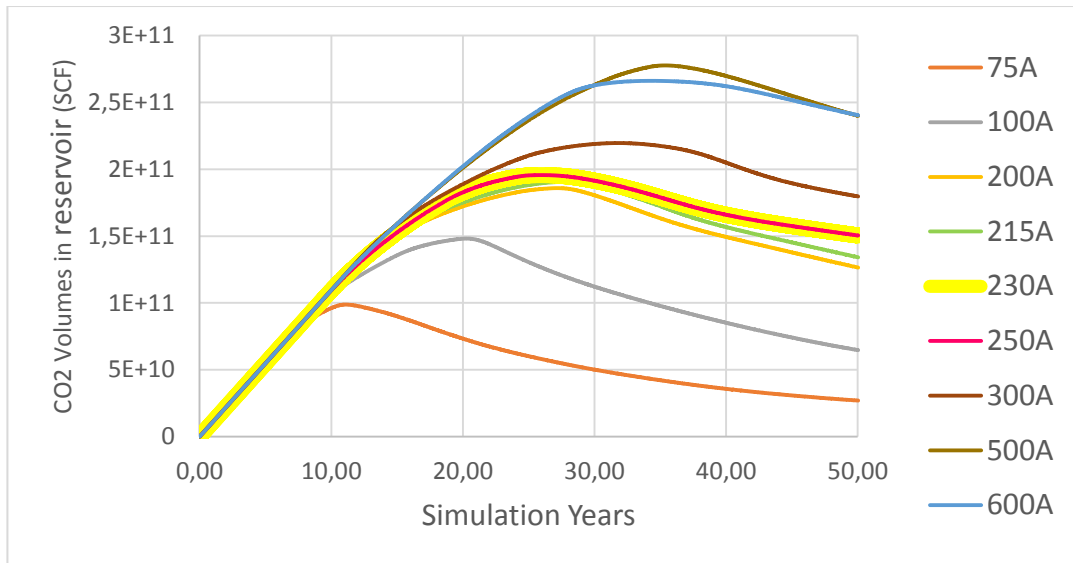


Figure 6.4. CO<sub>2</sub> Volumes in reservoir for various pattern sizes

As scenario 2 simulations were initially aimed to compare different pattern areas for the full field development, it should be noted, that different pattern areas correspond to different number of patterns, and thus number of wells, which has a significant effect on the oil recovery. On the other hand, as proximity of production and injection wells change with each pattern area, the CO<sub>2</sub> breakthrough and thus amount of carbon sequestrated change as well. It is difficult to decide which pattern size is the most optimal one, since financial and time aspects should be considered, as both cost and time required for development increase with decreasing area of the pattern.

Table 6.2 summarizes results of each simulation in Scenario 2:

Table 6.2 Scenario 2 outcomes

Pattern area (acres)	<i>RF</i>	<i>Max CO<sub>2</sub></i>
		<i>deposited (scf)</i>
75	9.66	9.88E+10
100	6.59	1.48E+11
200	5.38	1.86E+11
215	5.22	1.91E+11

230	3.77	1.96E+11
250	3.77	1.96E+11
400	2.33	2.30E+11
500	2.10	2.78E+11
600	1.76	2.66E+11

### 6.3 Scenario 3

Scenario 3 was performed to analyze how various CO<sub>2</sub> injection rates will influence recovery of the oil and storage of carbon dioxide. The results indicate, that with higher injection rate both recovery factor and deposition increase.

Field development without injection was also simulated to observe the difference between lowest injection rate simulated with primary recovery. As it can be observed from the Figure 6.5, even an injection of 10MM scf can boost oil production by 1.5 times, with RF of 5.81 without injection and 8.62 with 10MM scf. However, as injection rises, the rate of increase in recovery factor declines. This can be clearly seen from the Figure 6.6. So, by increasing injection rate to 1000MM scf, recovery factor increases by just 1.06 times compared to 500MM scf and by 2.28 times compared to no injection.

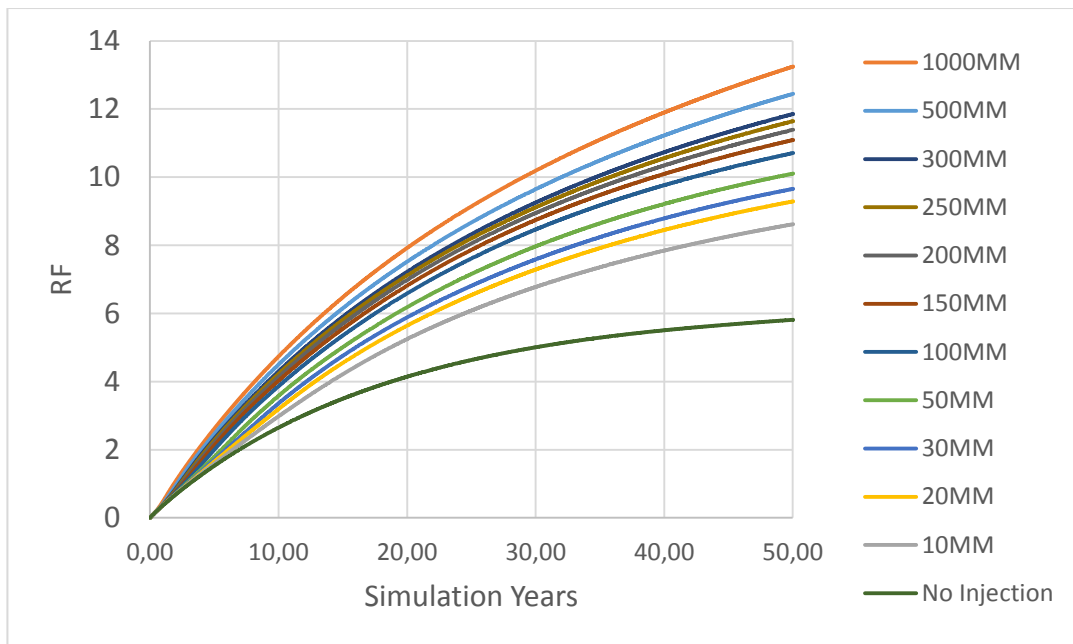


Figure 6.5. Oil Recovery Factors for various CO<sub>2</sub> injection rates

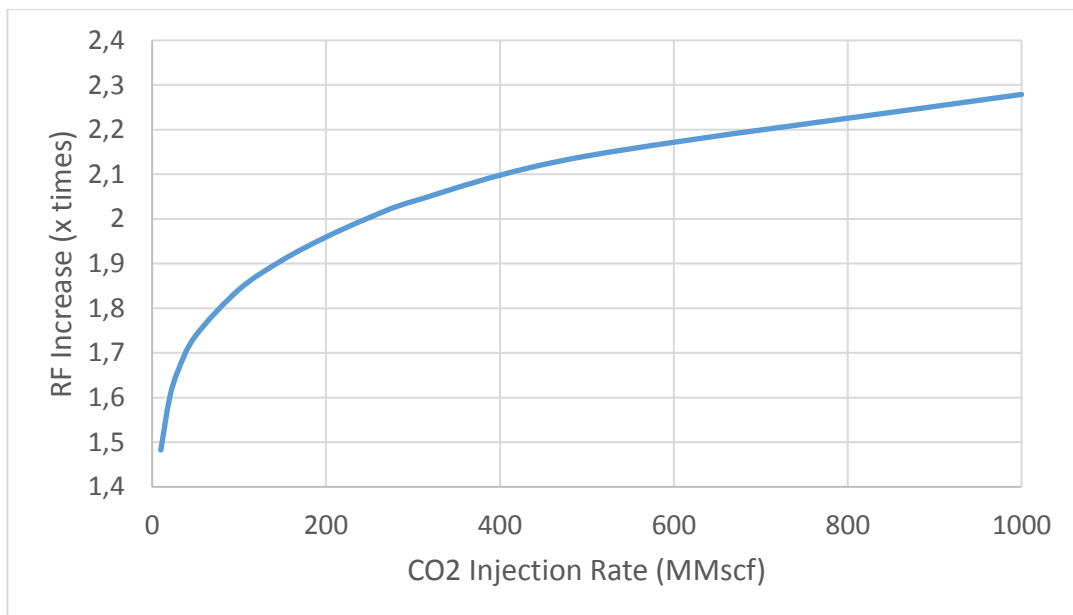


Figure 6.6. Rate of oil recovery factor increase vs CO<sub>2</sub> injection rate

Regarding the volumes of carbon dioxide stored, they are also rising with increasing injection rate. However, the higher the injection rate, the earlier is the CO<sub>2</sub> breakthrough to the production wells. For this case, years passed before

breakthrough for each injection rate can be observed on Figure 6.7. Nevertheless, at the end of 50-year injection-production period, the higher rate still results in higher amounts of deposited carbon.

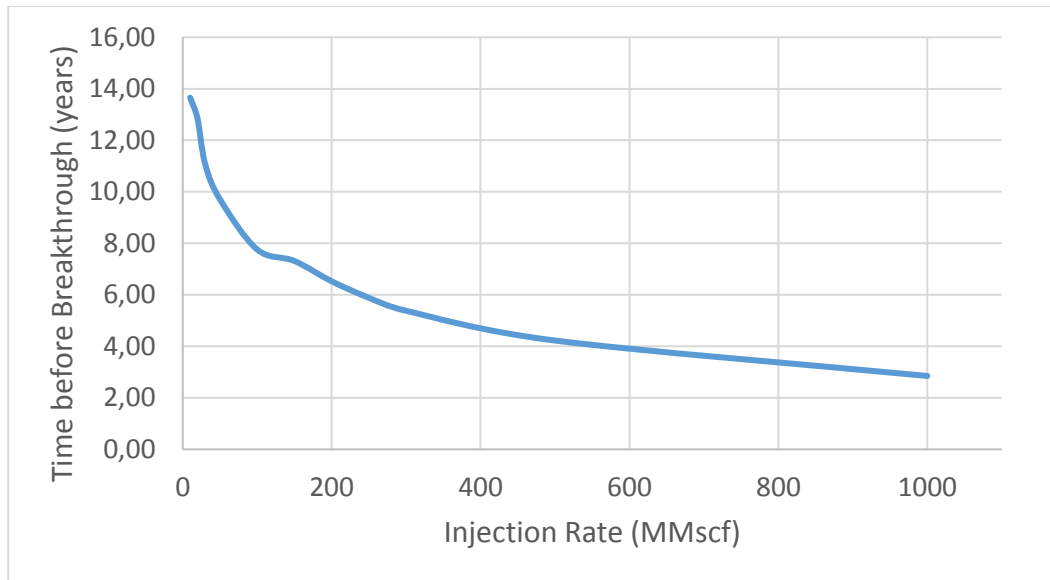


Figure 6.7. Time before CO<sub>2</sub> Breakthrough to production wells

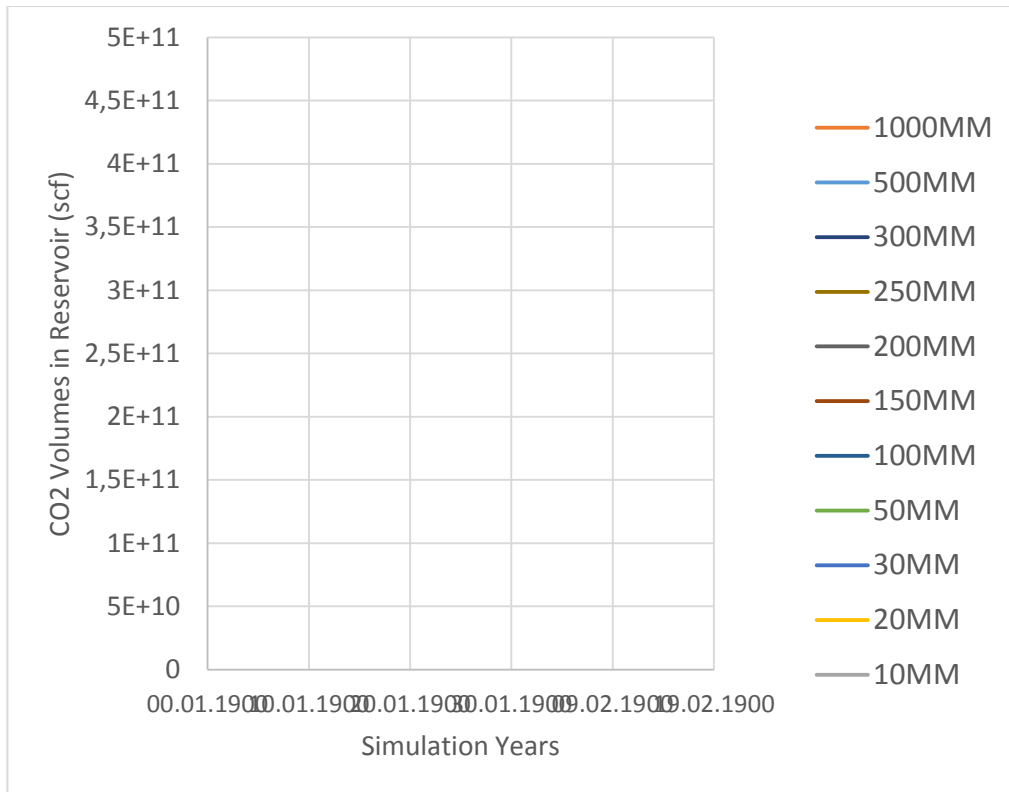


Figure 6.8. CO<sub>2</sub> Volumes in reservoir for various CO<sub>2</sub> injection rates

Table 6.3 below summarizes results of simulations of each case in this scenario:

Table 6.3 Scenario 3 outcomes

Injection Rate (MMscf)	<i>RF</i>	<i>Max CO<sub>2</sub> Stored</i> (scf)	<i>CO<sub>2</sub> Stored at 50-year</i> (scf)
0	5.81	N/A	N/A
10	8.62	4.01E+10	1.65E+10
20	9.29	7.17E+10	2.32E+10
30	9.66	9.88E+10	2.70E+10
50	10.11	1.38E+11	3.18E+10
100	10.71	2.02E+11	4.00E+10
150	11.09	2.44E+11	4.77E+10
200	11.39	2.77E+11	5.51E+10

Table 6.3 (cont'd)

250	11.65	3.02E+11	6.24E+10
300	11.86	3.22E+11	6.91E+10
500	12.45	3.77E+11	9.07E+10
1000	13.25	4.52E+11	1.33E+11

#### 6.4 Scenario 4

As it was discussed in section 5.1.1.3.4 scenario 4 was focused on simulating CO<sub>2</sub> injection in different zones: oil zone, water zone, and both of them. All three cases showed similar results in terms of oil recovery, with small differences among them. So, injecting into the oil zone showed just 1.023 times higher recovery factor than injecting into the aquifer and 1.021 times higher than injecting into both oil and water zones. Difference between water zone and both zones injection can be considered negligible, with RF in both zones being 1.0017 times higher than water zone injection. Results can be observed on Figure 6.9.

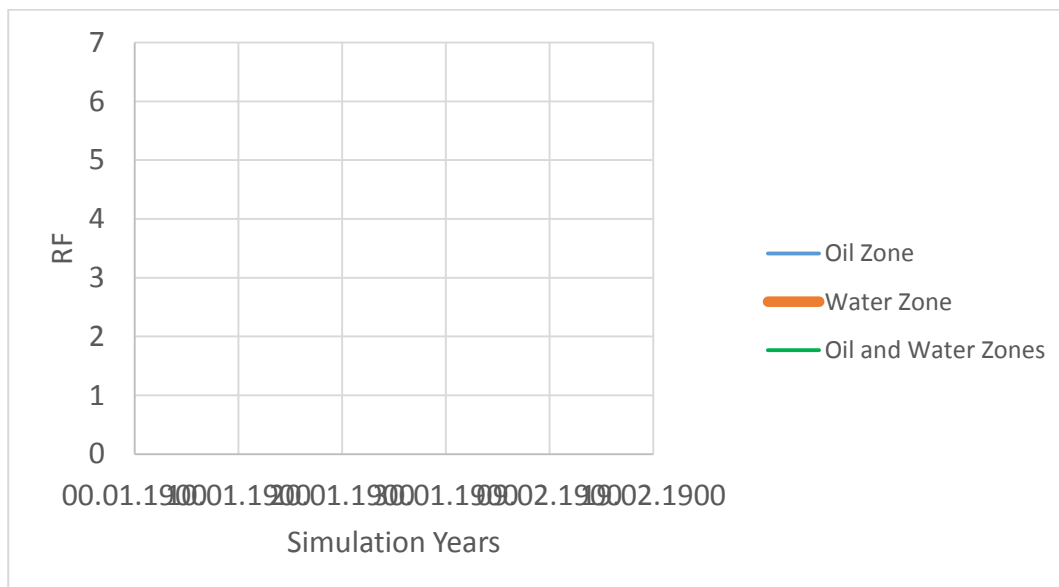


Figure 6.9. Oil Recovery Factors for CO<sub>2</sub> injection into various zones

As for the carbon dioxide deposition, the results are slightly different. While injection into water zone and both zones together show relatively similar results in almost the same sequestration, injection into the oil zone is slightly different.

As you can see from the Figure 6.10, while injecting CO<sub>2</sub> into water and oil zones, or just water zone, the amount of carbon dioxide deposited in the reservoir starts rising quickly, until it reaches its peak after around 4-5 years of operations. Since major part of the CO<sub>2</sub> in these cases dissolves in water, decline in the amount of carbon in the reservoir is associated with water breakthrough to the production wells. With increasing water production, the amount of carbon dioxide decreases, since production rate of the CO<sub>2</sub> dissolved is higher than injection rate. It continues, until the water production rate decreases, which is associated with the decreased average reservoir pressure.

In case of oil zone injection, the peak for the CO<sub>2</sub> deposited at a moment in time is lower, than the one in the cases described above. This is due to the fact, that the contact between carbon dioxide and water comes later, and the production rate of free CO<sub>2</sub> is higher than the one dissolved in water. Furthermore, as it can be seen in the Figure 6.10, at some point, amount of carbon sequestered starts increasing again. This is due to the fact, that it dissolves in water at that moment, and increase continues until injection rate is lower than production of combined dissolved and free carbon dioxide. It can also be seen, that for some time, the pressure in case of oil zone injection is higher, than water and combined injection. This is due to the fact, that there is more free CO<sub>2</sub> available at that moment, which leads to the higher reservoir pressures.

Table 6.4 summarizes results of simulations of each case in this scenario:

Table 6.4 Scenario 4 outcomes

Injected Zone	<i>RF</i>	<i>Max CO<sub>2</sub> Stored</i>	<i>CO<sub>2</sub> Stored at 50-year</i>
		( <i>scf</i> )	( <i>scf</i> )
Oil	5.76	3.80E+11	2.43E+11
Water	5.63	4.24E+11	2.60E+11
Oil & Water	5.64	4.24E+11	2.61E+11

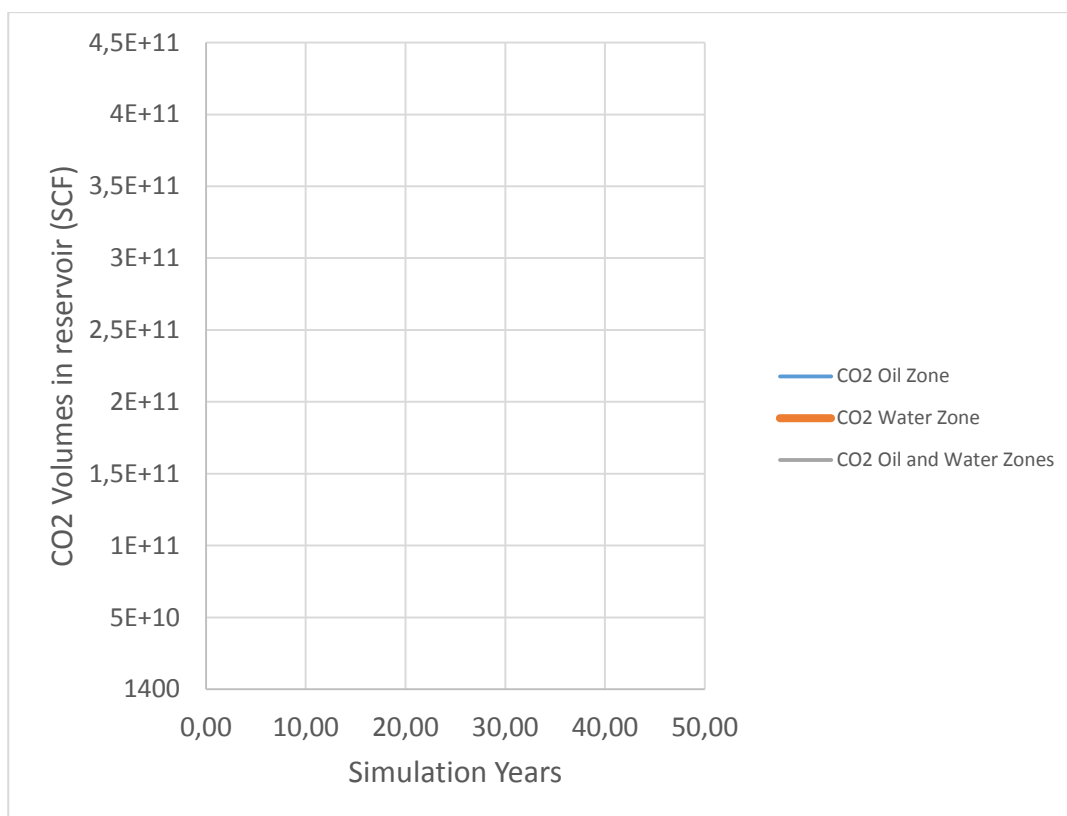


Figure 6.10. CO<sub>2</sub> Volumes in reservoir for injection into various zones

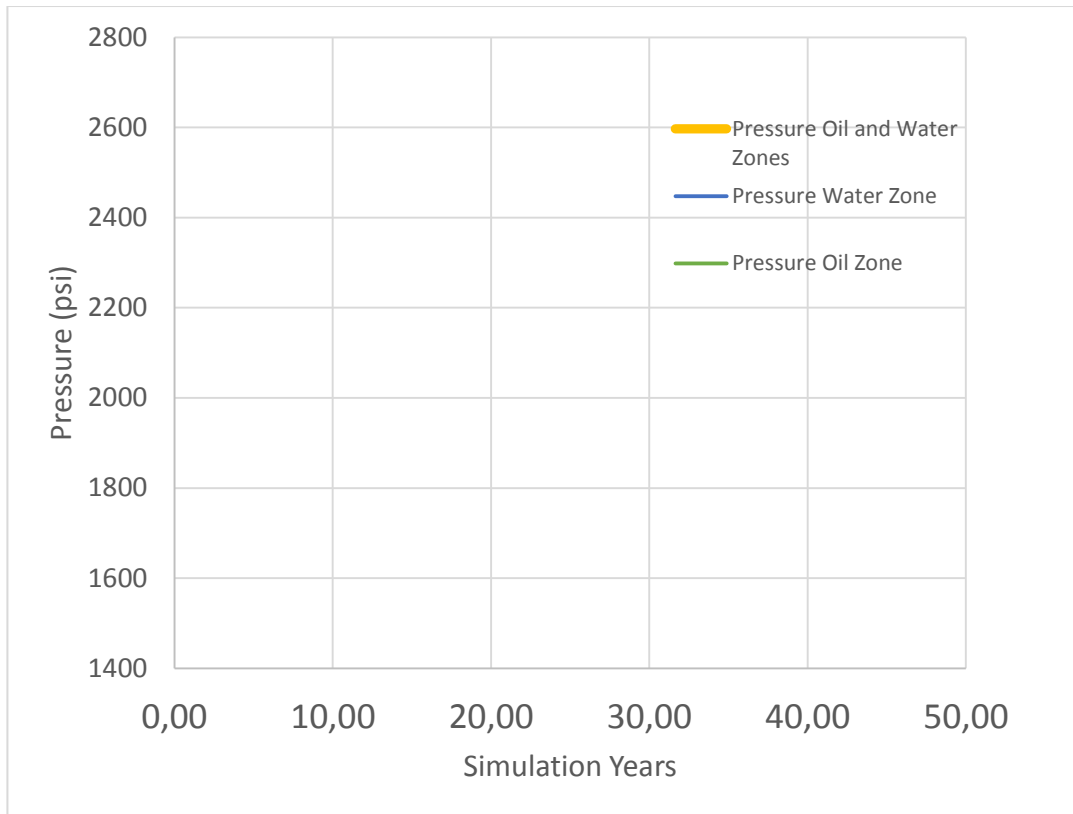


Figure 6.11. Reservoir Pressures for CO<sub>2</sub> injection into various zones

## 6.5 Scenario 5

Scenario 5 simulations indicate that with the right configuration, water alternating gas (WAG) injection can be the most efficient way of CO<sub>2</sub> injection in terms carbon sequestration and EOR co-optimization in heavy oil fields, contradicting to the statement done by Vega and Kavscek in 2010 (Vega & Kavscek, 2010).

As for oil recovery factor, results, as expected, showed that by implementing WAG there is a chance to produce much more oil, compared to single carbon dioxide injection. The Figure 6.12 represents the outcomes for all WAG and pure CO<sub>2</sub> injection simulations. As it can be seen on the plot, any WAG injection can result with at least 29%-30% more oil RF at the end of simulated period, with 2:1 cycle showing the best result of increasing oil production by almost 38%. Furthermore, as

it can be seen from the graph, the duration of a cycle for 1:1 configuration, does not affect the results, as 3 months and 6 months' cycle periods result in the same recovery factors. Detailed results for increase in RF can be found in the Table 6.5.

Table 6.5 Oil Recovery Factors increase for various WAG configurations

WAG Cycles (Months)	RF Increase (%)
3 H <sub>2</sub> O – 3 CO <sub>2</sub> (1:1)	33.9
3 H <sub>2</sub> O – 6 CO <sub>2</sub> (1:2)	29.6
6 H <sub>2</sub> O – 3 CO <sub>2</sub> (2:1)	37.8
6 H <sub>2</sub> O – 6 CO <sub>2</sub> (1:1)	33.9

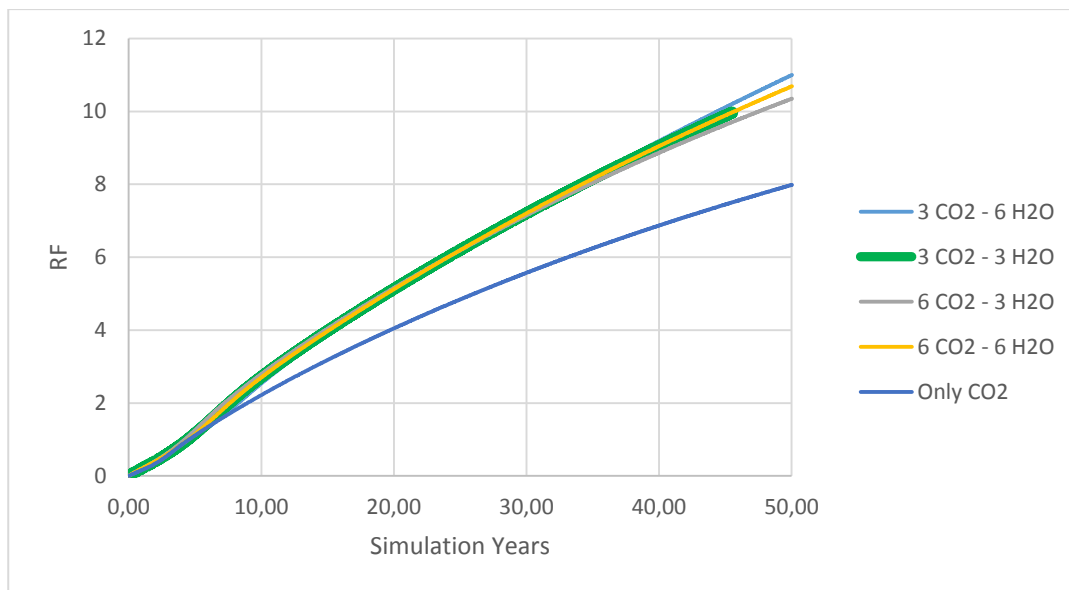


Figure 6.12. Oil Recovery Factors for various WAG configurations

Now going to the CO<sub>2</sub> stored during the process, the results are a bit more controversial. As it has been mentioned in the section 2.2.3.3.3, according to Vega and Kavscek, the carbon dioxide stored during WAG process is less, than the one in pure CO<sub>2</sub> injection (Vega & Kavscek, 2010). So, as per simulations conducted by Kavscek and Cakici in 2005, during WAG injections, water occupies significant

amount of pore volume, resulting in less volume remaining for carbon storage (Kovscek & Cakici, 2005). However, noting that water injection strongly reduces CO<sub>2</sub> mobility(Kovscek & Cakici, 2005), which in return reduces its production, may results in delayed carbon dioxide breakthrough. So, the results of the simulations indicate, that by injection water in much smaller rates, compared to CO<sub>2</sub> rates, we may actually stabilize the amount of CO<sub>2</sub> stored in the reservoir and continue oil production for much longer time. As simulation indicated, having 100 and less bbls/day of H<sub>2</sub>O injection, will significantly reduce mobility of carbon dioxide, while occupying small reservoir volume. By the end of 50 year WAG operations, it can be seen, that water saturations increase from 0.21 irreducible saturation, to just around 0.3. As for the amount of carbon dioxide stored, even though that the maximum value is slightly less compared to conventional carbon injection, by the end of 50 year period, 2:1 and 1:1 cycle WAG results in slightly higher amounts sequestered.

Detailed results for increase in CO<sub>2</sub> storage can be found in the Table 6.5.

Table 6.6 Change in CO<sub>2</sub> volumes in reservoir for various WAG configurations

WAG Cycles (Months)	Increase in CO <sub>2</sub> Stored (%)
3 H <sub>2</sub> O – 3 CO <sub>2</sub> (1:1)	10
3 H <sub>2</sub> O – 6 CO <sub>2</sub> (1:2)	-1.7
6 H <sub>2</sub> O – 3 CO <sub>2</sub> (2:1)	12
6 H <sub>2</sub> O – 6 CO <sub>2</sub> (1:1)	10

The most stable results for CO<sub>2</sub> storage are coming from 2:1 cycle, considering the fact, that more water results in less carbon dioxide mobility. However, noting that 1:1 cycle results are quite close to 2:1, and considering the fact, that this cycle showed second best results for RF, the most optimum WAG cycle can be considered 1:1, with either 3 months or 6 months.

The results are shown on the Figure 6.13.

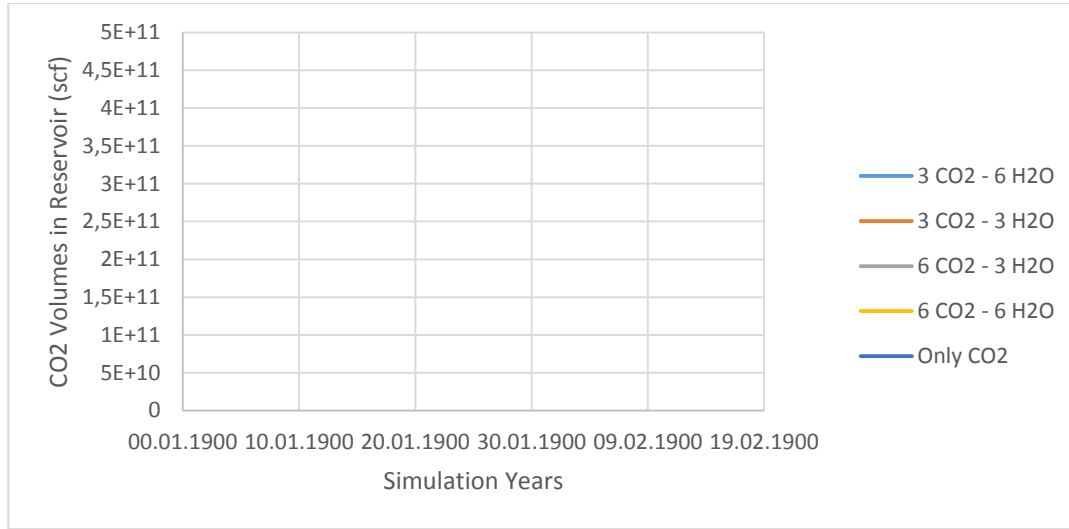


Figure 6.13. CO<sub>2</sub> Volumes in reservoir for various WAG configurations

## 6.6 Economical considerations

Even though technically maximizing both oil recovery and carbon dioxide sequestration is possible, realistically operator companies responsible for the process will try to maximize their profit. The profit for CO<sub>2</sub> sequestration and EOR co-optimization can be calculated from the following equation (Veld et al., 2013):

$$\text{profit} = p_{\text{oil}} q_{\text{oil}}^{\text{prd}} + s_{\text{CO}_2} q_{\text{CO}_2}^{\text{seq}} - p_{\text{CO}_2} q_{\text{CO}_2}^{\text{seq}} - c^{\text{rec}} q_{\text{CO}_2}^{\text{rec}} - c^{\text{oth}} \quad (6.1)$$

Where  $p_{\text{oil}}$  is the unit price for oil,  $p_{\text{CO}_2}$  is the unit price for CO<sub>2</sub> purchased for sequestration purposes,  $s_{\text{CO}_2}$  subsidies for the CO<sub>2</sub> sequestrated,  $c^{\text{rec}}$  is unit cost for carbon dioxide recycling process, and  $c^{\text{oth}}$  is the cost of other operations.

Currently, oil production is the main source of revenue from CO<sub>2</sub> sequestration during EOR. On average, companies agree to pay up to 2% of oil price for carbon dioxide (Núñez-López & Moskal, 2019). Therefore, for the operator companies which are buying CO<sub>2</sub> it is natural to try to reduce amount of carbon dioxide injected, while increasing oil recovery factor. To implement full scale sequestration during

Enhanced-Oil-Recovery, the revenue should be high enough for the company to profit from the process. Firstly, stable high oil prices, will influence company's aim to recover as much oil as possible during high oil price period, which will result in higher demand for CO<sub>2</sub>-EOR. Furthermore, as it can be seen from equation above, introducing subsidies for CO<sub>2</sub> sequestration will increase company's profit, which is one of the government's method to motivate operator company. To make the process even more profitable, carbon dioxide recycling should be taking into account. As it can be seen from the simulations conducted above, after CO<sub>2</sub> breakthrough significant amount of it is being produced together with oil, which may be postponed by optimizign pattern area or implementing WAG. In addition, recycled carbon dioxide can be re-injected into the reservoir, thus reducing the required amount of CO<sub>2</sub> to be purchased. Finally, increasing taxes to the produced CO<sub>2</sub> during industrial processes, and development in carbon capture technologies, which in terms makes the process cheaper, will reduce the price of CO<sub>2</sub> to be purchase for sequestration. Moreover, significant increase in tax, may reduce carbon dioxide price to negative, which may be considered as a subsidy for carbon sequestration (Veld et al., 2013).

Considering all of the discussed above, results of the simulations indicate, that for the case of both oil and CO<sub>2</sub> purchase price being high, co-optimization shift more to the EOR side, meaning that it will be more profitable for the company to implement strategies resulting in higher oil RF, e.g using inverted 9 spot pattern, while minimizing pattern area. Furhermore, considering high purchase cost of carbon dioxide, injected amount should be minimized, based on the profit.

For the case of oil price being low, and either subsidies for CO<sub>2</sub> injection or negative CO<sub>2</sub> purchase price, co-optimization will shift to the carbon storage project side. So, it would be beneficial to increase amount of carbon dioxide stored, by implementing 5 spot injection, while maximizing overall injection rate, using maximum possible pattern area, which will be limited by number of wells and injection pressure per single well, and injection into the oil zone.

Finally, for the case of high oil price and subsidies for CO<sub>2</sub> injection, inverted 5 spot, with maximum possible injection rate, injecting into the oil zone will be most beneficial in terms of profit.

It should be noted, that in all three cases, implementation of WAG injection is beneficial and will increase the overall profit.

## CHAPTER 7

### CONCLUSION

CO<sub>2</sub> is one of the major greenhouse gases contributing to the global warming and climate change. Apart from reduction in greenhouse gases emissions, one of the main methods for climate change mitigation is carbon capture, utilization and storage, which include carbon dioxide sequestration in hydrocarbon reservoirs. However, noting that most of the oil reservoirs are still producing, and CO<sub>2</sub>-EOR proves to be efficient in many oil reservoirs, the most optimum way for carbon storage is to co-optimize both CO<sub>2</sub> sequestration and oil recovery processes. Taking into account efficiency of immiscible CO<sub>2</sub>-EOR in Bati Raman heavy oil field, the study has been conducted for optimization of sequestration in immiscible heavy oil environment.

The study included sets of numerical simulations to evaluate effect of change in different injection strategies on oil recovery factor and amount of carbon dioxide stored in the reservoir. The parameters that were evaluated are injection patterns; patterns' area; carbon dioxide injection rates; CO<sub>2</sub> injection into oil zone, water zone, and both oil and water zones; and finally efficiency of water-alternating-gas injection compared to conventional carbon dioxide injection. The model was constructed using CMG's Builder and simulations were conducted using CMG's IMEX softwares.

First scenario simulations investigated effects of different injection patterns. Results indicate that while inverted 9 spot and 5 spot patterns are the most efficient in terms of oil recovery factor and carbon dioxide deposition respectively, the optimum ones are to be considered inverted 5 spot and inverted 7 spot patterns. Furthermore, since inverted 5 spot is simpler and requires less wells to be drilled, it is superior in comparison to inverted 7 spot.

For the second scenario pattern size was evaluated to understand how increase or decrease in pattern area influences oil recovery and carbon dioxide sequestration for whole field development. Results indicate that, while with decrease of pattern area oil RF increases, CO<sub>2</sub> sequestration on contrary decreases. In addition, well spacing affects carbon dioxide breakthrough to the production wells, which should also be taken into account while designing field development. Furthermore, simulations indicate, that number of wells affect the results at least as strongly as well spacing. Identification of efficient pattern area should be considered on field to field basis considering financial and time aspects as well.

Third scenario evaluated effect of carbon dioxide injection rates. Results indicate, that increase in injection rates results in higher recovery factors and carbon dioxide deposited. However, as the injection rate increases, rate of increase in oil RF decreases. Furthermore, for field development, it should be noted, that higher injection rate results in earlier carbon dioxide breakthrough, which in terms results in decrease of carbon sequestered.

Fourth scenario simulations were aimed to identify reservoir zone most suitable for oil recovery and carbon dioxide deposition. In terms of oil recovery factor, injection zone does not really affect the results, with differences being negligible. As for CO<sub>2</sub> deposition, it is most efficient to inject just into the oil zone, however, the injection should be stopped at earlier time. Injection into water or both zones show similar and more stable results, and are better for injection for longer periods.

Fifth scenario simulations evaluated feasibility of water-alternating-gas injection for co-optimization purposes. Results indicate, that implementing WAG results in up to 38% increase in oil recovery factor while injecting water for 2 times longer period than carbon dioxide. As for carbon sequestration, simulations indicate, that injection of water in small amounts significantly reduces mobility of carbon dioxide, and thus prevent its early breakthrough and show more stable CO<sub>2</sub> deposition. Same as recovery factor, injecting water for 2 times longer period than carbon dioxide show higher results in terms of carbon sequestered as well.

Overall, while some of the parameters, such as inverted 5-spot pattern, and WAG implementation, are more obvious to be used for the purpose of co-optimization, others need to be chosen on field to field basis. Pattern size, injection rate, and injection zone, are dependent on how long the CO<sub>2</sub> injection and oil recovery are planned to continue, as these parameters affect time for CO<sub>2</sub> breakthrough, and thus both oil production rate and amount of carbon dioxide stored. Furthermore, the parameters need to be optimized with regards to oil and CO<sub>2</sub> markets, since the operations discussed in this study need to provide profit to the operator company, and thus need to be considered at the time of implementation.



## REFERENCES

- Al-Bayati, D., Saeedi, A., Myers, M., White, C., & Xie, Q. (2018). *An Experimental Investigation of Immiscible CO<sub>2</sub> Flooding Efficiency in Sandstone Reservoirs: Influence of Permeability Heterogeneity*. <https://doi.org/10.2118/190876-MS>
- Alper, E., & Yuksel Orhan, O. (2017). CO<sub>2</sub> utilization: Developments in conversion processes. *Petroleum*, 3(1), 109–126. <https://doi.org/https://doi.org/10.1016/j.petlm.2016.11.003>
- Ansarizadeh, M., Dodds, K., Gurpinar, O., Pekot, L. J., Kalfa, Ü., Sahin, S., Uysal, S., Ramakrishnan, T. S., Sacuta, N., & Whittaker, S. (2015). Carbon dioxide-challenges and opportunities. In *Oilfield Review* (Vol. 27).
- Aresta, M., & Dibenedetto, A. (2010). 14 - Industrial utilization of carbon dioxide (CO<sub>2</sub>). In M. M. B. T.-D. and I. in C. D. (CO<sub>2</sub>) C. and S. T. Maroto-Valer (Ed.), *Woodhead Publishing Series in Energy* (Vol. 2, pp. 377–410). Woodhead Publishing. <https://doi.org/https://doi.org/10.1533/9781845699581.4.377>
- Babadagli, T., Sahin, S., Kalfa, U., Celebioglu, D., Karabakal, U., & Topguder, N. N. S. (2008). Development of Heavy Oil Fractured Carbonate Bati Raman Field: Evaluation of Steam Injection Potential and Improving Ongoing CO<sub>2</sub> Injection. In *SPE Annual Technical Conference and Exhibition* (p. 22). Society of Petroleum Engineers. <https://doi.org/10.2118/115400-MS>
- Bachu, S. (2010). 2 - Screening and selection criteria, and characterisation techniques for the geological sequestration of carbon dioxide (CO<sub>2</sub>). In M. M. B. T.-D. and I. in C. D. (CO<sub>2</sub>) C. and S. T. Maroto-Valer (Ed.), *Woodhead Publishing Series in Energy* (Vol. 2, pp. 27–56). Woodhead Publishing. <https://doi.org/https://doi.org/10.1533/9781845699581.1.27>
- Bhatti, A. A., Raza, A., Mahmood, S. M., & Gholami, R. (2019). Assessing the application of miscible CO<sub>2</sub> flooding in oil reservoirs: a case study from Pakistan. *Journal of Petroleum Exploration and Production Technology*, 9(1), 685–701. <https://doi.org/10.1007/s13202-018-0504-x>
- Bouzalakos, S. (2010). Overview of carbon dioxide (CO<sub>2</sub>) capture and storage technology. *Developments and Innovation in Carbon Dioxide (CO<sub>2</sub>) Capture and Storage Technology*, 1–24. <https://doi.org/10.1533/9781845699581.1>
- CMG. (2019). *CMG IMEX Product Brochure 2019*. [https://www.cmgl.ca/sites/default/files/sites/default/files/uploads/docs/CMG\\_I\\_MEX\\_Product\\_Brochure\\_2019.pdf](https://www.cmgl.ca/sites/default/files/sites/default/files/uploads/docs/CMG_I_MEX_Product_Brochure_2019.pdf)
- Computer Modelling Group. (2018). *IMEX User Guide*.

- Cuéllar-Franca, R. M., & Azapagic, A. (2015). Carbon capture, storage and utilisation technologies: A critical analysis and comparison of their life cycle environmental impacts. *Journal of CO2 Utilization*, 9, 82–102.  
<https://doi.org/https://doi.org/10.1016/j.jcou.2014.12.001>
- De Silva, G. P. D., Ranjith, P. G., & Perera, M. S. A. (2015). Geochemical aspects of CO2 sequestration in deep saline aquifers: A review. *Fuel*, 155, 128–143.  
<https://doi.org/https://doi.org/10.1016/j.fuel.2015.03.045>
- Emera, M. K., & Sarma, H. K. (2007). Prediction of CO2 Solubility in Oil and the Effects on the Oil Physical Properties. *Energy Sources, Part A: Recovery, Utilization, and Environmental Effects*, 29(13), 1233–1242.  
<https://doi.org/10.1080/00908310500434481>
- Evans, S. (2014). Around the world in 22 carbon capture projects. *CarbonBrief*.  
<https://www.carbonbrief.org/around-the-world-in-22-carbon-capture-projects>
- Ganzer, L., & Reinicke, K. M. (2017). Enhanced Oil Recovery. In *Kirk- Othmer Encyclopedia of Chemical Technology*.  
<https://doi.org/doi:10.1002/0471238961.0514080102151803.a01.pub3>
- Gaspar Ravagnani, A. T. F. S., Ligerio, E. L., & Suslick, S. B. (2009). CO2 sequestration through enhanced oil recovery in a mature oil field. *Journal of Petroleum Science and Engineering*, 65(3–4), 129–138.  
<https://doi.org/10.1016/J.PETROL.2008.12.015>
- Golomb, D., & Pennell, S. (2010). 11 - Ocean sequestration of carbon dioxide (CO2). In M. M. B. T.-D. and I. in C. D. (CO2) C. and S. T. Maroto-Valer (Ed.), *Woodhead Publishing Series in Energy* (Vol. 2, pp. 304–323). Woodhead Publishing.  
<https://doi.org/https://doi.org/10.1533/9781845699581.3.304>
- Hamouda, A., & Chughtai, S. (2018). Miscible CO2 Flooding for EOR in the Presence of Natural Gas Components in Displacing and Displaced Fluids. In *Energies* (Vol. 11). <https://doi.org/10.3390/en11020391>
- Holm, L. W., & Josendal, V. A. (1974). Mechanisms of Oil Displacement By Carbon Dioxide. *Journal of Petroleum Technology*, 26(12), 1427–1438.  
<https://doi.org/10.2118/4736-PA>
- Huang Chung-Sung, C.-H. and T. (2014). A Review: CO2 Utilization. *Aerosol and Air Quality Research*, 14(2), 480–499.  
<https://doi.org/10.4209/aaqr.2013.10.0326>
- Hughes, R. G. (2010). *Evaluation and Enhancement of Carbon Dioxide Flooding Through Sweep Improvement*. <https://www.osti.gov/servlets/purl/983791>
- Ibrahim, A., & Nasr-El-Din, H. (2015). *CO2 Sequestration in Unmineable Coal Seams*. <https://doi.org/10.2118/176458-MS>

- IEA. (2015). Storing CO<sub>2</sub> through Enhanced Oil Recovery. *Insights Series*.  
[https://nachhaltigwirtschaften.at/resources/iea\\_pdf/reports/iea\\_ghg\\_storing\\_co2\\_trough\\_enhanced\\_oil\\_recovery.pdf](https://nachhaltigwirtschaften.at/resources/iea_pdf/reports/iea_ghg_storing_co2_trough_enhanced_oil_recovery.pdf)
- IPCC. (2014). *AR5 Synthesis Report: Climate Change 2014*.  
<https://www.ipcc.ch/report/ar5/syr/>
- IRGC. (2008). *Regulation of Carbon Capture and Storage*.  
<https://irgc.org/issues/carbon-capture-and-storage/regulation-of-carbon-capture-and-geological-storage/>
- Jain, R., Urban, L., Balbach, H., Webb, M. D., Jain, R., Urban, L., Balbach, H., & Webb, M. D. (2012). Contemporary Issues in Environmental Assessment. *Handbook of Environmental Engineering Assessment*, 361–447.  
<https://doi.org/10.1016/B978-0-12-388444-2.00013-0>
- Kambale, J., & Tripathi, V. (2010). BIOTIC AND ABIOTIC PROCESSES AS A CARBON SEQUESTRATION STRATEGY. In *Journal of Environmental Research And Development* (Vol. 5).
- Kovscek, A. R., & Cakici, M. D. (2005). Geologic storage of carbon dioxide and enhanced oil recovery. II. Cooptimization of storage and recovery. *Energy Conversion and Management*, 46(11), 1941–1956.  
<https://doi.org/https://doi.org/10.1016/j.enconman.2004.09.009>
- Lal, R. (2010). Terrestrial sequestration of carbon dioxide (CO<sub>2</sub>). *Developments and Innovation in Carbon Dioxide (CO<sub>2</sub>) Capture and Storage Technology*, 271–303. <https://doi.org/10.1533/9781845699581.3.271>
- Lasater, J. A. (1958). Bubble Point Pressure Correlation. *Journal of Petroleum Technology*, 10(05), 65–67. <https://doi.org/10.2118/957-G>
- Le Gallo, Y., Couillens, P., & Manai, T. (2002). CO<sub>2</sub> Sequestration in Depleted Oil or Gas Reservoirs. In *SPE International Conference on Health, Safety and Environment in Oil and Gas Exploration and Production* (p. 3). Society of Petroleum Engineers. <https://doi.org/10.2118/74104-MS>
- Mazzotti, M., Pini, R., Storti, G., & Burlini, L. (2010). 5 - Carbon dioxide (CO<sub>2</sub>) sequestration in unmineable coal seams and use for enhanced coalbed methane recovery (ECBM). In M. M. B. T.-D. and I. in C. D. (CO<sub>2</sub>) C. and S. T. Maroto-Valer (Ed.), *Woodhead Publishing Series in Energy* (Vol. 2, pp. 127–165). Woodhead Publishing.  
<https://doi.org/https://doi.org/10.1533/9781845699581.1.127>
- Metz, B., Davidson, O., de Coninck, H., Loos, M., & Meyer, L. (2005). *Carbon Dioxide Capture and Storage*. <https://www.ipcc.ch/report/carbon-dioxide-capture-and-storage/>
- Michael, K., Golab, A., Shulakova, V., Ennis-King, J., Allinson, G., Sharma, S., & Aiken, T. (2010). Geological storage of CO<sub>2</sub> in saline aquifers—A review of

- the experience from existing storage operations. *International Journal of Greenhouse Gas Control*, 4(4), 659–667.  
<https://doi.org/https://doi.org/10.1016/j.ijggc.2009.12.011>
- MIT. (n.d.-a). *Boundary Dam Fact Sheet: Carbon Dioxide Capture and Storage Project*. Carbon Capture and Sequestration Technologies.  
[http://sequestration.mit.edu/tools/projects/boundary\\_dam.html](http://sequestration.mit.edu/tools/projects/boundary_dam.html)
- MIT. (n.d.-b). *Kemper County IGCC Fact Sheet: Carbon Dioxide Capture and Storage Project*. Carbon Capture and Sequestration Technologies.  
<https://sequestration.mit.edu/tools/projects/kemper.html>
- MIT. (n.d.-c). *White Rose\* Project Fact Sheet: Carbon Dioxide Capture and Storage Project (\*Formerly UK Oxy CCS Project)*. Carbon Capture and Sequestration Technologies.  
[http://sequestration.mit.edu/tools/projects/white\\_rose.html](http://sequestration.mit.edu/tools/projects/white_rose.html)
- Mungan, N. (1981). Carbon Dioxide Flooding-fundamentals. *Journal of Canadian Petroleum Technology*, 20(01). <https://doi.org/10.2118/81-01-03>
- Nair, P. K. R. (2012). Carbon sequestration studies in agroforestry systems: a reality-check. *Agroforestry Systems*, 86(2), 243–253.  
<https://doi.org/10.1007/s10457-011-9434-z>
- NASA. (n.d.). *The Causes of Climate Change*.
- Núñez-López, V., & Moskal, E. (2019). Potential of CO<sub>2</sub>-EOR for Near-Term Decarbonization . In *Frontiers in Climate* (Vol. 1, p. 5).  
<https://www.frontiersin.org/article/10.3389/fclim.2019.00005>
- Perera, S., Pathegama, ranjith, Rathnaweera, T., Ranathunga, A., Koay, A., & Choi, X. (2016). A Review of CO<sub>2</sub>-Enhanced Oil Recovery with a Simulated Sensitivity Analysis. In *Energies: Vol. 9(7)*.  
<https://doi.org/10.3390/en9070481>
- Post, W. M., Amonette, J. E., Birdsey, R., Garten, C. T. J., Izaurrealde, R. C., Jardine, Philip, M., Jastrow, J., Lal, R., & Marland, G. (2009). Terrestrial biological carbon sequestration: science for enhancement and implementation. *Geophysical Monograph Series*, 183, 73–78.  
<https://www.fs.usda.gov/treearch/pubs/38906>
- Rosenbauer, R. J., & Thomas, B. (2010). 3 - Carbon dioxide (CO<sub>2</sub>) sequestration in deep saline aquifers and formations. In M. M. B. T.-D. and I. in C. D. (CO<sub>2</sub>) C. and S. T. Maroto-Valer (Ed.), *Woodhead Publishing Series in Energy* (Vol. 2, pp. 57–103). Woodhead Publishing.  
<https://doi.org/https://doi.org/10.1533/9781845699581.1.57>
- Rubin, E. S., Mantripragada, H., Marks, A., Versteeg, P., & Kitchin, J. (2012). The outlook for improved carbon capture technology. *Progress in Energy and Combustion Science*, 38(5), 630–671.

<https://doi.org/10.1016/J.PECS.2012.03.003>

- Sahin, S., Kalfa, U., Celebioglu, D., Duygu, E., & Lahna, H. (2012). *A Quarter Century of Progress in the Application of CO<sub>2</sub> Immiscible EOR Project in Bati Raman Heavy Oil Field in Turkey*. <https://doi.org/10.2118/157865-MS>
- Soares, C. (2015). *Chapter 11 - Gaseous Emissions and the Environment* (C. B. T.-G. T. (Second E. Soares (ed.); pp. 637–667). Butterworth-Heinemann. <https://doi.org/https://doi.org/10.1016/B978-0-12-410461-7.00011-0>
- Todd, M. R., & Longstaff, W. J. (1972). The Development, Testing, and Application Of a Numerical Simulator for Predicting Miscible Flood Performance. *Journal of Petroleum Technology*, 24(07), 874–882. <https://doi.org/10.2118/3484-PA>
- United Nations Climate Change. (2019a). *The Paris Agreement*. <https://unfccc.int/process-and-meetings/the-paris-agreement/the-paris-agreement>
- United Nations Climate Change. (2019b). *What is the Kyoto Protocol?* <https://unfccc.int/process-and-meetings/the-kyoto-protocol/what-is-the-kyoto-protocol/what-is-the-kyoto-protocol>
- Vega, B., & Kovscek, A. R. (2010). 4 - Carbon dioxide (CO<sub>2</sub>) sequestration in oil and gas reservoirs and use for enhanced oil recovery (EOR). In M. M. B. T.-D. and I. in C. D. (CO<sub>2</sub>) C. and S. T. Maroto-Valer (Ed.), *Woodhead Publishing Series in Energy* (Vol. 2, pp. 104–126). Woodhead Publishing. <https://doi.org/https://doi.org/10.1533/9781845699581.1.104>
- Veld, K. van t, Mason, C. F., & Leach, A. (2013). The Economics of CO<sub>2</sub> Sequestration Through Enhanced Oil Recovery. *Energy Procedia*, 37, 6909–6919. <https://doi.org/https://doi.org/10.1016/j.egypro.2013.06.623>
- Verma, M. K. (2015). Fundamentals of carbon dioxide-enhanced oil recovery (CO<sub>2</sub>-EOR): a supporting document of the assessment methodology for hydrocarbon recovery using CO<sub>2</sub>-EOR associated with carbon sequestration. In *Open-File Report*. <https://doi.org/10.3133/ofr20151071>
- Yang, F., Bai, B., Tang, D., Shari, D.-N., & David, W. (2010). Characteristics of CO<sub>2</sub> sequestration in saline aquifers. *Petroleum Science*, 7(1), 83–92. <https://doi.org/10.1007/s12182-010-0010-3>



## APPENDICES

### A. Scenario 1 Raw Material

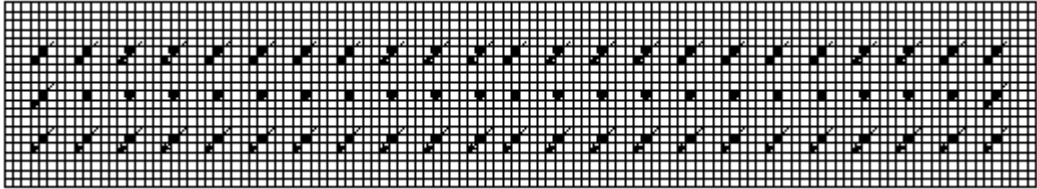


Figure 7.1. Peripheral injection top view

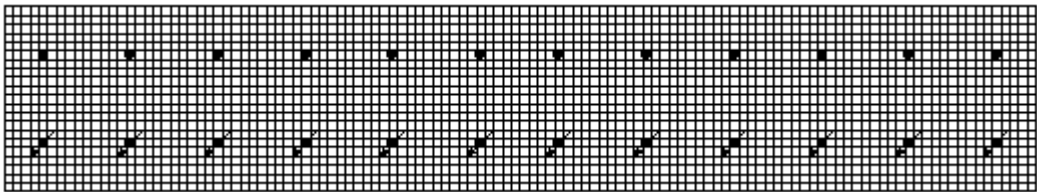


Figure 7.2. Directline injection top view

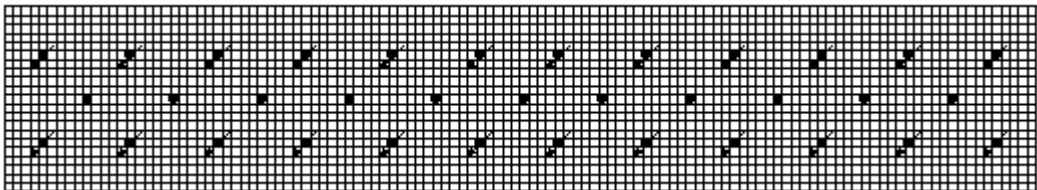


Figure 7.3. 5-Spot pattern injection top view

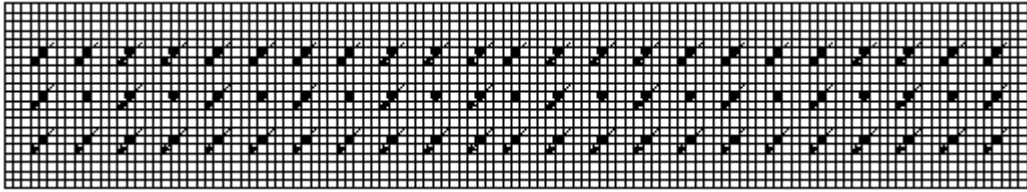


Figure 7.4. 9-Spot pattern injection top view

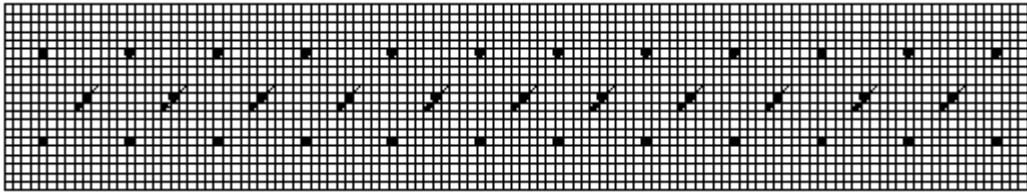


Figure 7.5. Inverted 5-Spot pattern injection top view

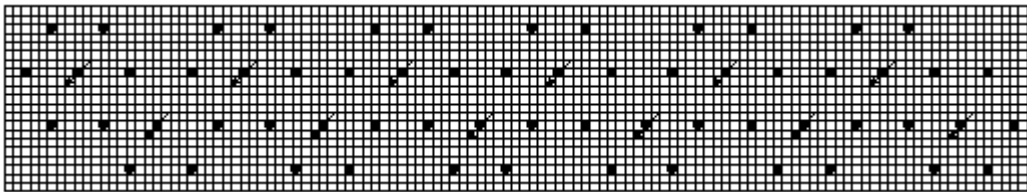


Figure 7.6. Inverted 7-Spot pattern injection top view

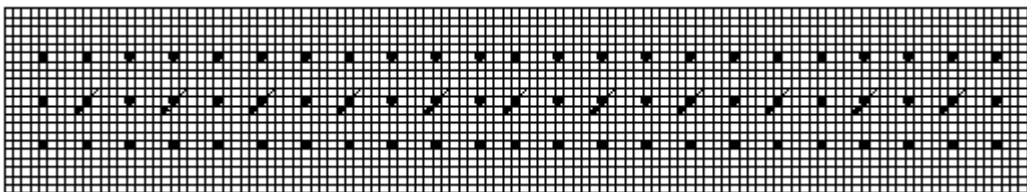


Figure 7.7. Inverted 9-Spot pattern injection top view

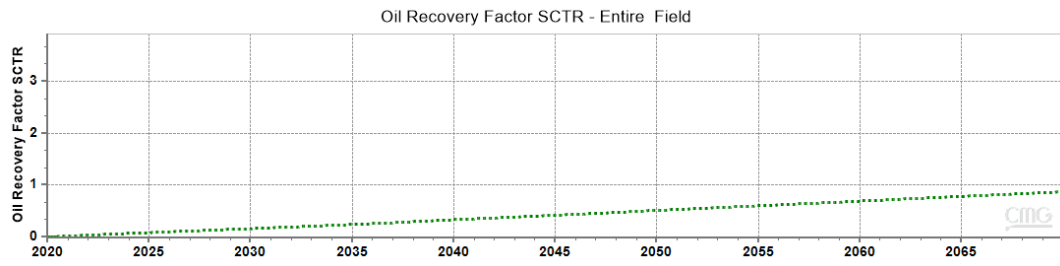


Figure 7.8. Directline Injection RF

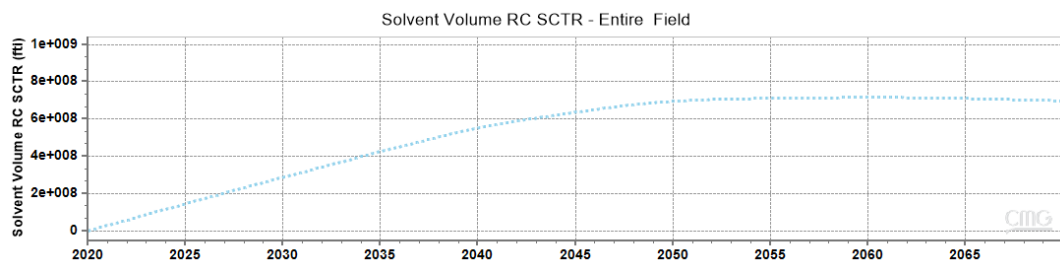


Figure 7.9. Directline Injection CO<sub>2</sub> Volumes

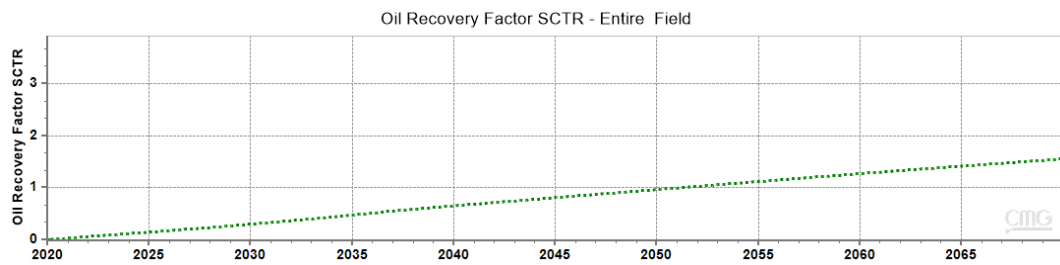


Figure 7.10. Peripheral Injection RF

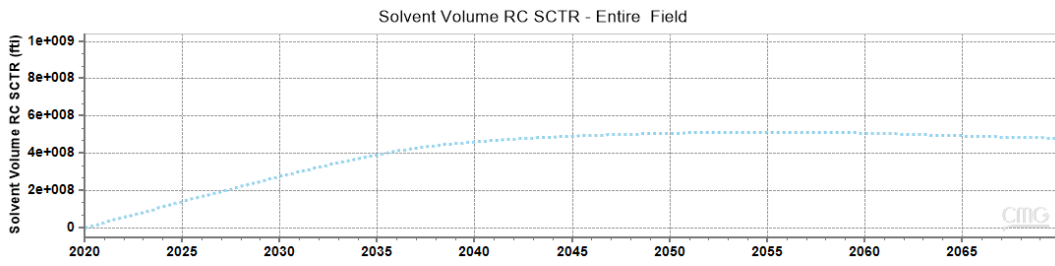


Figure 7.11. Peripheral Injection CO<sub>2</sub> Volumes

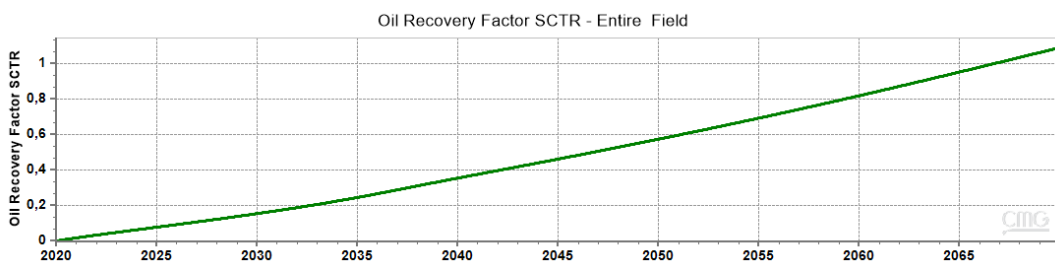


Figure 7.12. 5-Spot Pattern Injection RF

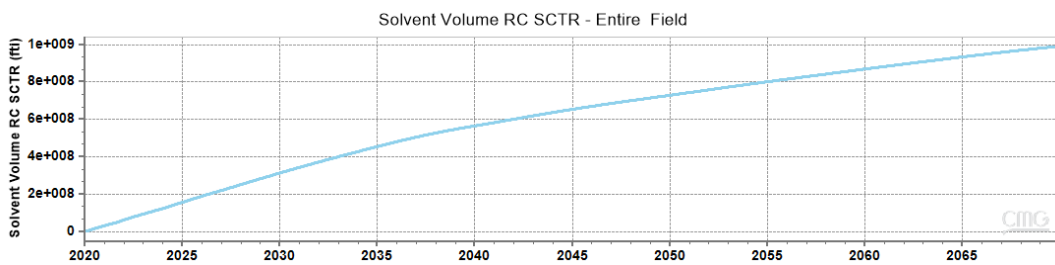


Figure 7.13. 5-Spot Pattern Injection CO<sub>2</sub> Volumes

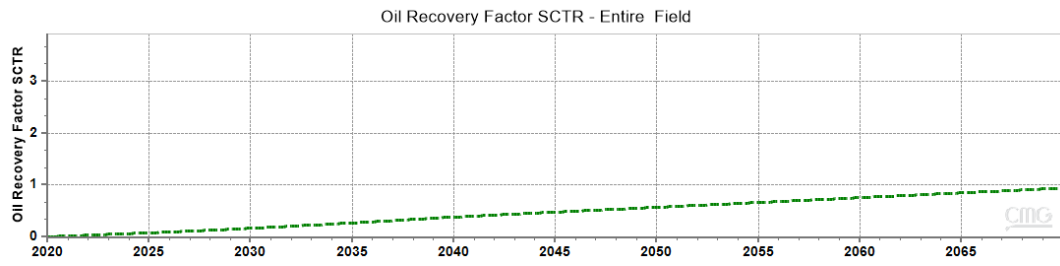


Figure 7.14. 9-Spot Pattern Injection RF

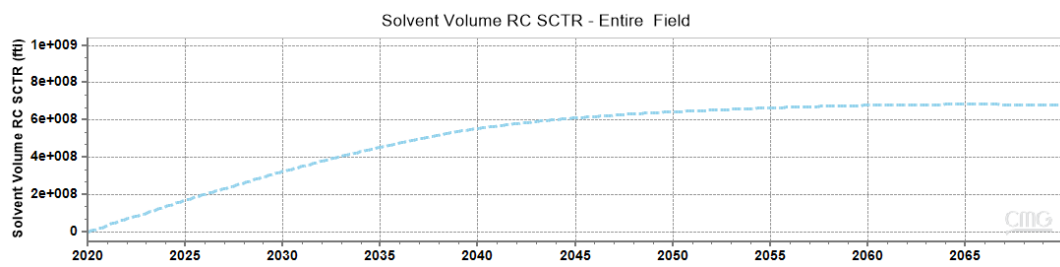


Figure 7.15. 9-Spot Pattern Injection CO<sub>2</sub> Volumes

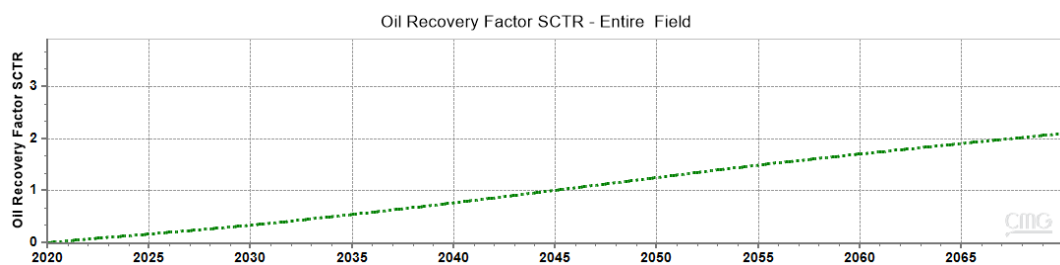


Figure 7.16. Inverted 5-Spot Pattern Injection RF

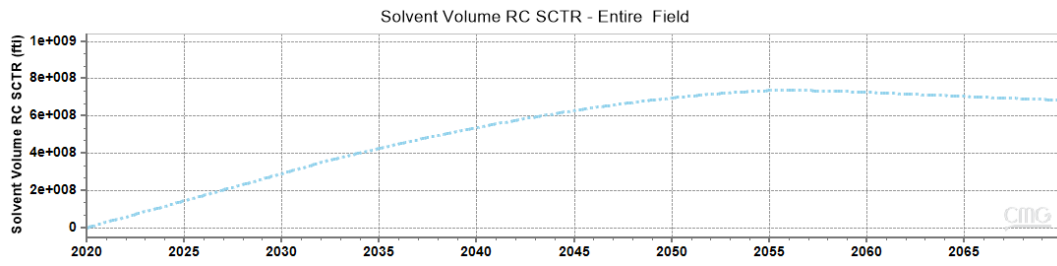


Figure 7.17. Inverted 5-Spot Pattern Injection CO<sub>2</sub> Volumes

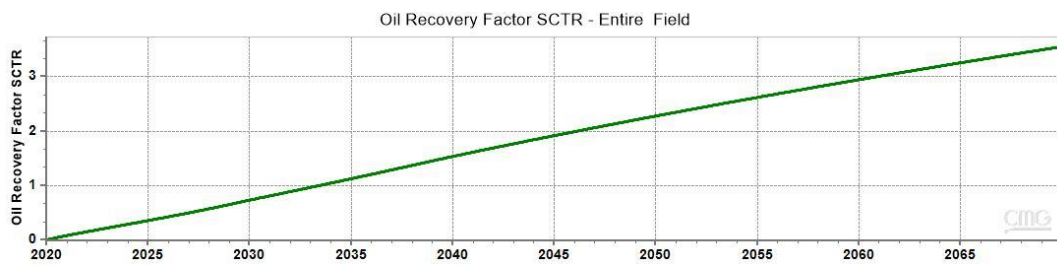


Figure 7.18. Inverted 7-Spot Pattern Injection RF

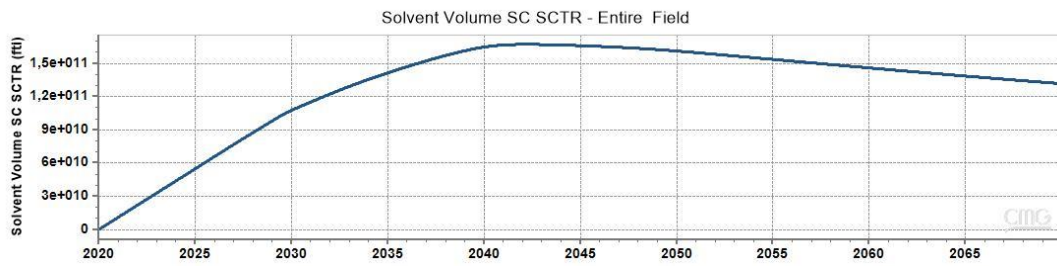


Figure 7.19. Inverted 7-Spot Pattern Injection CO<sub>2</sub> Volumes

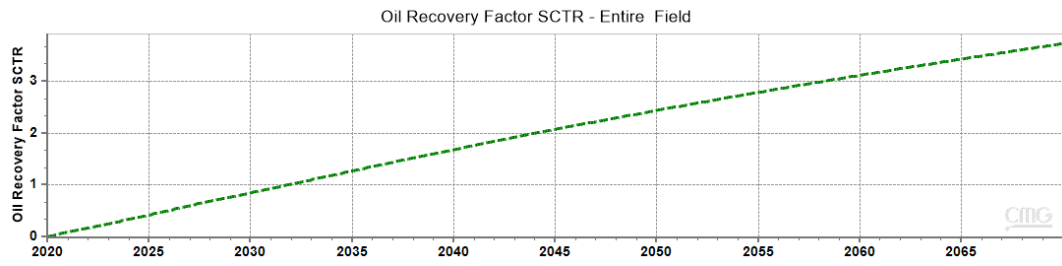


Figure 7.20. Inverted 9-Spot Pattern Injection RF

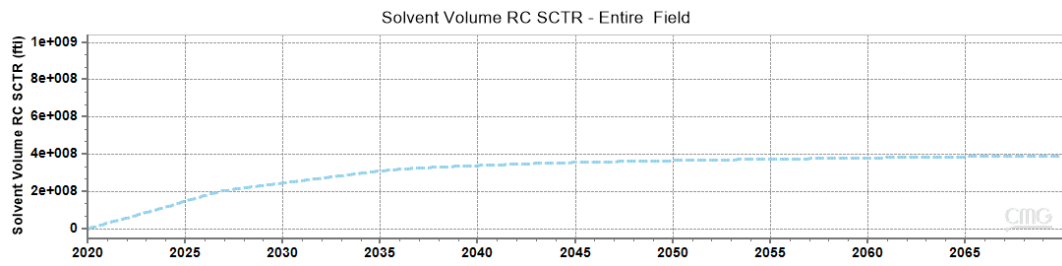


Figure 7.21. Inverted 9-Spot Pattern Injection CO<sub>2</sub> Volumes

## B. Scenario 2 Raw Material

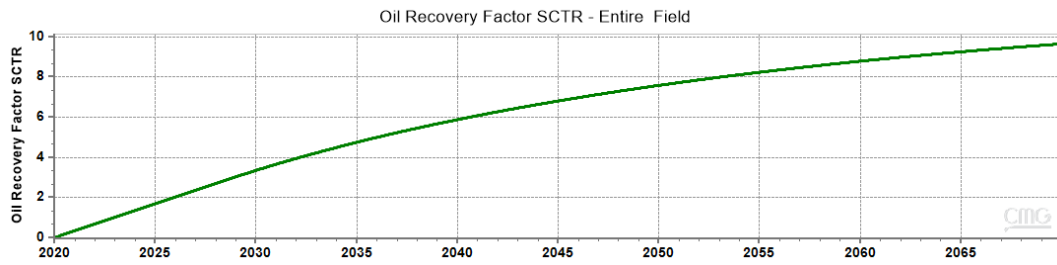


Figure 7.22. 75 Acres Pattern Size RF

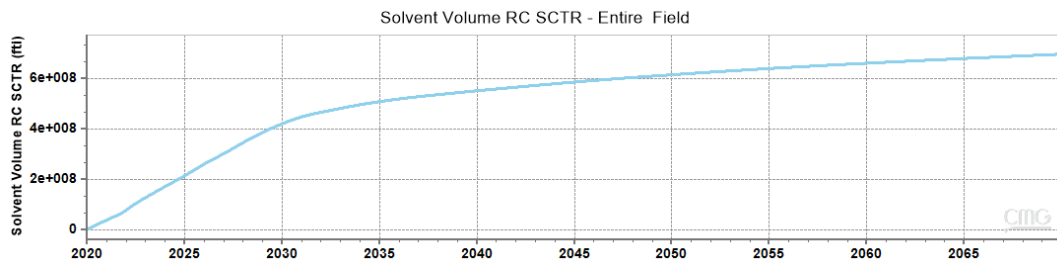


Figure 7.23. 75 Acres Pattern Size CO<sub>2</sub> Volumes

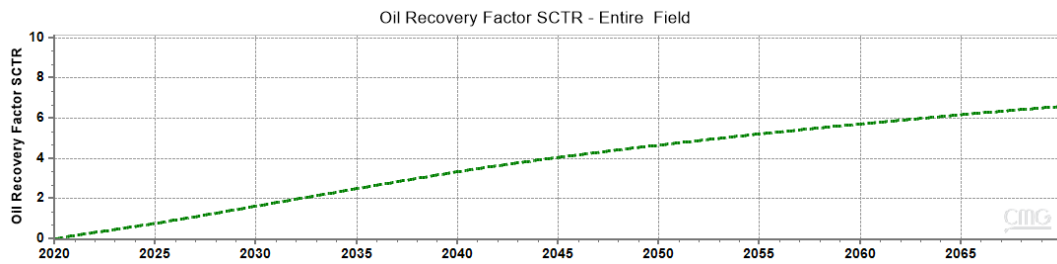


Figure 7.24. 100 Acres Pattern Size RF

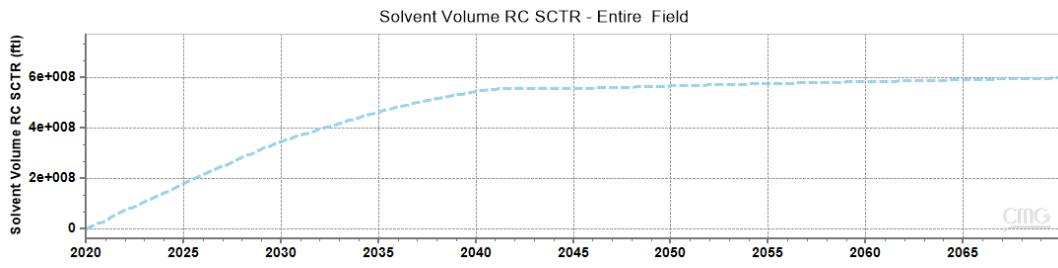


Figure 7.25. 100 Acres Pattern Size CO<sub>2</sub> Volumes

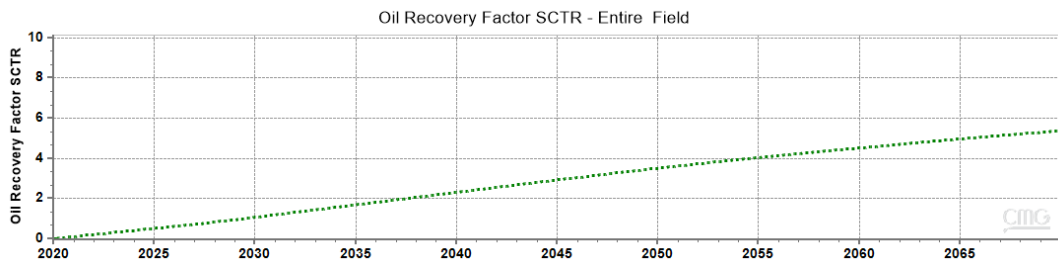


Figure 7.26. 200 Acres Pattern Size RF

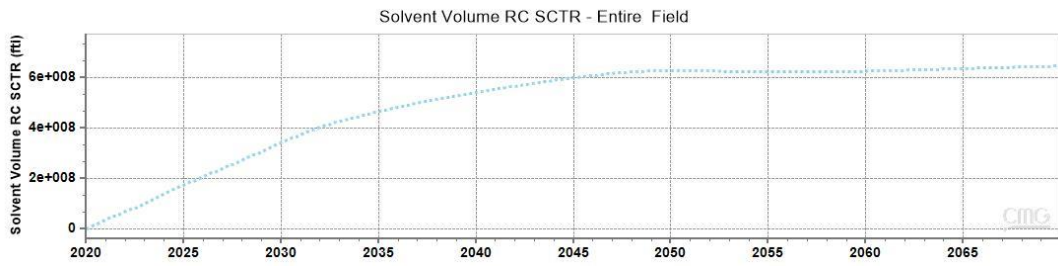


Figure 7.27. 200 Acres Pattern Size CO<sub>2</sub> Volumes

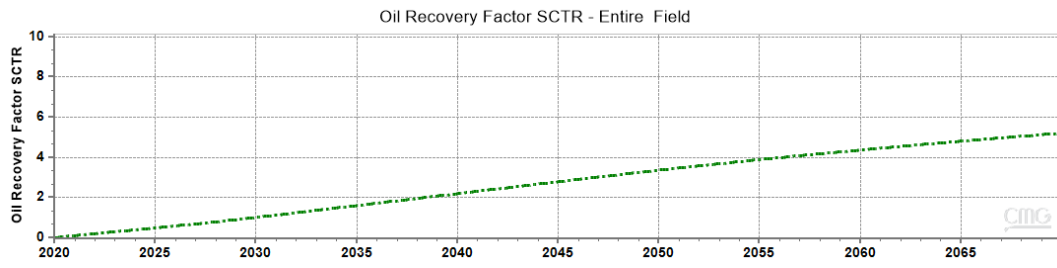


Figure 7.28. 215 Acres Pattern Size RF

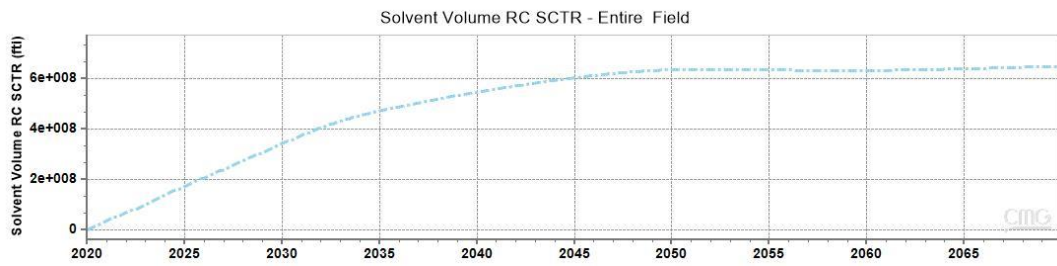


Figure 7.29. 215 Acres Pattern Size CO<sub>2</sub> Volumes

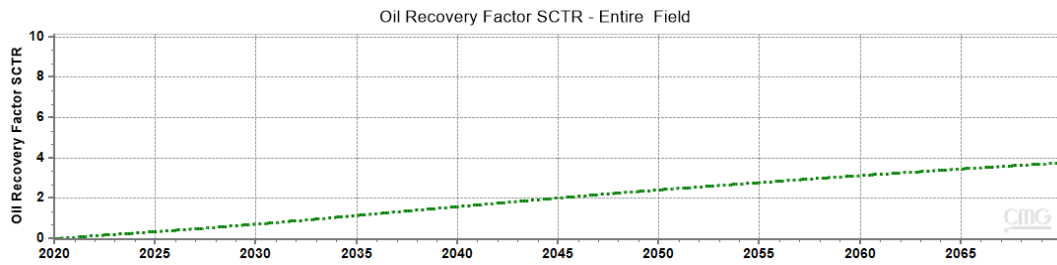


Figure 7.30. 230 Acres Pattern Size RF

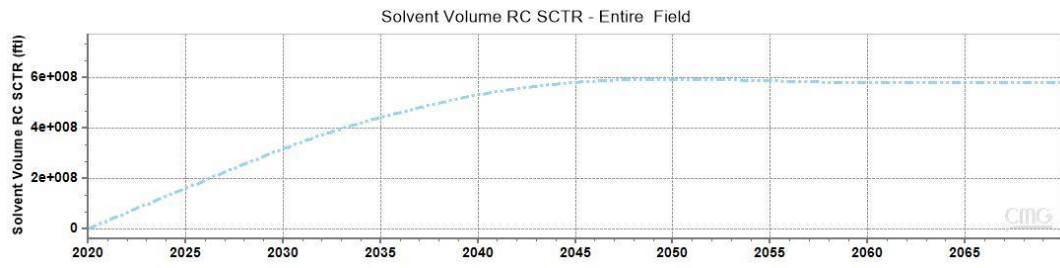


Figure 7.31. 230 Acres Pattern Size CO<sub>2</sub> Volumes

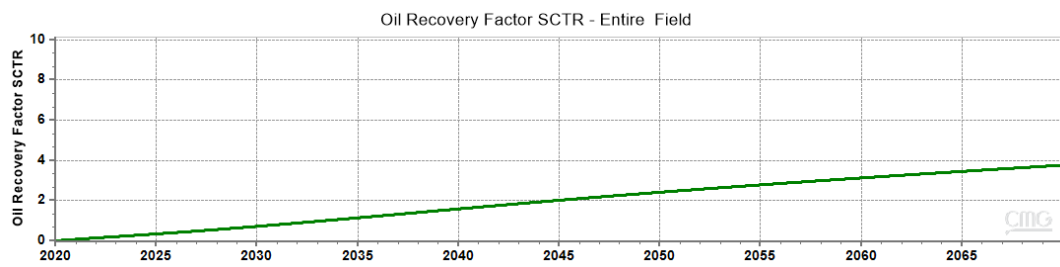


Figure 7.32. 250 Acres Pattern Size RF

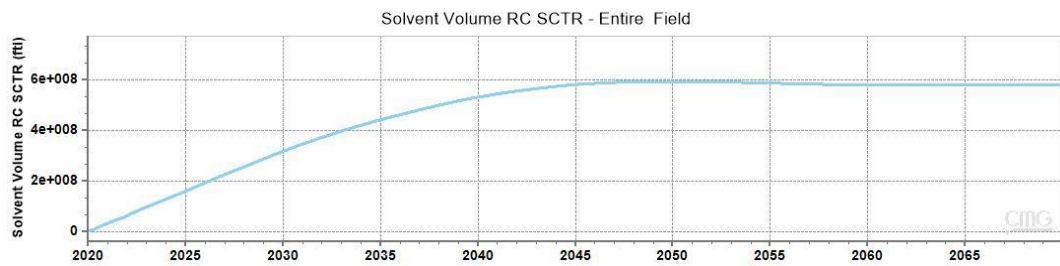


Figure 7.33. 250 Acres Pattern Size CO<sub>2</sub> Volumes

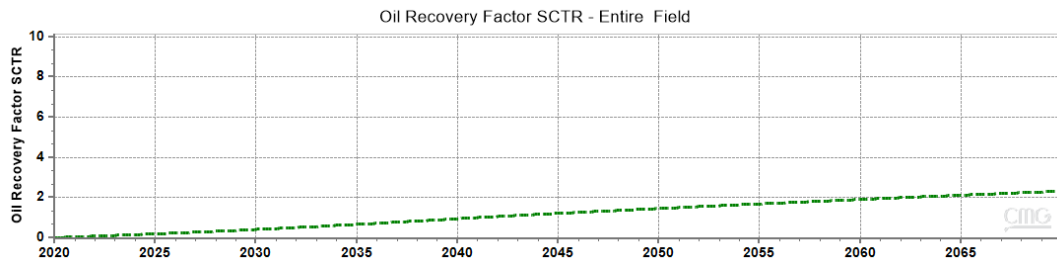


Figure 7.34. 400 Acres Pattern Size RF

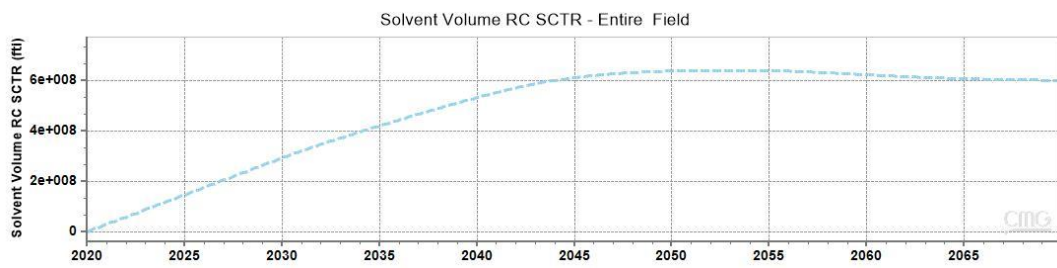


Figure 7.35. 400 Acres Pattern Size CO<sub>2</sub> Volumes

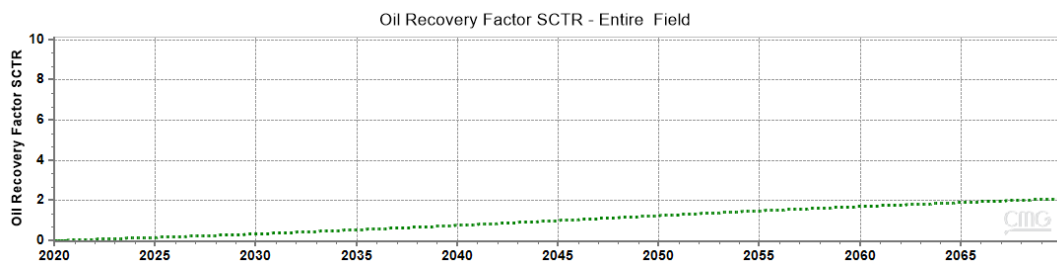


Figure 7.36. 500 Acres Pattern Size RF

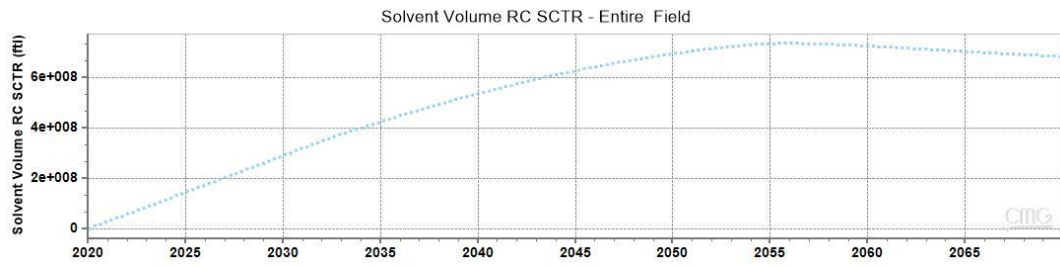


Figure 7.37. 500 Acres Pattern Size CO<sub>2</sub> Volumes

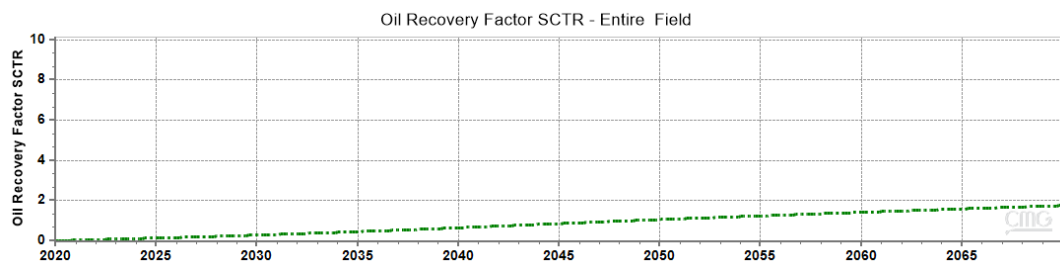


Figure 7.38. 600 Acres Pattern Size RF

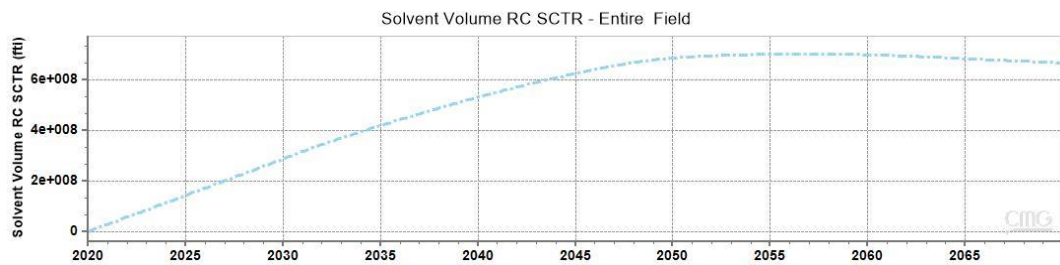


Figure 7.39. 600 Acres Pattern Size CO<sub>2</sub> Volumes

### C. Scenario 3 Raw Material

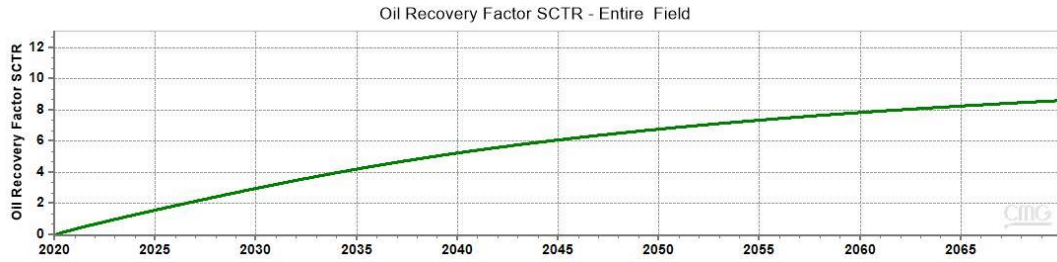


Figure 7.40. RF at 10 MMscf injection

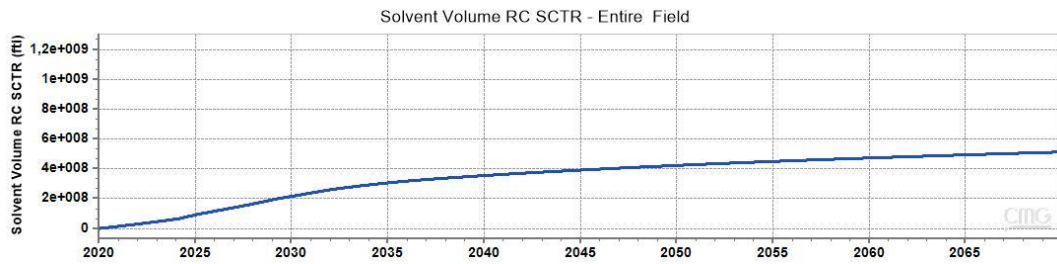


Figure 7.41. CO<sub>2</sub> Volumes at 10 MMscf injection

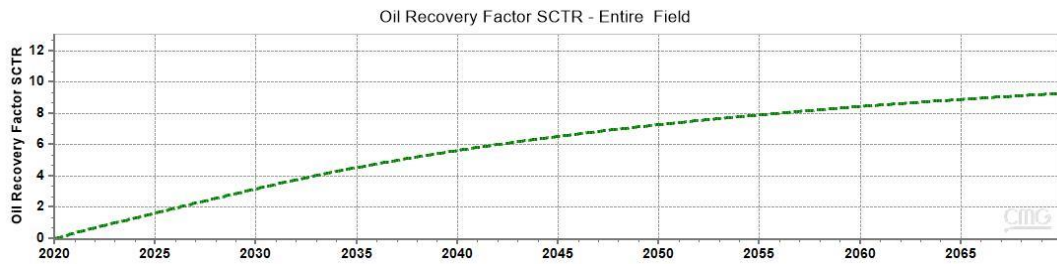


Figure 7.42. RF at 20 MMscf injection

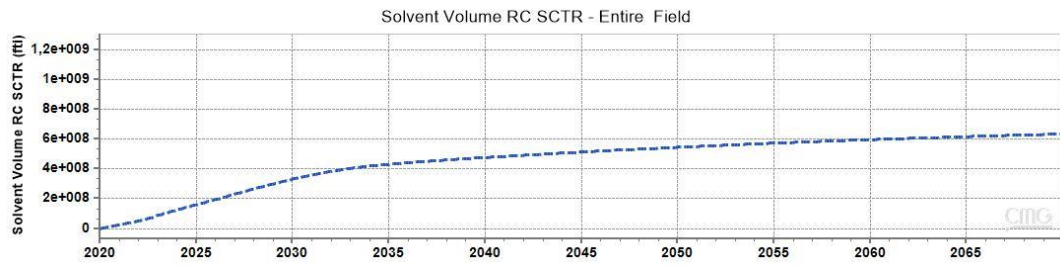


Figure 7.43. CO<sub>2</sub> Volumes at 20 MMscf injection

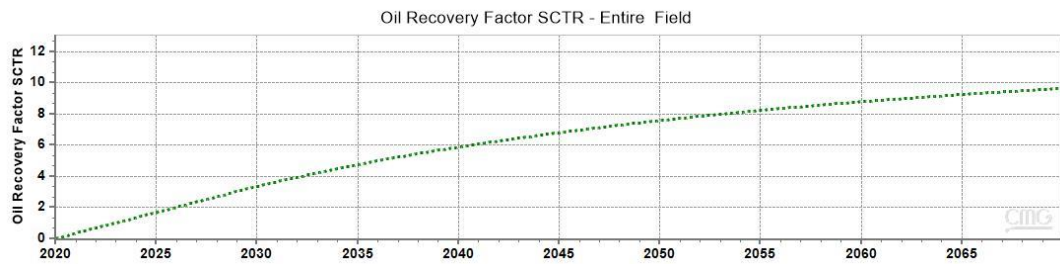


Figure 7.44. RF at 30 MMscf injection

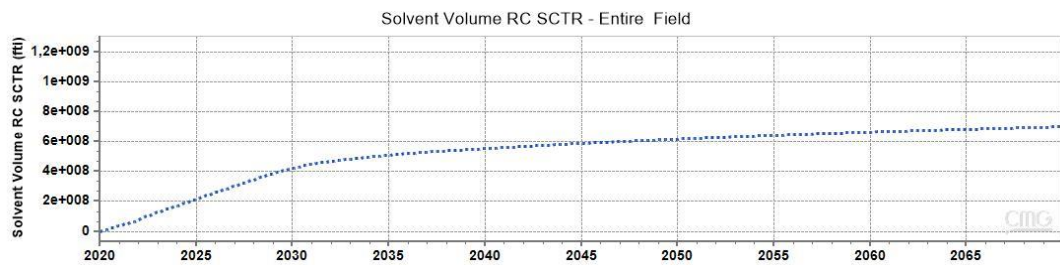


Figure 7.45. CO<sub>2</sub> Volumes at 30 MMscf injection

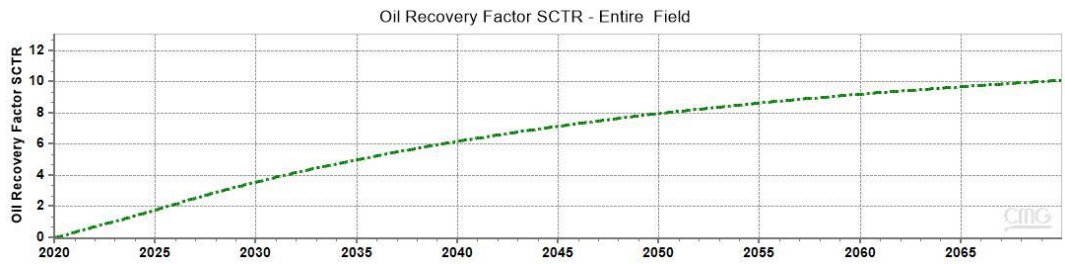


Figure 7.46. RF at 50 MMscf injection

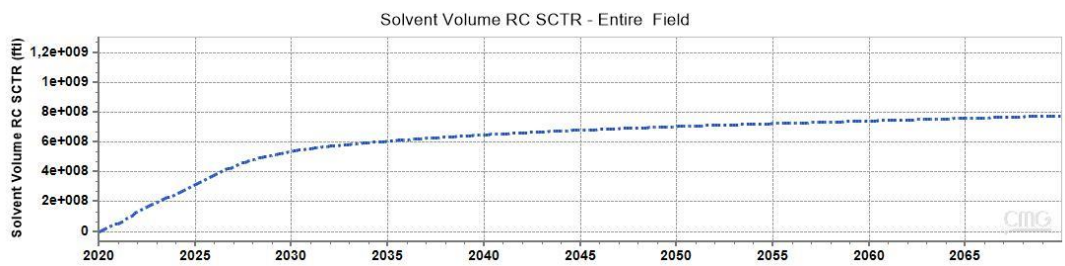


Figure 7.47. CO<sub>2</sub> Volumes at 50 MMscf injection

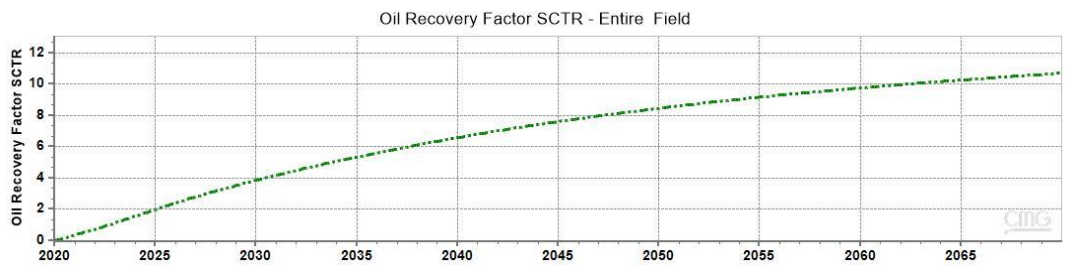


Figure 7.48. RF at 100 MMscf injection

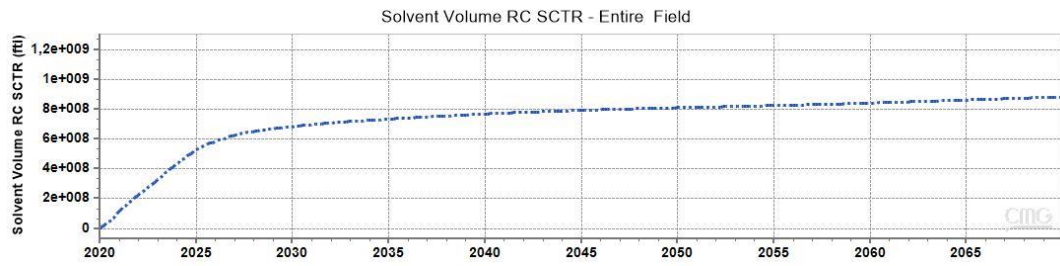


Figure 7.49. CO<sub>2</sub> Volumes at 100 MMscf injection

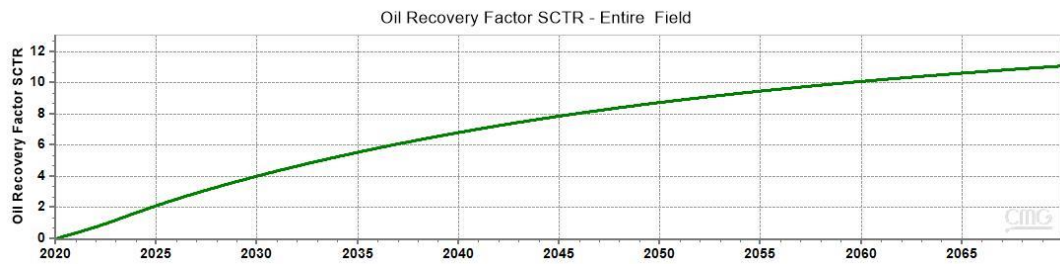


Figure 7.50. RF at 150 MMscf injection

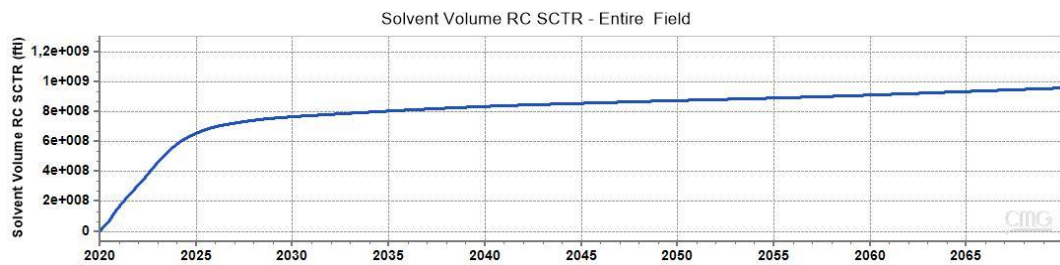


Figure 7.51. CO<sub>2</sub> Volumes at 150 MMscf injection

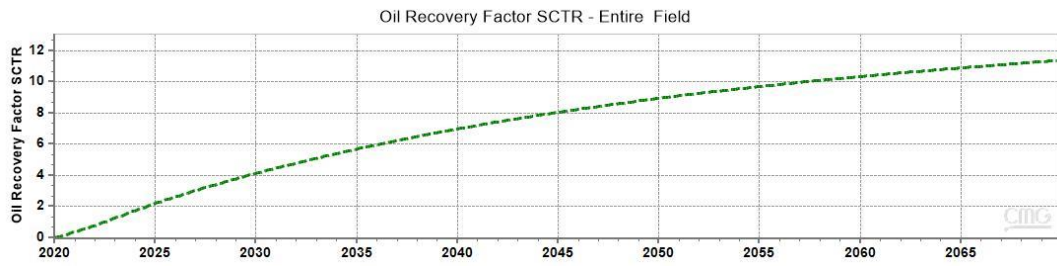


Figure 7.52. RF st 200 MMscf injection

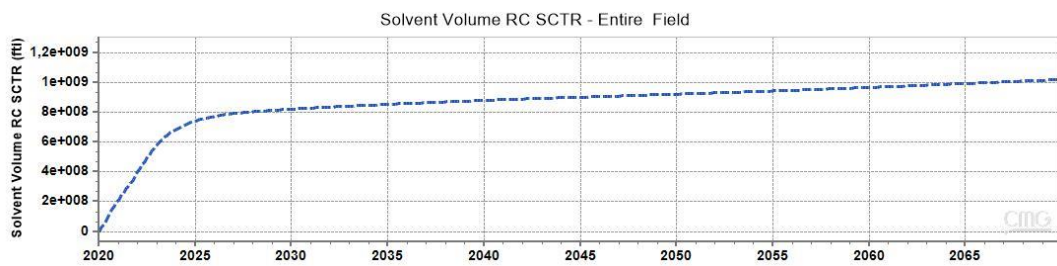


Figure 7.53. CO<sub>2</sub> Volumes at 200 MMscf injection

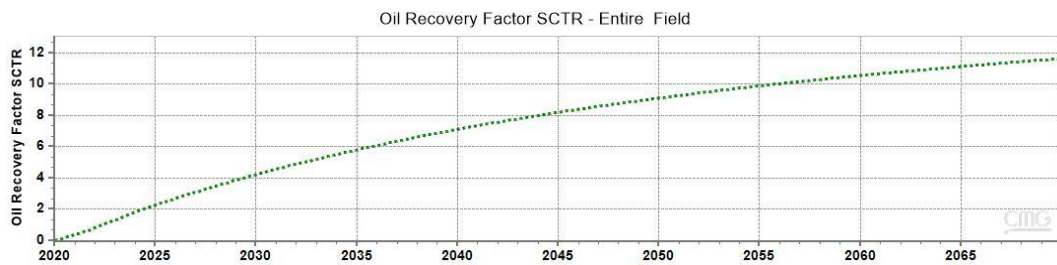


Figure 7.54. RF at 250 MMscf injection

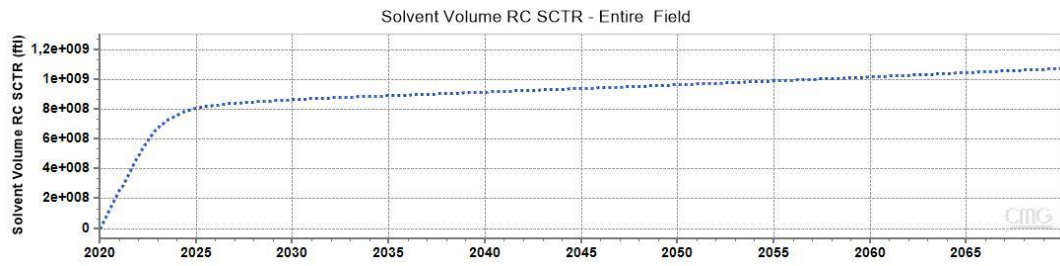


Figure 7.55. CO<sub>2</sub> Volumes at 250 MMscf injection

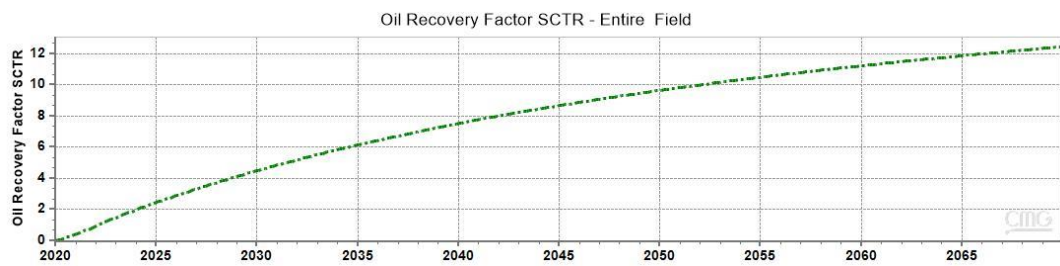


Figure 7.56. RF at 500 MMscf injection

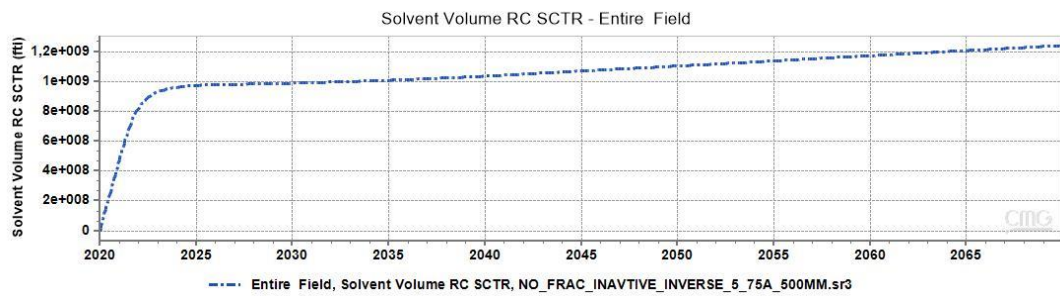


Figure 7.57. CO<sub>2</sub> Volumes at 500 MMscf injection

#### D. Scenario 4 Raw Material

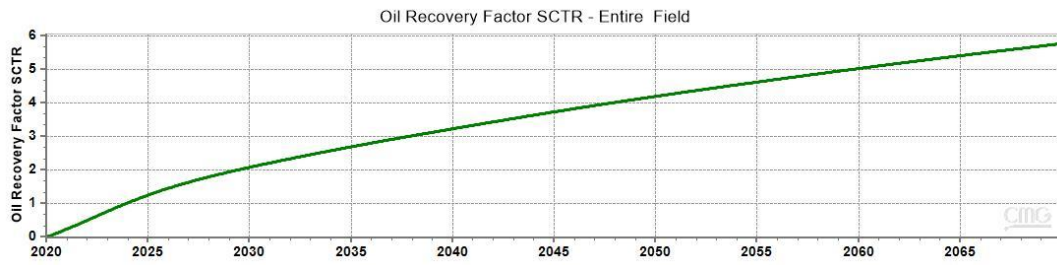


Figure 7.58. RF for CO<sub>2</sub> Injection into Oil Zone

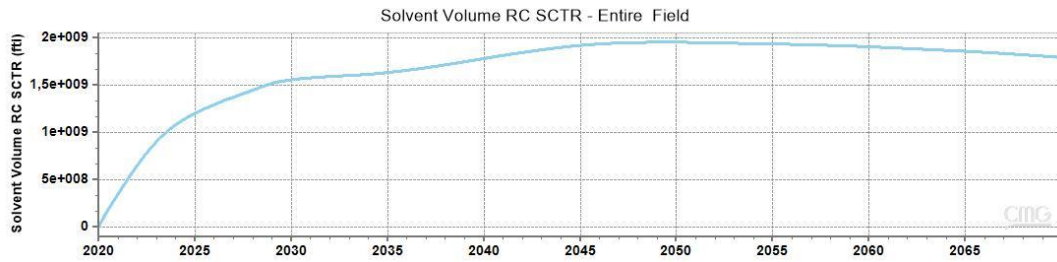


Figure 7.59. CO<sub>2</sub> Volumes for Injection into Oil Zone

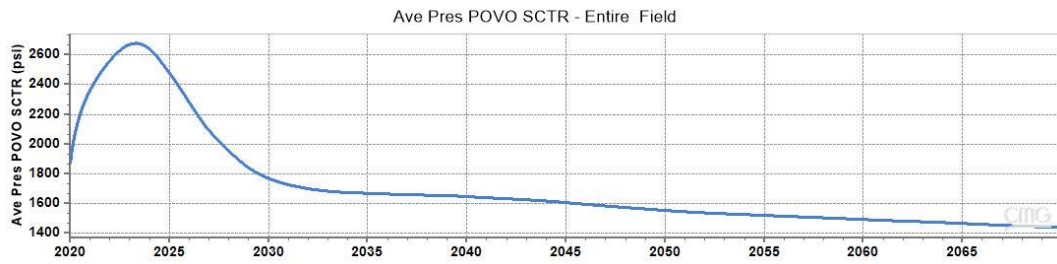


Figure 7.60. Reservoir Pressure While CO<sub>2</sub> Injection into Oil Zone

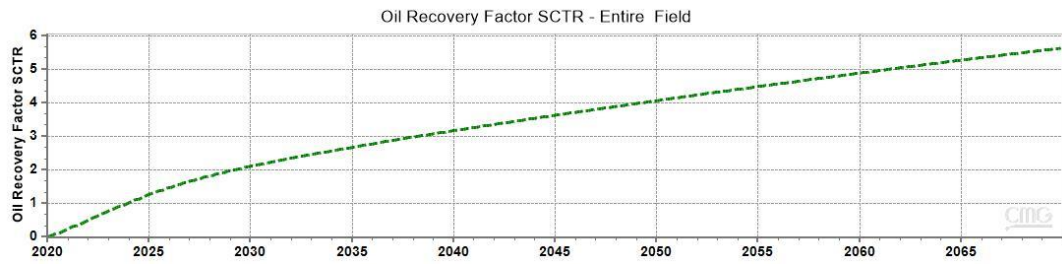


Figure 7.61. RF for CO<sub>2</sub> Injection into Water Zone

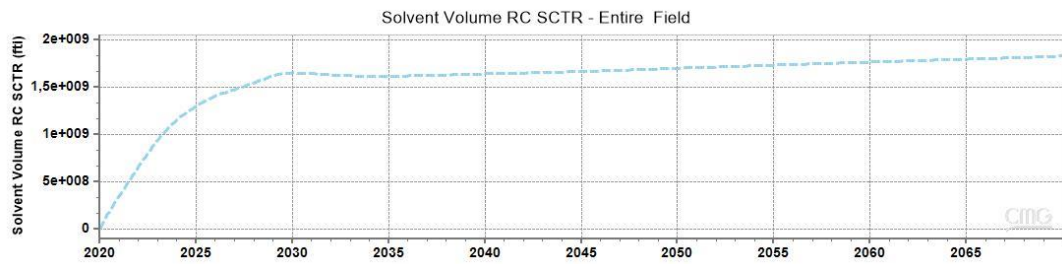


Figure 7.62. CO<sub>2</sub> Volumes for Injection into Water Zone

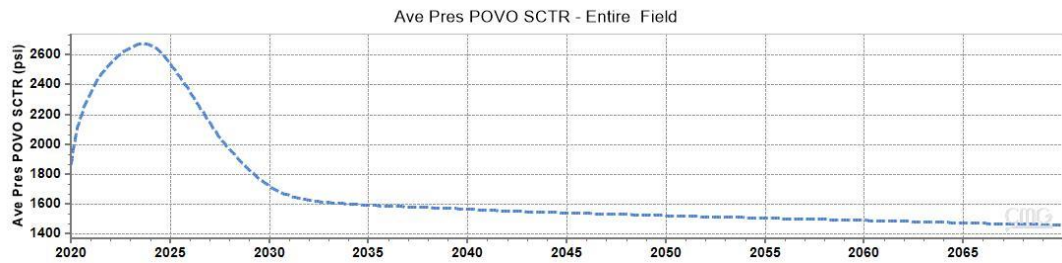


Figure 7.63. Reservoir Pressure While CO<sub>2</sub> Injection into Water Zone

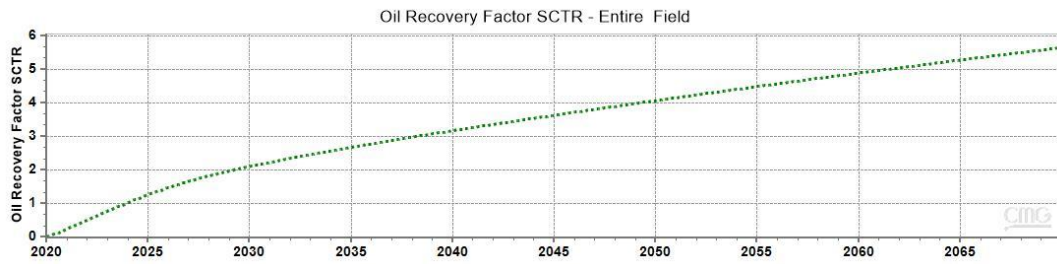


Figure 7.64. RF for CO<sub>2</sub> Injection into Both Oil and Water Zones

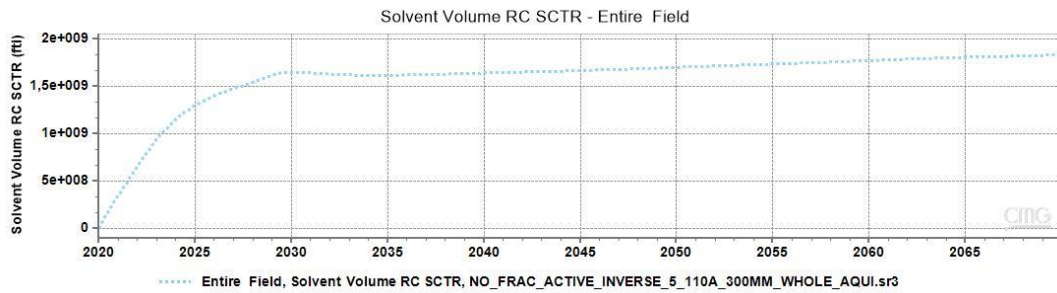


Figure 7.65. CO<sub>2</sub> Volumes for Injection into Both Oil and Water Zones

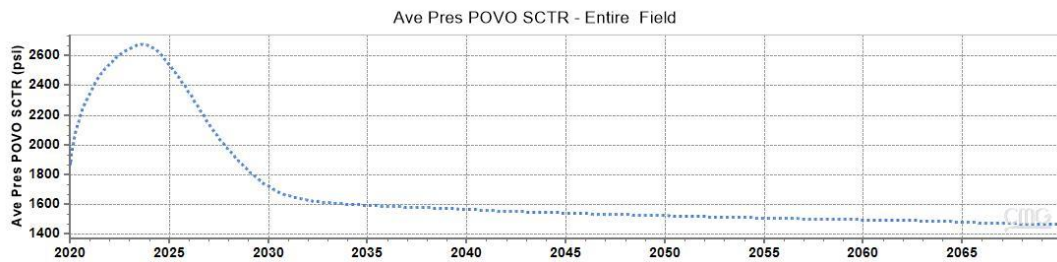


Figure 7.66. Reservoir Pressure While CO<sub>2</sub> Injection into Both Oil and Water Zones

## E. Scenario 5 Raw Material

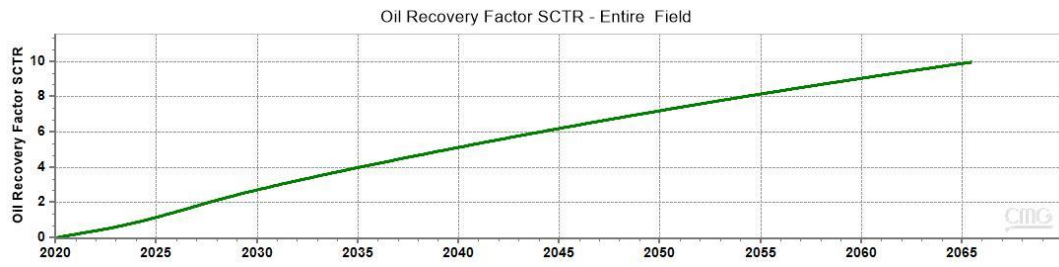


Figure 7.67. RF for 1:1 WAG Cycle ( 3 month each )

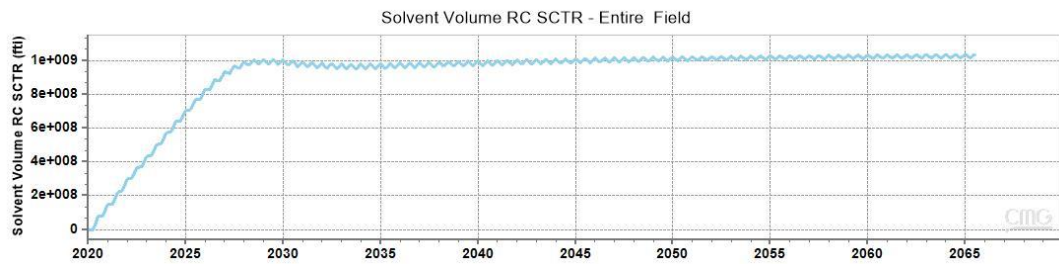


Figure 7.68. CO<sub>2</sub> Volume for 1:1 WAG Cycle ( 3 months each )

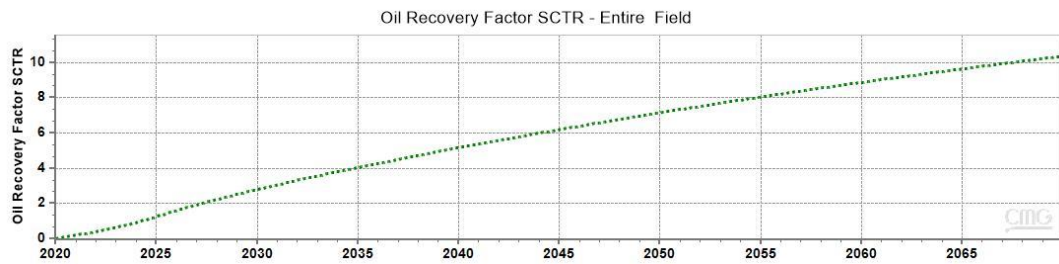


Figure 7.69. RF for 1:2 WAG Cycle ( 3 months H<sub>2</sub>O – 6 months CO<sub>2</sub> )

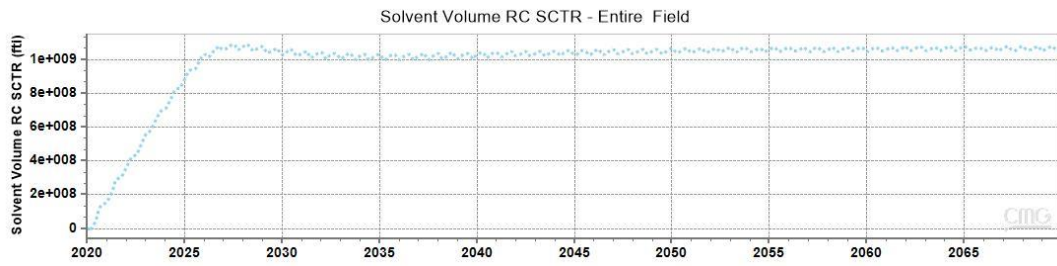


Figure 7.70. CO<sub>2</sub> Volume for 1:2 WAG Cycle ( 3 months H<sub>2</sub>O – 6 months CO<sub>2</sub> )

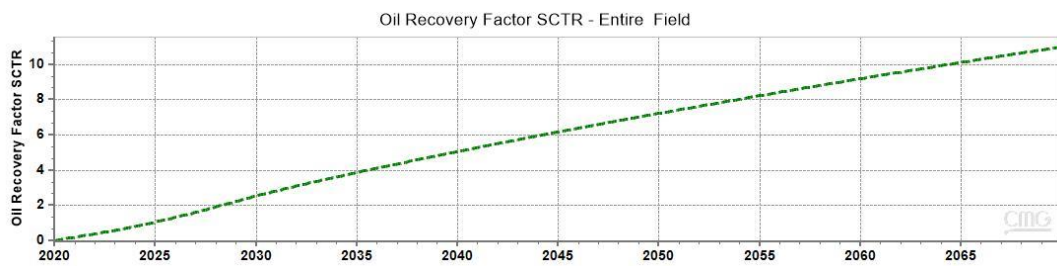


Figure 7.71. RF for 2:1 WAG Cycle ( 6 months H<sub>2</sub>O – 3 months CO<sub>2</sub> )

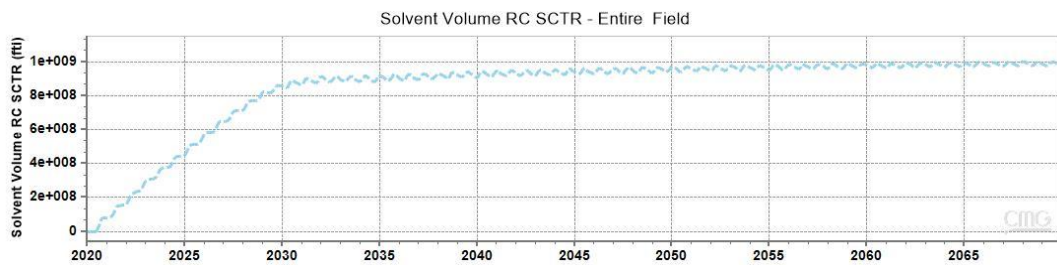


Figure 7.72. CO<sub>2</sub> Volume for 2:1 WAG Cycle ( 6 months H<sub>2</sub>O – 3 months CO<sub>2</sub> )

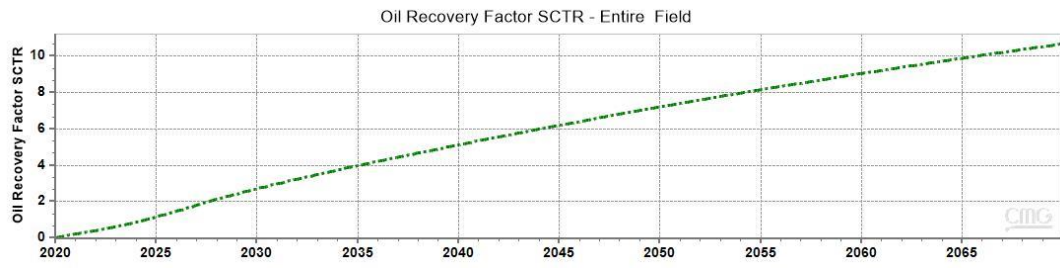


Figure 7.73. RF for 1:1 WAG Cycle ( 6 month each )

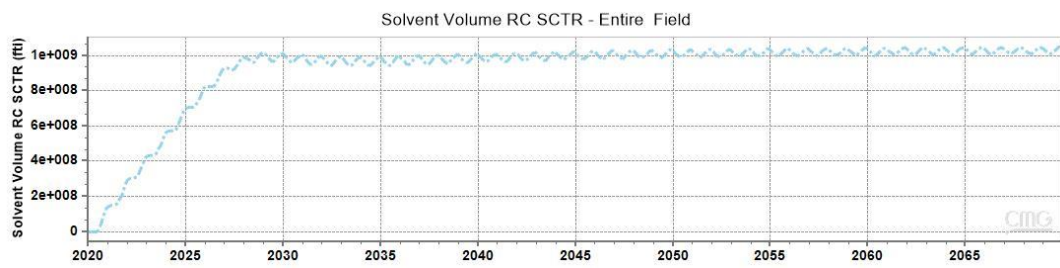


Figure 7.74. CO<sub>2</sub> Volume for 1:1 WAG Cycle ( 6 month each )